Université de Montréal

ANALYSIS OF THE ESOPHAGOGASTRIC JUNCTION USING THE 3D HIGH RESOLUTION MANOMETRY

By Frédéric NICODÈME

Department of Physiology
Faculty of Medicine

Thesis prepared at NORTHWESTERN UNIVERSTY
and presented at UNIVERSITÉ DE MONTRÉAL
(Faculté des études supérieures et postdoctorales)
for the degree of
Philosophiæ Doctor in Physiology

October 2013

ANALYSIS OF THE ESOPHAGOGASTRIC JUNCTION USING THE 3D HIGH RESOLUTION MANOMETRY

JURY MEMBERS

President	**Dre Marie-Josée HÉBERT** **Centre Hospitalier de l'Université de Montréal, QC**
Directors	**Dr André DURANCEAU** **Centre Hospitalier de l'Université de Montréal, QC** **Dr Peter J. KAHRILAS** **Northwestern University, Chicago, IL** **Dr John E. PANDOLFINO** **Northwestern University, Chicago, IL**
External Reviewer	**Dr Nicholas E. DIAMANT** **Queen's University, Kingston, ON**
Reviewer	**Dr Mickael BOUIN** **Centre Hospitalier de l'Université de Montréal, QC**
Dean's representative	**Dr Pierre POITRAS** **Centre Hospitalier de l'Université de Montréal, QC**

To my wife Johanne, to Alexandre,

To my parents and grand-parents,

To my brother, sister and their families,

To my friends,

To Thomas.

RÉSUMÉ (English)

Background & Aims: Conventional water-perfused manometry and high resolution manometry permitted the development of a variety of manometric methodologies and metrics to understand the motility of the esophagus and to quantify esophagogastric junction (EGJ) characteristics. However, the anatomy in the area of the EGJ is complex and intraluminal manometry recordings detect pressure signals referable both to intrinsic esophageal structures and to adjacent extrinsic structures impinging on the esophagus. Both have distinct sphincteric mechanisms within the EGJ. The dominant pressure signals detected near the EGJ are attributable to the lower esophageal sphincter (LES) and the crural diaphragm (CD). However, neither of these technologies were able to distinguish between the different components of the EGJ.

When analyzing EGJ characteristics as a reflection of its competence against reflux, the more widely used manometric parameters are the EGJ length and the respiratory inversion point (RIP), defined as the location at which inspiratory pressure deflections change from positive (abdomen) to negative (chest). However, the significance of these metrics has not gained wide acceptance in the gastroenterology community as evident in a recent American Gastroenterology Association Institute (AGAI) Position Statement (1) concluding that 'The current role of manometry in gastroesophageal reflux disease (GERD) is to exclude motor disorders as a cause of the continued symptoms'.

During deglutition, the objective quantitative measurement of EGJ relaxation, the integrative relaxation pressure (IRP), permits one to distinguish between normal and abnormal EGJ relaxation. However, comparison between spatial pressure variation plots and relaxation pressures derived from circumferentially averaged pressures suggest a persistent high pressure at the hiatal center during a period that flow is known to be occurring whereas this was not seen using nadir radial pressure data.

Recently, a 3D-high resolution manometry (3D-HRM) assembly (Given Imaging, Duluth, GA) has been developed with the potential to simplify the assessment of EGJ pressure morphology and physiology. The 3D segment of the array permits high resolution recording both axially and radially while maintaining a stationary sensor position. Consequently, 3D-HRM should allow for the measurement of important EGJ parameters such as length and RIP. Data extracted from the 3D-HRM recording may also allow differentiating pressure signals within the EGJ attributable to the intrinsic sphincter and to the surrounding elements. Moreover, 3D-HRM preserves the individual pressure values of each radially dispersed sensor within the array, permitting one to overcome the apparent persistent high pressure during the deglutitive relaxation.

Thus, the aims of this work were 1) to describe the EGJ pressure morphology at rest, comparing measures made with real time 3D-HRM to simulations of a conventional pull-through protocol and to define the pressure signatures attributable to the diaphragmatic and LES pressure components within the 3D-HRM recording; 2) to assess deglutitive EGJ relaxation by testing the hypothesis that the 3D-HRM array using an analysis paradigm based

on finding the minimal radial pressure at each axial level (3D-eSleeve) should provide a representation of the luminal pressure gradient across the EGJ that is more relevant to predicting periods of trans-sphincteric flow using barium transit on fluoroscopy as the comparator. We also sought to adapt the IRP metric to the 3D-HRM array using the 3D-eSleeve principle (3D-IRP) and compare normative values obtained with this new paradigm to standard IRP calculations.

Methods: Patients were studied with a 3D-HRM assembly. The 3D-HRM assembly incorporated a 9 cm 3D-HRM segment into an otherwise standard HRM assembly; the 3D segment was comprised of 12 rings of 8 radially dispersed independent pressure sensors, spaced 7.5mm apart.

At rest, 9 volunteers were studied and recordings were done during a station pull-through of the 3D-HRM segment withdrawing it across the EGJ at 5 mm increments with each position held for 30s (sufficient to capture several respiratory cycles). Conventional measures of 'LES length' were made using 4 radially dispersed sensors within the 3D-HRM array, defining the margins of the sphincter by a 2 mmHg pressure increase relative to gastric or esophageal pressure. In the 3D-HRM, the proximal and distal limits of the EGJ were defined as the axial locations first detecting a 360° circumferential pressure increase of 2 mmHg relative to the stomach. RIP was determined, A) in the tracing mode: using the pull-through of 4 single sensors spaced 7.5 mm apart [RIP is the average value of 4 radially dispersed sensors] and B) in a stationary position using the software pressure inversion point

(PIP) tool. In the esophageal pressure topography (EPT) mode, the tracing changed progressively from a thoracic pattern to an abdominal pattern, and the RIP was localized within the inversion zone with the PIP tool tracing.

For the study of the EGJ deglutitive relaxation, 25 volunteers underwent 3 consecutive 10-swallows protocols of 5 ml of water in the supine position with both the standard (once) and 3D-HRM (twice) devices in random sequence. During the 3D-HRM studies, the EGJ was measured once with the 3D-sleeve segment and once with a proximal (non-3D sleeve portion) of the device incorporating standard HRM sensors. For each subject, the IRP was calculated in four ways: 1) conventional method with the standard HRM device, 2) conventional method with a standard HRM segment of the 3D-HRM device, 3) conventional method using the 3D-HRM sleeve segment, and 4) a novel 3D-HRM eSleeve paradigm (3D-IRP) localizing the radial pressure minimum at each locus along the eSleeve. Fourteen additional subjects then underwent synchronized simultaneous videofluoroscopy and 3D-HRM (including two 5-ml barium swallows). Pressure data were exported to MATLAB™ and four pressures were measured simultaneously: 1) esophageal body pressure 2cm above EGJ, 2) intragastric pressure, 3) radially average eSleeve pressure and 4) 3D-eSleeve pressure. Data were plotted to determine the flow permissive time (FPT) characterized as periods during which a pressure gradient through the EGJ is present (esophageal pressure > EGJ relaxation pressure (radial average or 3D-eSleeve paradigm) > gastric pressure). FPT was calculated during a 10s time window after upper sphincter relaxation. The presence or absence of bolus transit or FPT was coded with dichotomous values for each 0.1 s. We

calculated the corresponding sensitivity and specificity for both radial average and 3D-eSleeve analyses of FPT with bolus transit evident on fluoroscopy being the reference.

Results: 3D-HRM recordings suggested that sphincter length assessed by a pull-through method greatly exaggerated the estimate of LES length by failing to discriminate among circumferential contractile pressure and asymmetric extrinsic pressure signals attributable to diaphragmatic and vascular structures. Real-time 3D EGJ recordings found that the dominant constituents of EGJ pressure at rest were attributable to the diaphragm.

The 3D-IRP was significantly less than all other calculations of IRP with the upper limit of normal being 12 mmHg vs. 17 mmHg for the standard IRP. The sensitivity (0.78) and the specificity (0.88) of the 3D-eSleeve were also better than the standard eSleeve (0.55 and 0.85, respectively) for predicting flow permissive time verified fluoroscopically.

Discussion & Conclusion: Our observations suggest that the 3D-HRM permits real-time recording of EGJ pressure morphology facilitating analysis of the EGJ constituents responsible for its function as a reflux barrier at rest. The axial and radial spatial resolution of the 9 cm 3D-HRM segment may permit further studies to differentiate pressure signals within the EGJ attributable to the LES and to extrinsic structures (diaphragm and vascular artifacts). These attributes of the 3D-HRM device suggest it to be a promising new tool in the study of GERD pathophysiology.

During deglutition, we evaluated the feasibility of improving the measurement of IRP utilizing a novel 3D-HRM assembly and a novel 3D-eSleeve concept based on finding the axial maximum of the radial minimum pressures at each sensor ring along the sleeve segment. Our findings suggest that this approach is more accurate than standard HRM and other methods that utilize a radially averaged pressure within the EGJ. Although we can only speculate on how much this will improve clinical management, 3D-HRM will certainly improve the accuracy of EGJ relaxation measurements and this will certainly impact research endeavors focused on modeling EGJ function during swallowing and reflux.

KEY WORDS

- Esophagogastric junction
- Esophageal manometry
- 3D-High resolution manometry
- Deglutition physiology
- Gastroesophageal reflux

RÉSUMÉ (Français)

Contexte & Objectifs : La manométrie perfusée conventionnelle et la manométrie haute résolution (HRM) ont permis le développement d'une variété de paramètres pour mieux comprendre la motilité de l'œsophage et quantifier les caractéristiques de la jonction œsophago-gastrique (JOG). Cependant, l'anatomie de la JOG est complexe et les enregistrements de manométrie détectent à la fois la pression des structures intrinsèques et des structures extrinsèques à l'œsophage. Ces différents composants ont des rôles distincts au niveau de la JOG. Les pressions dominantes ainsi détectées au niveau de la JOG sont attribuables au sphincter œsophagien inférieur (SOI) et aux piliers du diaphragme (CD), mais aucune des technologies manométriques actuelles n'est capable de distinguer ces différents composants de la JOG.

Lorsqu'on analyse les caractéristiques de la JOG au repos, celle ci se comporte avant tout comme une barrière antireflux. Les paramètres manométriques les plus couramment utilisés dans ce but sont la longueur de la JOG et le point d'inversion respiratoire (RIP), défini comme le lieu où le pic de la courbe de pression inspiratoire change de positif (dans l'abdomen) à négatif (dans le thorax), lors de la classique manœuvre de « pull-through ». Cependant, l'importance de ces mesures reste marginale comme en témoigne une récente prise de position de l'American Gastroenterology Association Institute (AGAI) (1) qui concluait que « le rôle actuel de la manométrie dans le reflux gastro-œsophagien (RGO) est d'exclure les troubles moteurs comme cause des symptômes présentés par la patient ».

Lors de la déglutition, la mesure objective de la relaxation de la JOG est la pression de relaxation intégrée (IRP), qui permet de faire la distinction entre une relaxation normale et une relaxation anormale de la JOG. Toutefois, puisque la HRM utilise des pressions moyennes à chaque niveau de capteurs, certaines études de manométrie laissent suggérer qu'il existe une zone de haute pression persistante au niveau de la JOG même si un transit est mis en évidence en vidéofluoroscopie.

Récemment, la manométrie haute résolution « 3D » (3D-HRM) a été développée (Given Imaging, Duluth, GA) avec le potentiel de simplifier l'évaluation de la morphologie et de la physiologie de la JOG. Le segment « 3D » de ce cathéter de HRM permet l'enregistrement de la pression à la fois de façon axiale et radiale tout en maintenant une position fixe de la sonde, et évitant ainsi la manœuvre de « pull-through ». Par conséquent, la 3D-HRM devrait permettre la mesure de paramètres importants de la JOG tels que sa longueur et le RIP. Les données extraites de l'enregistrement fait par 3D-HRM permettraient également de différencier les signaux de pression attribuables au SOI des éléments qui l'entourent. De plus, l'enregistrement des pressions de façon radiaire permettrait d'enregistrer la pression minimale de chaque niveau de capteurs et devrait corriger cette zone de haute pression parfois persistante lors la déglutition.

Ainsi, les objectifs de ce travail étaient: 1) de décrire la morphologie de la JOG au repos en tant que barrière antireflux, en comparant les mesures effectuées avec la 3D-HRM en temps réel, par rapport à celle simulées lors d'une manœuvre de « pull-through » et de déterminer quelles sont les signatures des pressions attribuables au SOI et au diaphragme;

2) d'évaluer la relaxation de la JOG pendant la déglutition en testant l'hypothèse selon laquelle la 3D-HRM permet le développement d'un nouveau paradigme (appelé « 3D eSleeve ») pour le calcul de l'IRP, fondé sur l'utilisation de la pression radiale minimale à chaque niveau de capteur de pression le long de la JOG. Ce nouveau paradigme sera comparé à une étude de transit en vidéofluoroscopie pour évaluer le gradient de pression à travers la JOG.

Méthodes : Nous avons utilisé un cathéter 3D-HRM, qui incorpore un segment dit « 3D » de 9 cm au sein d'un cathéter HRM par ailleurs standard. Le segment 3D est composé de 12 niveaux (espacés de 7.5mm) de 8 capteurs de pression disposés radialement, soit un total de 96 capteurs.

Neuf volontaires ont été étudiés au repos, où des enregistrements ont été effectués en temps réel et pendant une manœuvre de « pull-through » du segment 3D (mobilisation successive du cathéter de 5 mm, pour que le segment 3D se déplace le long de la JOG). Les mesures de la longueur du SOI et la détermination du RIP ont été réalisées. La longueur de la JOG a été mesurée lors du « pull-through » en utilisant 4 capteurs du segment 3D dispersés radialement et les marges de la JOG ont été définies par une augmentation de la pression de 2 mmHg par rapport à la pression gastrique ou de l'œsophage. Pour le calcul en temps réel, les limites distale et proximale de la JOG ont été définies par une augmentation de pression circonférentielle de 2 mmHg par rapport à la pression de l'estomac. Le RIP a été déterminée, A) dans le mode de tracé conventionnel avec la méthode du « pull-through » [le RIP est la valeur moyenne de 4 mesures] et B) en position fixe, dans le mode de représentation

topographique de la pression de l'œsophage, en utilisant l'outil logiciel pour déterminer le point d'inversion de la pression (PIP).

Pour l'étude de la relaxation de la JOG lors de la déglutition, 25 volontaires ont été étudiés et ont subi 3 études de manométrie (10 déglutitions de 5ml d'eau) en position couchée avec un cathéter HRM standard et un cathéter 3D-HRM. Avec la 3D-HRM, l'analyse a été effectuée une fois avec le segment 3D et une fois avec une partie non 3D du cathéter (capteurs standard de HRM). Ainsi, pour chaque individu, l'IRP a été calculée de quatre façons: 1) avec la méthode conventionnelle en utilisant le cathéter HRM standard, 2) avec la méthode conventionnelle en utilisant le segment standard du cathéter 3D-HRM, 3) avec la méthode conventionnelle en utilisant le segment « 3D » du cathéter 3D-HRM, et 4) avec le nouveau paradigme (3D eSleeve) qui recueille la pression minimale de chaque niveau de capteurs (segment 3D).

Quatorze autres sujets ont subi une vidéofluoroscopie simultanée à l'étude de manométrie avec le cathéter 3D-HRM. Les données de pression ont été exportés vers MATLAB ™ et quatre pressions ont été mesurées simultanément : 1) la pression du corps de l'œsophage, 2cm au-dessus de la JOG, 2) la pression intragastrique, 3) la pression radiale moyenne de la JOG (pression du eSleeve) et 4) la pression de la JOG en utilisant la pression minimale de chaque niveau de capteurs (pression du 3D eSleeve). Ces données ont permis de déterminer le temps permissif d'écoulement du bolus (FPT), caractérisé par la période au cours de laquelle un gradient de pression existe à travers la JOG (pression œsophagienne > pression de relaxation de la JOG > pression gastrique). La présence ou l'absence du bolus

en vidéofluoroscopie et le FPT ont été codés avec des valeurs dichotomiques pour chaque période de 0,1 s. Nous avons alors calculé la sensibilité et la spécificité correspondant à la valeur du FPT pour la pression du eSleeve et pour la pression du 3D eSleeve, avec la vidéofluoroscopie pour référence.

Résultats : Les enregistrements avec la 3D-HRM laissent suggérer que la longueur du sphincter évaluée avec la méthode du « pull-through » était grandement exagéré en incorporant dans la mesure du SOI les signaux de pression extrinsèques à l'œsophage, asymétriques et attribuables aux piliers du diaphragme et aux structures vasculaires. L'enregistrement en temps réel a permis de constater que les principaux constituants de la pression de la JOG au repos étaient attribuables au diaphragme.

L'IRP calculé avec le nouveau paradigme 3D eSleeve était significativement inférieur à tous les autres calculs d'IRP avec une limite supérieure de la normale de 12 mmHg contre 17 mmHg pour l'IRP calculé avec la HRM standard. La sensibilité (0,78) et la spécificité (0,88) du 3D eSleeve étaient meilleurs que le eSleeve standard (0,55 et 0,85 respectivement) pour prédire le FPT par rapport à la vidéofluoroscopie.

Discussion et conclusion : Nos observations suggèrent que la 3D-HRM permet l'enregistrement en temps réel des attributs de la JOG, facilitant l'analyse des constituants responsables de sa fonction au repos en tant que barrière antireflux. La résolution spatiale axiale et radiale du segment « 3D » pourrait permettre de poursuivre cette étude pour quantifier les signaux de pression de la JOG attribuable au SOI et aux structures extrinsèques

(diaphragme et artéfacts vasculaires). Ces attributs du cathéter 3D-HRM suggèrent qu'il s'agit d'un nouvel outil prometteur pour l'étude de la physiopathologie du RGO.

Au cours de la déglutition, nous avons évalué la faisabilité d'améliorer la mesure de l'IRP en utilisant ce nouveau cathéter de manométrie 3D avec un nouveau paradigme (3D eSleeve) basé sur l'utilisation de la pression radiale minimale à chaque niveau de capteurs de pression. Nos résultats suggèrent que cette approche est plus précise que celle de la manométrie haute résolution standard. La 3D-HRM devrait certainement améliorer la précision des mesures de relaxation de la JOG et cela devrait avoir un impact sur la recherche pour modéliser la JOG au cours de la déglutition et dans le RGO.

MOTS CLEF

- Jonction œsophago-gastrique
- Manométrie de l'œsophage
- Manométrie haute résolution 3D
- Physiologie de la déglutition
- Reflux gastro œsophagien

INDEX OF CONTENT

LIST OF FIGURES

LIST OF TABLES

ACKNOWLEDGMENTS

André Duranceau, for his everyday support and trust,

Peter J. Kahrilas and **John E. Pandolfino**, for their availability, their time and their teaching,

Zhiyue Lin, for his advices during my stay in Chicago,

Kristina, Lubomyr, **Gabriella**, **Chang**, **Tim**, **Meghan**, **Jordan** and **Chrissy**, for their precious help**.**

INTRODUCTION

Esophageal manometry has been used in humans since the early 1950s (2-4). The first measurements of esophageal pressure were provided by balloon-tipped catheters containing a small amount of air, which were introduced into the lower esophagus.

Subsequently, the water-perfused system (conventional manometry) was developed with catheters composed of a bundle of thin polyvinyl tubes with side holes, positioned at 3-5 cm intervals, providing point pressure measurements (Figure 1). Esophageal contractions that occlude the lumen interfere with the continuous low rate (but high pressure) flow through the channels and therefore raise the pressure in the corresponding channel. This pressure information is continuously monitored and transmitted to a recorder (Figure 2).

The limitations of the water-perfused systems are that the differences between vertical catheter tip position and pressure transducer can significantly influence the measured pressure and air contained in the fluid column can dampen the recording (5). Furthermore, much information is lost or missing given the widely spaced side-holes and because pressure is only recorded in one radial orientation of the catheter circumference. The station pull-through technique was introduced by Code and colleagues in 1956 to improve on this (6). Thus, the catheter was pulled gradually across the esophagogastric junction (EGJ) to evaluate its entire length and the maximum generated pressure. This maneuver, however, is time-consuming, not well tolerated, potentially affects EGJ pressure, and cannot be used to assess

sphincter relaxation or movement (7). This problem was ameliorated by Dent, who introduced a perfused sleeve sensor in 1976 that detects the highest pressure along its length and allows continuous measurement of the maximum EGJ pressure (8). The sleeve length is generally 6 cm in adults, although EGJ movement may exceed that length during reflux events or esophageal shortening during spasm. Conventional water-perfused manometry entails a catheter with 4 to 8 sensors including a sleeve sensor (9).

Figure 1. Illustration of different extrusions used for conventional water-perfused manometry catheters.

Picture from the personal collection of Dr Kahrilas, Northwestern University, Chicago.

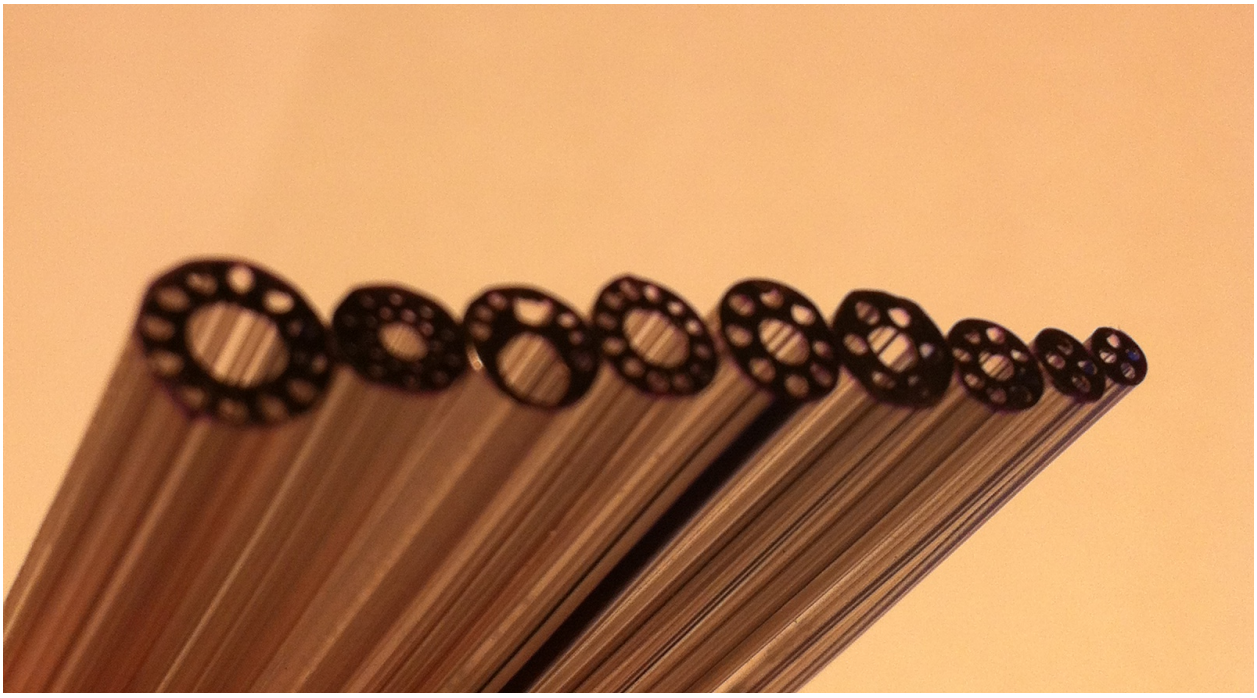

Figure 2. Example of a manometric study with a conventional water-perfused manometry.

Schematic representation of the manometry catheter positioned in the esophagus, with 5 pressure records along the esophagus and the Dent sleeve positioned within the EGJ. The resulting tracing mode recording is illustrated (Figure courtesy of Dr Pandolfino, Northwestern University, Chicago).

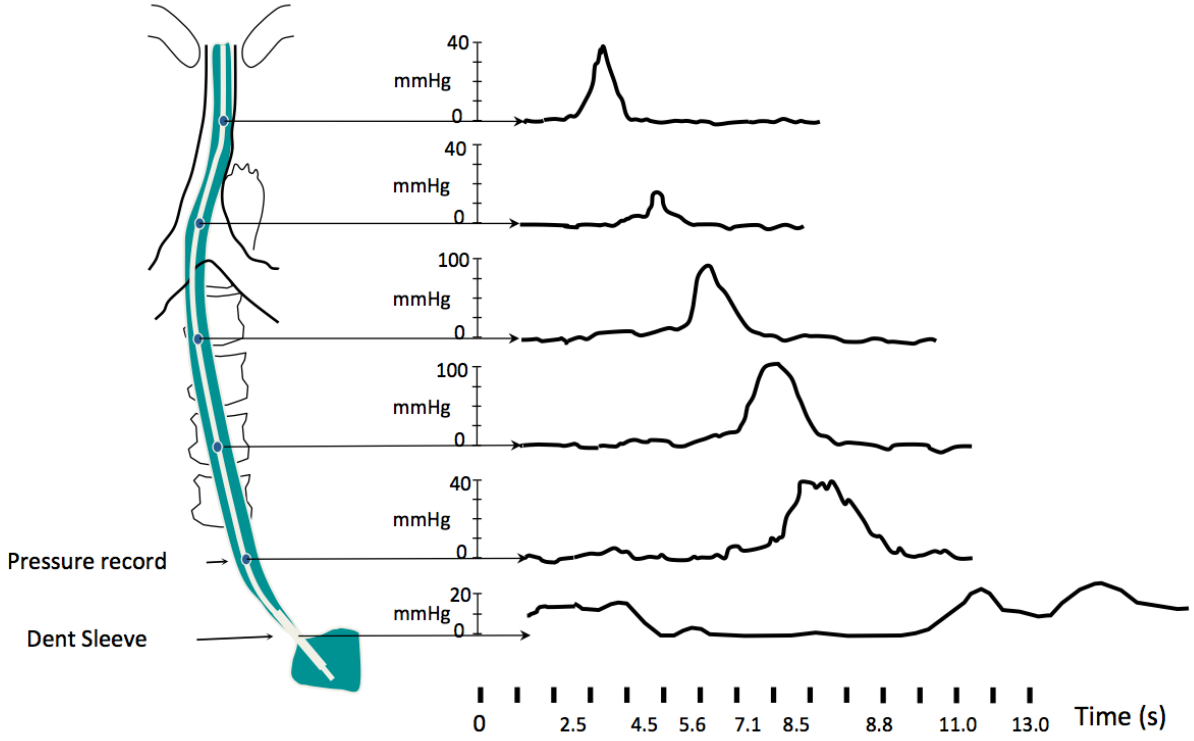

Although there have been numerous technical advances in conventional manometry, multiple maneuvers and need for catheter movement for EGJ measurements prolong test time and increase the level of expertise needed to conduct the test accurately. Even in those with expertise, inter-observer agreement in the interpretation of manometric findings is poor (10). The association between manometric findings and symptom severity or disease course is also poor (11). Water-perfused systems are cumbersome and catheters are stiff

and uncomfortable. Moreover, the large distance between sensors produces an information gap and may not detect important findings.

Initially described by Clouse and Staiano (12,13), high-resolution manometry (HRM) with esophageal pressure topography (EPT) circumvents many of the limitations of conventional manometry by utilizing enhanced spatial pressure resolution and data visualization. The evolution of the technical aspect of manometry allows the development of novel metrics to quantify the distinct aspects of the esophageal function and permit the determination of classifications to better understand the pathophysiology and to propose to the patients the best available therapeutics.

REVIEW OF LITERATURE ON HIGH RESOLUTION MANOMETRY (HRM)

1) Technical aspects of esophageal high resolution manometry

a) Pressure sensors

The concept of high resolution manometry (HRM) is to provide a sufficient number of pressure sensors within the esophagus to monitor intraluminal pressure as a continuum along the entire length of the esophagus. HRM probes are comprised of 18 to 36 pressure sensors depending on the company that commercialize these devices (Given Imaging, MMS, or Sandhill). Pressure sensors are water-perfused or solid-state pressure sensors: 1) Water-perfused pressures sensors were initially used for HRM. 2) Solid-state sensors consist of strain gauge transducers (MMS, Sandhill) or TactArray™ devices, a proprietary transducer technology (Given Imaging). For strain gauge transducers, pressure is measured unidirectionally whereas it is measured circumferentially (360° around with averaged pressure) for TactArray™ devices.

The Given Imaging HRM catheter consists of 36 pressure sensors spaced 1 cm apart (Figure 3) whereas the MMS consists of 36 unidirectional strain gauge pressure sensors spaced at 1 cm interval and the Sandhill probe consists of 32 pressure sensors: from the distal to the proximal extremity 15 sensors spaced at 1 cm apart, 8 sensors spaced at 1.5 cm and 9 sensors 1 cm apart.

Figure 3. Picture of the standard HRM catheter, by Given Imaging.

Illustration of the Given Imaging standard HRM catheter, showing the 36 pressure sensors rings disposed each centimeter along the catheter. Each ring contains one TactArray™ device that averages the pressure at each centimeter.

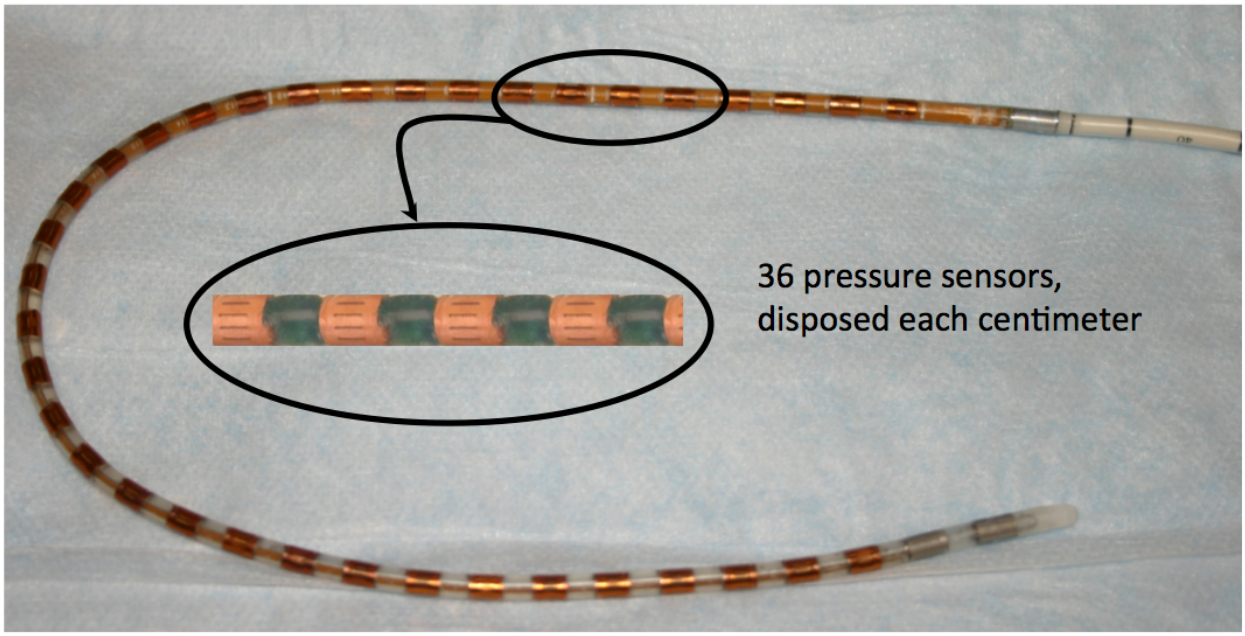

In all cases, the probe is connected to a recording unit and a computer (via a pneumohydraulic pump in case of water-perfused pressure sensors).

b) Esophageal pressure topography (EPT)

The difference between conventional manometry and HRM is the quantity of information available for analysis. With conventional manometry, intraluminal pressures are analyzed from a set of two-dimensional tracings (Figures 2 & 4). Clouse *et al.* (12) hypothesized that more information could be extracted by considering spatial relationships of pressure data. They applied cubic spline interpolation between pressure sensors. Thus,

they developed a three-dimensional plotting method connecting data in space as well as time and defined a topographic pressure plot, fundamental to high resolution interpretation and analysis (Figure 5).

Figure 4. Manometric study with a HRM catheter without EPT.

This figure illustrates the fact that HRM is the evolution of conventional manometry: using the tracing mode, the pressure recorded is similar to the pressure recorded using the conventional manometry. However, the resulting tracings are difficult to understand and interpret, due to the mixing curves (Figure courtesy of Dr Pandolfino, Northwestern University, Chicago).

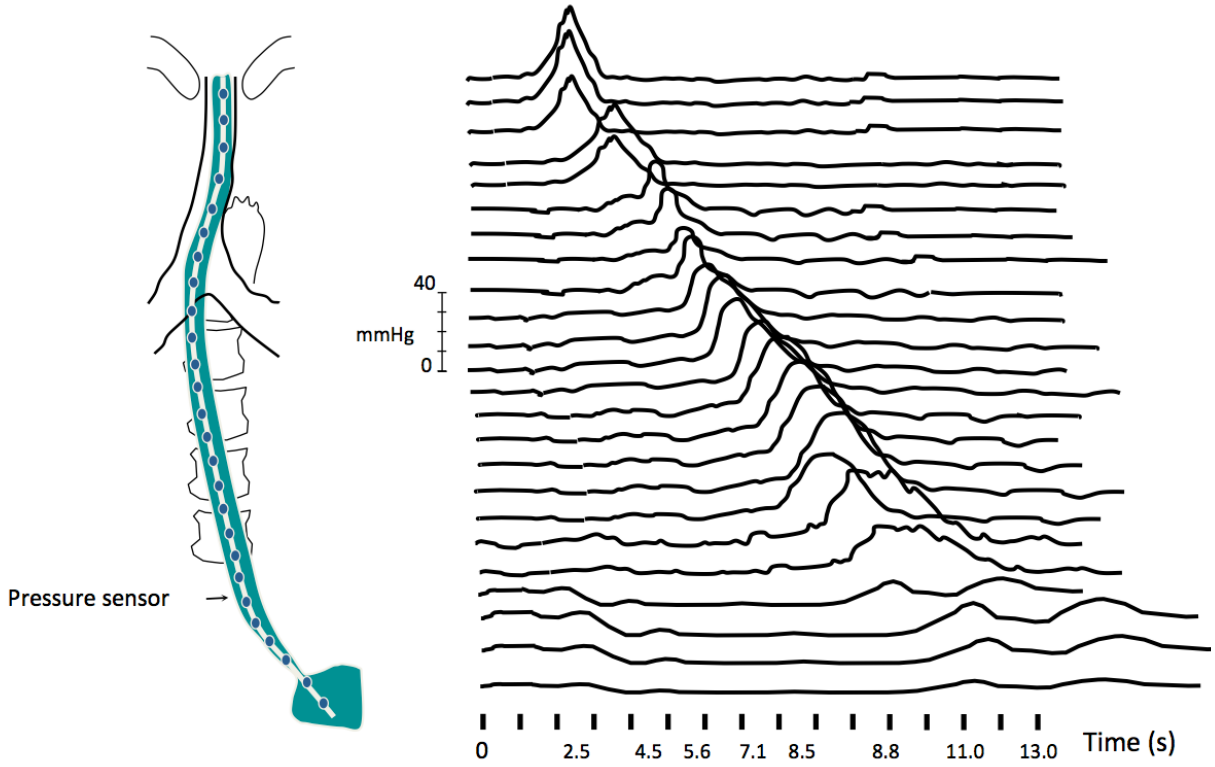

Figure 5. Description of the esophageal pressure topography.

Illustration of the development of esophageal pressure topography (12): in panel A, the raw data as recorded by the pressure sensors, with cubic spline interpolation between the records. Information is presented in 3 axes: time, distance from the nares and pressure. Panel B shows the topographic isobaric lines with different colors depending of the pressure value. Panel C presents the actual EPT mode.

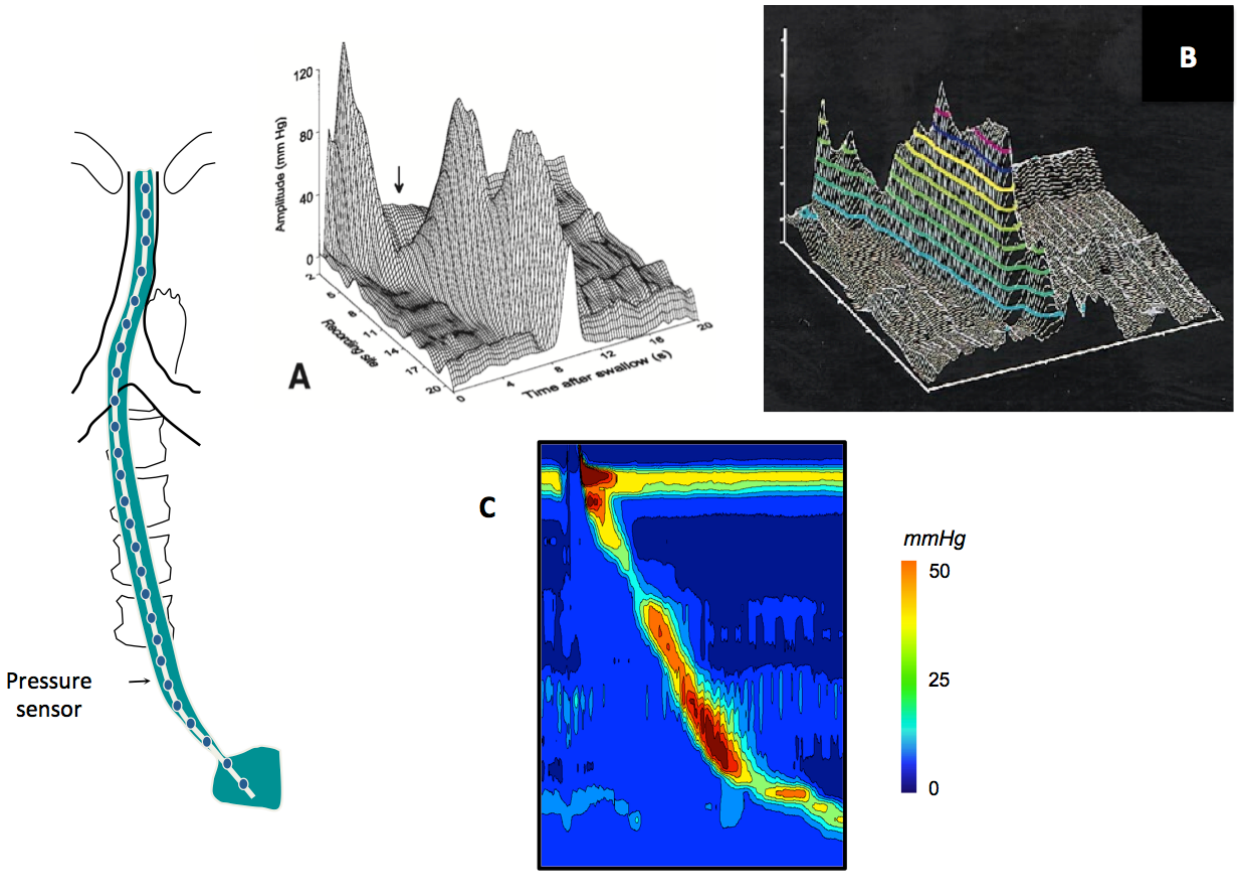

c) Manometry protocol

The manometry catheter is inserted transnasally and positioned to record from the hypopharynx to the stomach with at least 3 intragastric sensors. The catheter is fixed in place by taping it to the nose. A typical manometry protocol includes a 30-s baseline recording without swallowing and ten 5-ml water swallows in supine position. Normal values have been established with this protocol in 75 controls for Given Imaging system (14-17) and in 20 controls for the solid state sensors MMS system (18).

Some authors have proposed to perform HRM in an upright (or sitting) position reasoning that it is more physiologic than the supine position. Hence, normal values are also available for the upright position (19). Moving upright to supine resulted in a shorter transition zone, and a slower and more vigorous esophageal contraction. Comparing the diagnosis of esophageal motility disorders in 100 consecutive patients Roman *et al.* showed that the diagnosis was concordant in the supine and upright positions in 72 patients (20). Xiao *et al.* showed that changing position elicited a significant change in diagnosis in about 10% of studies (21). Later on, it will be important to remember that the Chicago classification for esophageal motility disorders is intended for use with studies done in the supine position.

Different physiological challenges including different bolus viscosity and high volume (10 ml and 20 ml water swallows) have been proposed to increase diagnostic yield, especially in patients with dysphagia. Basseri *et al.* showed that an apple sauce challenge increased

the identification of classifiable motor disorders in a series of 41 patients with dysphagia (22). Similarly, the percentage of ineffective motility was increased with bread swallows compared to water swallows in one study (23). On the other hand, Daum *et al.* noticed an increased percentage of effective contractions with bread swallows in patients with non-erosive reflux disease (24). Only patients with erosive reflux disease failed to respond to physiologic challenge of solid bolus. Sweis *et al.* established normal values for solid swallows (bread) and noticed a lower proportion of peristaltic swallows with solid than liquid in controls (19). Multiple water swallows might also be used as physiologic challenge (24). The patient is provided with 200 ml of water to drink within 30 s using multiple swallows. Recently, Xiao *et al.* (21) showed that provocative bolus challenges with viscous liquid and marshmallows increased the detection of EGJ outflow obstruction (see below: definition of esophageal motility disorders).

In summary, performing manometric evaluations in both supine and upright positions with provocative swallows may increase the yield of standard HRM technique.

2) Analysis of esophageal motility in EPT

Specific HRM metrics have been developed to analyze EPT plots. Each of these parameters has been developed to assess a specific function of the esophagus at rest, during the deglutitive process or after swallowing. Parameters described in this section are illustrated in Figure 6.

Figure 6. HRM parameters.

EPT of a swallow with basic HRM parameters, permitting to classify the esophageal motility.

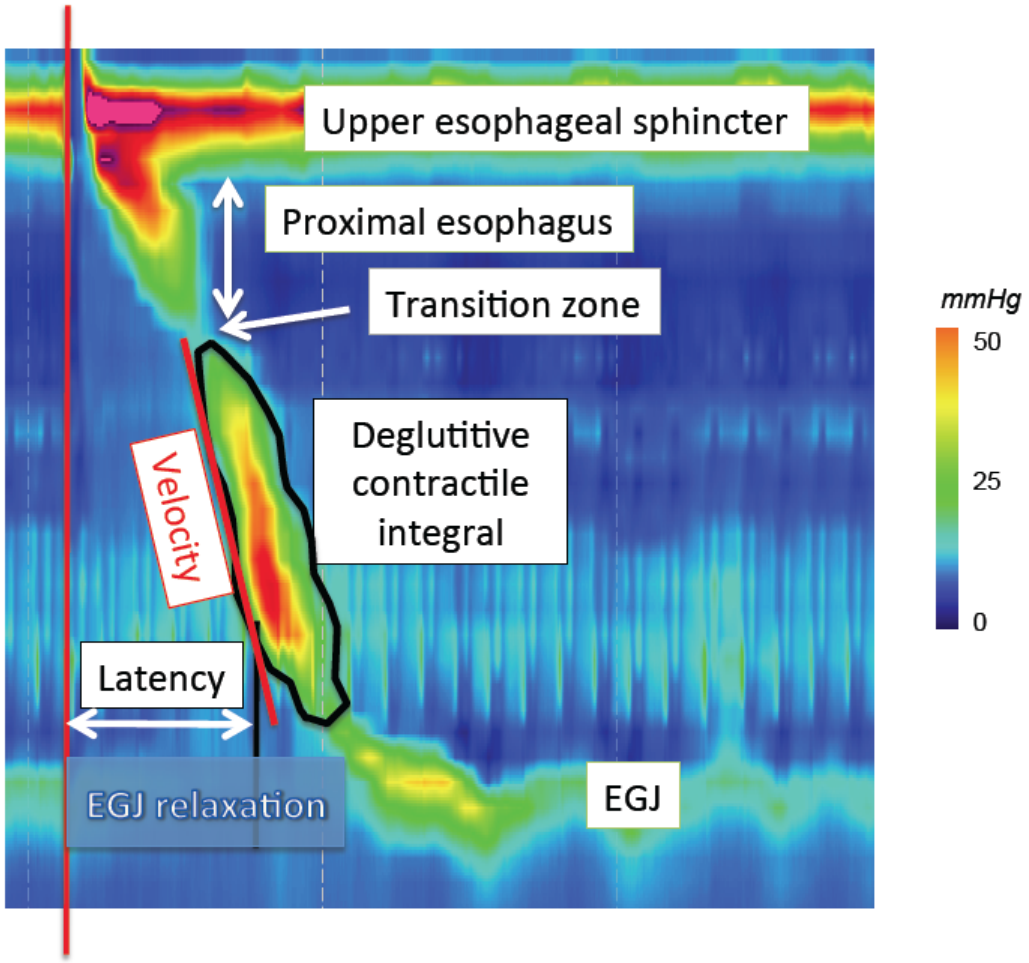

a) Esophagogastric junction (EGJ)

EGJ is the portion of the esophagus that is the most studied in the literature (15,17,25-38).

EGJ morphology evaluated in EPT is composed of the lower esophageal sphincter (LES) and crural diaphragm (CD), which are usually superimposed. However in the case of

hiatal hernia, two high pressure zones (HPZs) can be distinguished corresponding respectively to LES and CD. Bredenoord *at al.* noticed an intermittent separation of the LES and CD in GERD patients using EPT (28). Further Pandolfino *et al.* proposed to classify EGJ in 3 types (32). Type I is defined as an absence of separation between LES and CD; type II as a minimal LES-CD separation (< 2cm); and type III as a LES-CD separation > 2 cm. The inter observer agreement to classify EGJ morphology was moderate in the only study in which it was tested (20).

Several EPT metrics have been proposed to assess EGJ relaxation: the single-sensor nadir pressure, the integrated relaxation resistance, the 3-s nadir eSleeve pressure, the 1-s integrated relaxation pressure (IRP) and the 4-s IRP (15). These metrics are calculated using an eSleeve measurement after the demarcation of the proximal and the distal border of the EGJ. The 4-s IRP had the best sensitivity and specificity to diagnose achalasia, and was selected to assess EGJ relaxation. Moreover, the term 'IRP' now implies '4-s IRP' in the HRM literature. 4-s IRP is the lowest mean EGJ pressure for 4 contiguous or non-contiguous seconds in the 10-s period following upper esophageal sphincter (UES) relaxation (deglutitive window) (15). A mean IRP (10 swallows) greater than 15 mmHg is considered as abnormal using the Given Imaging system (95^{th} percentile).

Normal values for EGJ resting pressure have been established for the Given Imaging system in 75 controls (15,39) and for the MMS solid state sensors in 20 controls (18) (Table 1).

Normal values are specific for sensors types and arrays with marked differences between devices.

Table 1. Normal values for IRPs using different HRM systems.

	Given Imaging (Mean ± SE)	***MMS (Mean ± SD)***
1s-IRP (mmHg)	6.7 ±0.3	22.47 ±7.85
4s-IRP (mmHg)	8.6 ±0.4	25.90 ±7.68

b) Esophageal peristalsis and contractions

1 Contraction architecture

EPT allows a topographic characterization of esophageal contractions. Clouse first distinguished 3 to 4 segments in the contraction wave with 2 to 3 troughs respectively (13,40). Two troughs were identified, a proximal one and a distal one. A third trough between the proximal and the distal one is sometimes present in controls and in patients. This middle trough is less prominent than the others. Some motility disorders may affect predominantly one of the segments: for instance Clouse noticed that nutcracker esophagus primarily affects the distal segment (40). Gyawali emphasized that high amplitude segment location might differentiate mechanical obstruction from functional obstruction in patients with elevated post deglutitive residual pressure across the LES (41). Thus, pressures shifted to the second segment with mechanical obstruction and to the third segment in the

functional obstruction. Moreover, among patients with non-cardiac chest pain, a shift in contractile vigor to the third segment was observed in acid sensitive subjects (42).

The proximal trough is also known as the transition zone (TZ) as it might correspond to the transition between the striated muscle of the proximal esophagus and the smooth muscle of the distal esophagus (43-46). Complete bolus transit requires coordination between the proximal and the distal contraction. Even if the transition zone is physiological, a greater spatial separation as well as a delay between proximal and distal esophageal contraction might be more frequent in patients with dysphagia and/or GERD than in controls (44,46,47).

Finally integrity of the contraction may predict the occurrence of complete/incomplete bolus transit. Using impedance combined HRM, Bulsiewicz *et al.* determined that the smallest defect predictive of incomplete bolus transit measured 2.1 cm at a 20-mmHg isobaric contour and 3.2 cm at a 30-mmHg isobaric contour (48). Consequently, it has been proposed to assess the integrity of contraction at a 20-mmHg isobaric contour (49). A failed contraction is defined as minimal (< 3cm) integrity of the 20-mmHg isobaric contour distal to the transition zone. A weak contraction with a large break is defined as the presence of a break > 5 cm in length in the 20-mmHg isobaric contour. It was constantly associated with incomplete bolus transit in a series of 16 controls (49). A weak contraction with small break is defined as the presence of 2-5 cm break in the 20-mmHg isobaric contour and was variably associated with incomplete bolus transit in the same series of controls. The contraction is considered intact when the 20-mmHg isobaric contour is without large or small breaks.

The contraction architecture is also characterized by a contractile deceleration point (CDP) (50). This inflection point is identified as the point along the 30-mmHg isobaric contour at which propagation velocity slows demarcating the tubular esophagus from the phrenic ampulla. It has been recently shown that the segment of concurrent contraction during normal peristalsis progressively increased as peristalsis progressed, peaked at the CDP, and then progressively decreased (51). The clinical relevance of abnormal extent or timing of concurrent contraction still remains to determine.

Double peaks contractions were observed by Clouse in symptomatic patients (52). Sampath *et al.* demonstrated that these multipeaked contractions might be the consequence of a respiratory artifact (53). Respiration related movement of the contracted segment in relation to the stationary sensors could create the multipeaked pattern. However in case of high amplitude contractions these multipeaked contractions are not always synchronized with respiration (54). This suggests that multipeaked contractions might be a distinct entity with physiological and clinical significance.

Finally, esophageal shortening which is easily observed in EPT might be used to assess esophageal longitudinal muscle contraction as suggested by Mittal (55,56).

2 Metrics to assess esophageal contraction

Using EPT, the vigor of the contraction is not quantified only by focal amplitude as in conventional manometry but by the 'volume' of the contraction. The metric used is the

distal contractile integral (DCI): this is the product of the integral of amplitude times the duration times the length of the contraction (expressed as mmHg-s-cm) between the proximal and the distal trough (16). Only pressures above 20 mmHg are taken into account in DCI calculation to exclude intra-bolus pressure (IBP). Using the Given Imaging system, a value greater than 5,000 mmHg-s-cm is considered as abnormal and a value greater than 8,000 mmHg-s-cm is never encountered in healthy volunteers.

The velocity of the contraction is assessed using the contractile front velocity (CFV) (50). This is the slope of the tangent approximating the 30-mmHg isobaric contour between the transition zone and the CDP. A value greater than 9 cm/s is considered as abnormal.

The last metric is the distal latency (DL) (57); this corresponds to the duration of deglutitive inhibition that precedes esophageal contraction. The DL is the time interval between UES relaxation and the CDP. A DL shorter than 4.5 s is considered as abnormal and defines a premature contraction (58).

3) Primary role of HRM: evaluation of esophageal motility disorders

a) Definition of esophageal motility disorders

Esophageal motility disorders have been described and classified, using the previously described EPT parameters.

- *Achalasia*

Achalasia is characterized by impaired EGJ relaxation and an absence of normal esophageal peristalsis. An impaired EGJ relaxation is defined as a mean IRP ≥ 15 mmHg in EPT. Pandolfino *et al.* proposed to subdivide achalasia into 3 clinically relevant subtypes according to the pattern of esophageal contraction and pressurization (59). Type I achalasia (classic achalasia) is characterized by absence of esophageal contractions and absence of esophageal pressurization; type II (achalasia with pressurization) by absence of esophageal contractions and ≥ 20% swallows with panesophageal pressurization; and type III (spastic achalasia) by ≥ 20% spastic contractions with or without pan-esophageal pressurization. Type II achalasia is associated with the best response to either pneumatic dilation or Heller myotomy, type III with the worst response and type I with an intermediate response. These findings have been confirmed in 3 other majors studies (60-62).

The interobserver and intraobserver agreement for differentiating achalasia from non-achalasia patients using these criteria was very good to excellent (63). More variability was seen in agreement when classifying achalasia subtypes: the Cohen's κ for inter-rater reliability for type I varied from low moderate to very good (κ=0.44-0.84), ranged for type II from good to very good (κ=0.68-0.93) and was very good for type III (κ=0.86-1.0).

HRM might also be helpful for a better understanding of achalasia physiopathology. When occurring in type II achalasia panesophageal pressurization seems to be the consequence of a distinct motor pattern characterized by contraction of both sphincters and the intervening esophageal longitudinal muscle, but without lumen-obliterating contraction of the circular muscle in the inter-sphincteric span (55,64). In type III achalasia the esophageal muscularis propria appears thickened (55).

- *EGJ Outflow obstruction*

EGJ outflow obstruction is defined as impaired EGJ relaxation associated with some instances of preserved peristalsis (65). It was encountered not only in patients with previous fundoplication but also in patients without any previous surgery or mechanical EGJ obstruction (41,65). The distinction between EGJ outflow obstruction and an achalasia variant can be difficult (65,66) in cases of associated hypertensive peristalsis (54). The location of the high amplitude segment in the distal or in the middle segment might be predictive of the etiology (mechanical or idiopathic) of EGJ obstruction (66).

- *Diffuse esophageal spasm*

Diffuse esophageal spasm (DES) was redefined in EPT (58). Simultaneous contractions appeared a heterogeneous entity. Using distal latency to define premature contraction

allows a more specific definition of DES compared to contractile front velocity (CFV). Thus, premature contractions were encountered in patients with DES or spastic achalasia. Pandolfino *et al.* proposed to define DES as the presence of at least 20% premature contractions (58).

- *Hypercontractile and hypertensive esophagus*

Hypertensive or nutcracker esophagus is defined as a mean DCI greater than 5,000 mmHg-s-cm in a context of a normal CFV (14). Hoshino *et al.* demonstrated that the threshold value of 8,000 mmHg-s-cm was more clinically significant than 5,000 mmHg-s-cm and was more frequently associated with chest pain and dysphagia (67). It was then proposed to define hypercontractile esophagus as the presence of at least one contraction with a DCI greater than 8,000 mmHg-s-cm (54). As these high DCI contractions were frequently multipeaked, it was suggested to nickname this disorder "jackhammer esophagus".

- *Weak, frequent failed and absent peristalsis*

Weak peristalsis was defined as the presence of more than 20% of contractions with large breaks or more than 30% of contractions with small breaks (49). It was more frequently

observed in patients with unexplained dysphagia than in controls whereas this motility disorder remains borderline normal.

Frequent failed peristalsis was defined as more than 30% of contractions with absent peristalsis and absent peristalsis as 100% of absent contractions.

b) The Chicago Classification of esophageal motility disorders

After having determined EPT metrics and quantified the normative data, the first priority was to classify the esophageal motility disorders (achalasia, esophageal spasm…) into a widely accepted classification. The Chicago Classification is the resulting classification of esophageal motility disorders in EPT, and excludes the evaluation of EGJ as an antireflux barrier. This classification is intended for patients without previous gastrointestinal surgery and currently does not include the evaluation of pharynx, UES, or proximal esophageal segment (68,69). The first iteration was published in 2008 (14). Through the work of the Chicago group and the international HRM Working Group this classification evolved and a second iteration was published in 2009 (39). Finally, after the meeting of the international HRM working group in Ascona, Switzerland, in April 2011, a new iteration of the classification has been proposed taking into account the most recent publications and was summarized by Bredenoord *et al.* in 2012 (68).

EPT metrics are applied to score individual swallows and a decision algorithm permits the classification of the motility disorders. The analysis of esophageal motility disorders is focused firstly on normal or impaired EGJ relaxation and then on swallow score. Impaired EGJ relaxation, defined as an IRP greater than the upper limit of normal, is encountered in achalasia and EGJ outflow obstruction. Other esophageal motility disorders are subdivided into motility disorders that are never observed in normal individuals (absent peristalsis, DES, hypercontractile esophagus) and peristaltic abnormalities, which are defined by exceeding statistical limits of normal (rapid contraction, hypertensive peristalsis, weak peristalsis, frequent failed peristalsis).

Recently, Lin, et al have developed a classification and regression tree (CART) model (70) to interpret the EPT metrics in an automated mode. His findings were that IRP cutoffs suggested by the CART model ranged from 10 to 17 mmHg. In consequence, IRP should not been viewed as a dichotomous value and thresholds can be modified to compensate for the associated esophageal body contractility (71). In a series of 100 consecutive patients the inter observer agreement was good to diagnose motility disorders with the classification of 2009 (20).

c) Comparison of HRM with esophageal conventional manometry

Few data are available concerning the comparison between HRM and conventional manometry for esophageal motility disorders: both examinations were realized in the same patient in only one study (25), focused on EGJ evaluation. Fifty-five patients underwent HRM 30 minutes after conventional manometry. There was no significant difference in measurement of LES resting pressure between the 2 techniques. However, the authors emphasized the tendency to overestimate overall and abdominal LES length with HRM.

Sadowski *et al.* compared 20 patients who underwent conventional manometry to 21 patients who underwent HRM (72). The main finding was that total procedure time was reduced with HRM compared to conventional manometry (30.7 min vs. 41.8 min, $p<0.05$). No significant difference was observed in the discomfort scores reported by the patients or in study quality.

Tracing and EPT analysis methods were compared in different studies using water-perfused HRM. Clouse found that the diagnostic agreement was 88.2% between the 2 methods in a population of 220 patients (52); conventional analysis could not identify 6 achalasia patients and 8 patients with incomplete LES relaxation. In a series of 95 barium swallows with concurrent esophageal videofluoroscopy and manometry, Fox showed that EPT was more accurate than conventional tracings to predict abnormal bolus transit (73). Some types of motor dysfunction including localized disturbances of peristalsis and abnormal

movement of LES during esophageal spasm were detected only by EPT analysis and not by conventional analysis or radiography. However in another study, the agreement to detect ineffective motility was very good between the 2 methods (κ coefficient from 0.79 to 0.90, depending on the bolus viscosity and the body position) (23).

4) Diagnostic role of esophageal HRM beyond the motility disorders

According to an AGA technical review the only established role for manometry in GERD was the exclusion of 'motor disorders as a cause of the continued symptoms' (1) and in other specific medical conditions (esophageal or not). However we should qualify this statement in view of recent developments in EPT interpretation recently developed to assess these specific conditions.

a) Gastro-esophageal reflux disease (GERD)

HRM might be helpful to better understand GERD physiopathology. It provides a better assessment of EGJ anatomy and physiology. Bredenoord *et al.* showed that LES-CD separation was associated with reflux occurrence (28). Cardiovascular compression, identified in healthy volunteers, might limit the spread of gastroesophageal reflux (74).

Transient lower esophageal sphincter relaxations (tLESRs) play an important role in GERD genesis in patients with or without hiatal hernia. Different studies emphasized that HRM might be more accurate than conventional manometry to detect tLESRs (75-77). HRM and perfused manometry with a Dent sleeve probe were recorded simultaneously in 2 of these studies (76,77). Criteria including nadir pressure, relaxation duration, percentage of relaxation and 4s-IRP pressure have been proposed to diagnose tLESRs in EPT (76). According to an ROC curve analyses, relaxation duration appeared to be the most discriminant parameter. Other criteria such as diaphragmatic inhibition, esophageal shortening (78) and UES relaxation (79,80) were frequently encountered in tLESRs and are easy to identify with HRM. Furthermore the interobserver agreement to detect tLESRs was almost perfect with HRM (κ=0.83) whereas it was only fair with conventional manometry (κ=0.38) (76). Terminating motor events were also studied in tLESRs using EPT: secondary peristalsis was the most common (81). Bredenoord *et al.* did not observe differences between tLESRs associated with reflux and those without (82). However a greater trans-sphincteric pressure gradient was noted in tLESRs associated with acid reflux than in those without reflux (83) and was greater in GERD patients than in controls (84). In patients with achalasia, tLESRs were characterized with diaphragmatic inhibition and esophageal shortening (85).

Ineffective esophageal motility (IEM), defined as a swallow response associated with poor bolus transit in the conventional line tracing (CLT) manometry, is believed to play an important role in GERD (86). A recent study (87) showed that the manometric correlate of

IEM in EPT is a mixture of failed swallows and weak swallows with breaks in the middle/distal troughs. A DCI value <450mmHg-s-cm can be used to predict ineffective swallow previously defined in CLT. IEM can be defined by >5 swallows with weak/failed peristalsis or with a DCI <450mmHg-s-cm.

Finally, the study by Hoshino (88) proposed a novel EPT metric (LES pressure integral) to quantify the strength of the EGJ as a reflux barrier at rest, utilizing the DCI tool. We recently worked on a modified version of the LES pressure integral that normalizes for respiratory rate and is referenced to intragastric pressure would better characterize the barrier function of the EGJ. This novel metric may be useful in distinguishing patients with functional heartburn from those with refractory GERD (Article in press, NMO 2014).

b) Other specific medical conditions

All patterns of disordered esophageal motility were observed in patients with eosinophilic esophagitis (EoE) (89-91). Moreover, pan-esophageal pressurization might be more frequent in patients with EoE than in controls (90,91). Scleroderma has also been characterized in EPT with esophageal dysmotility observed in 2/3 of patients (92).

HRM has also been used to study motility in different pulmonary conditions; esophageal motility disorders were found more frequently encountered in lung transplant

candidates than in controls in EPT (93). Decrease of esophageal pressure and increase of end inspiratory UES and EGJ pressures were observed during obstructive sleep apnea (94).

Other studies focused on the effect of anesthesia on upper and lower esophageal sphincters function (95-99). Propofol increased LES pressure whereas remifentanil decreased LES pressure. Both drugs decreased UES pressure.

c) Specific surgical conditions

HRM studies have been done in different groups of patients with fundoplication or bariatric surgery.

- Fundoplication

First of all, esophageal manometry is recommended in all patients before fundoplication. Indeed, some patients with achalasia have a clinical presentation of GERD, as it has been emphasized by the Amsterdam group using HRM (100).

In HRM studies done before and after fundoplication (83,101,102), the postsurgical condition was characterized by a disappearance of a double peaked HPZ at the EGJ level (101) as expected but, moreover, incomplete LES relaxation was noticed after fundoplication as well as increased IBP (102).

HRM has been proposed to evaluate patients with recurrent GERD after fundoplication. Ineffective motility, hypertensive LES, impaired LES relaxation (103) and dual HPZ (104) have been identified as potential explanations for symptoms. Finally, partial and complete fundoplication had been compared; axial EGJ pressure profile was less affected in patients with partial fundoplication than in those with complete fundoplication (105).

- Laparoscopic adjustable gastric band (LAGB)

HRM might be also of interest in patients with LAGB. Esophageal peristalsis was characterized with frequently repetitive contractions (106) and an increase in distal esophageal peristaltic pressure after band inflation (107). Different patterns of contractions were observed in LAGB patients associated with dysphagia: absent peristalsis, pseudo-achalasia, EGJ outflow obstruction, hypotensive peristalsis, and normal peristalsis (108,109). Different pressurization pattern were also observed: pan-esophageal pressurization, hiatal hernia pressurization or gastric pouch pressurization (108,110-112). These patterns were observed after regular water swallows (108) or semi-solid stress barium protocol (2 consecutive spoonful of barium-soaked porridge followed immediately by drinking of up to 80 ml of liquid barium via a straw) (110-112).

INTRODUCING THE 3D HRM FOR THE ASSESSMENT OF EGJ CHARACTERISTICS

Review of the literature showed that conventional manometry and HRM permitted the development of a variety of manometric methodologies and metrics to understand the motility of the esophagus and to quantify EGJ characteristics. However, the anatomy in the area of the EGJ is complex and intraluminal manometry recordings detect pressure signals referable both to intrinsic esophageal structures and to adjacent extrinsic structures impinging on the esophagus. Each have distinct sphincteric mechanisms within the EGJ (113). The dominant pressure signals detected near the EGJ are attributable to the LES, the CD, the lower thoracic aorta and the heart. Both previously described technologies were unable to distinguish between theses components of EGJ pressure.

When analyzing EGJ characteristics as a reflection of its competence against reflux (114), a station pull-through protocol was used as the standard to determine the length of the EGJ HPZ and to localize the RIP, defined as the location at which inspiratory pressure deflections changed from positive (abdomen) to negative (chest) (115). Surgeons have utilized the position of the RIP in relation to the HPZ to determine the intra-abdominal component of the EGJ as a predictor of fundoplication efficacy (116). However, the significance of HPZ length and intra-abdominal length have not gained wide acceptance in the gastroenterology community as evident in a recent AGAI Position Statement concluding

that 'The current role of manometry in gastroesophageal reflux disease (GERD) is to exclude motor disorders as a cause of the continued symptoms' (1). In essence, it was concluded that the quantitative assessment of EGJ pressure morphology achieved with conventional manometry lacked sufficient validation to be useful in clinical management.

On the other side, during deglutition, the objective quantitative measurement of EGJ relaxation, the IRP, permits to distinguish between normal and abnormal EGJ relaxation (117). As presented in the review, the IRP utilizes an electronic sleeve (eSleeve) paradigm to calculate the average pressure during the four seconds of most complete EGJ relaxation in the post-deglutitive period. This measurement was validated as a more accurate measure of EGJ relaxation than prior methods and currently has been adopted as a key measurement in the new HRM classification schemes for esophageal motor disorders (118). Although the IRP is conceptually sound as a metric of EGJ relaxation, it is a very technology-sensitive measurement and normative values of the metric must be linked to the assembly with which they were derived. In work published thus far, standard HRM (360 HRM, Given Imaging, Los Angeles) has been utilized.

Recently, the 3D-high resolution manometry (3D-HRM) assembly (Given Imaging, Duluth, GA) has been developed with the potential to greatly simplify the assessment of EGJ pressure morphology (119) and physiology. The 3D segment of the array permits high resolution recording both axially and radially while maintaining a stationary sensor position.

Consequently, 3D-HRM should allow for the measurement of EGJ parameters, as length, that were only possible with pull-through maneuvers in the past and these measurements can be made in real time permitting analysis of the respiratory and vascular effects. Moreover, data extracted from the 3D-HRM recording may allow differentiating pressure signals within the EGJ attributable to the intrinsic sphincter and to the surrounding elements. 3D-HRM preserves the individual pressure values of each radially dispersed sensor within the array.

The first published observations using the 3D-HRM assembly (119,120) suggest that the nadir pressure value at each axial level provide a higher fidelity recording of intraluminal pressure gradients and sphincter relaxation than do circumferentially averaged pressures on account of their being less influence of radial pressure asymmetries imparted by extrinsic structures. Illustrative of this, comparison between spatial pressure variation plots and relaxation pressures derived from circumferentially averaged pressures suggest a persistent high pressure at the hiatal center during a period that flow is known to be occurring (Figure 7) whereas this was not seen using the nadir radial pressure data. The above observations suggest that the 3D-HRM array using an analysis paradigm premised on finding the minimal radial pressure at each axial level (3D-eSleeve) should provide a representation of the luminal pressure gradient across the EGJ that is more relevant to predicting periods of trans-sphincteric flow.

Figure 7. EPT of a swallow from an asymptomatic patient with a standard HRM assembly.

Dots represent the same location in HRM and videofluoroscopy at times A, B and C. The synchronous videofluoroscopy shows that bolus is not present (red arrow) at time A, but shows that bolus is present (green arrow) at times B and C even though the pressure gradient suggests that this would be impossible.

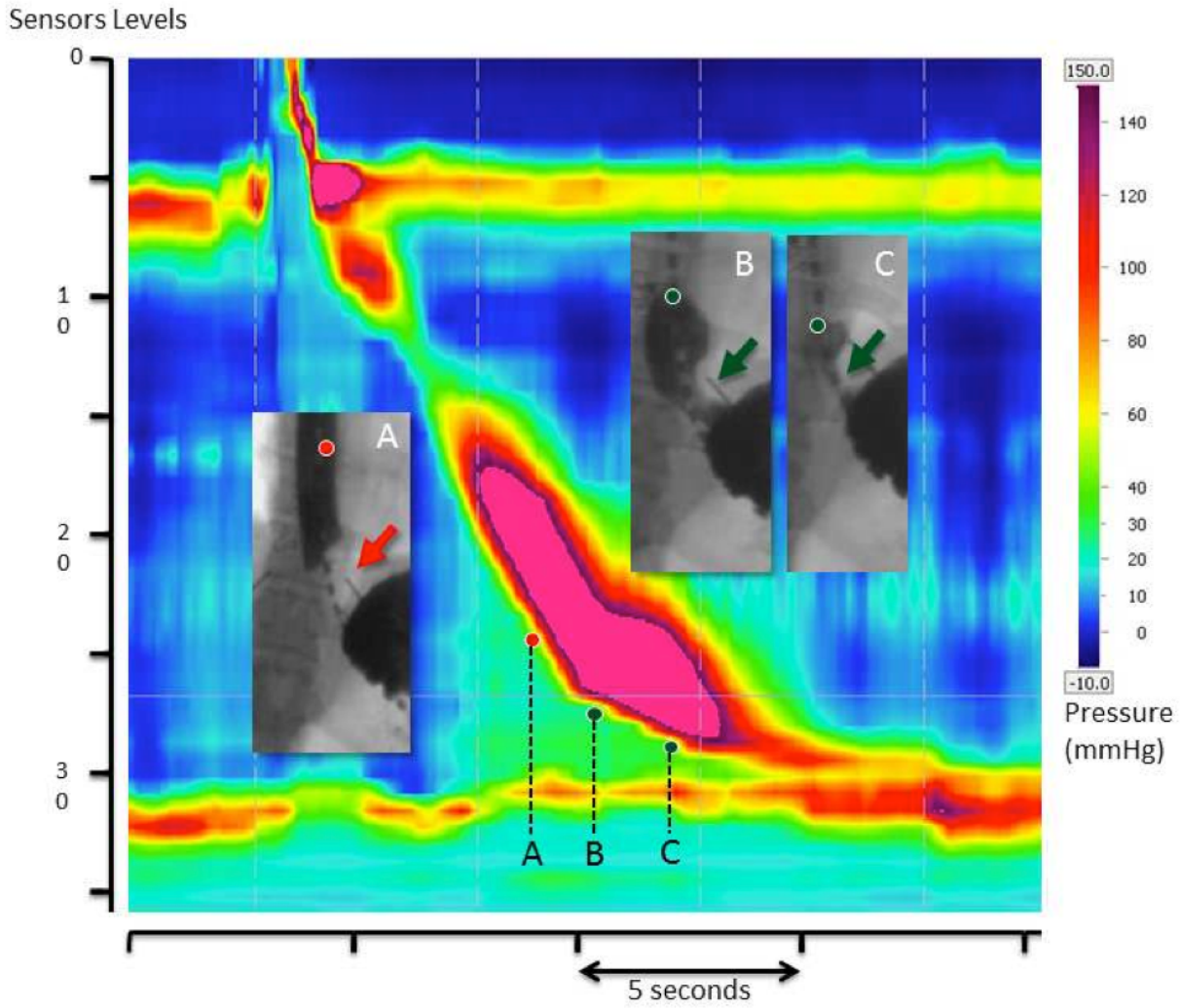

AIMS OF THE STUDY

We focused our studies on the analysis of the EGJ using 3D-HRM, in which the 3D segment of the array permitted high resolution recording both axially and radially within the EGJ. We studied the EGJ as an anti-reflux barrier at rest and during deglutition for the assessment of the coordinated relaxation of its different components:

- To describe the EGJ pressure morphology at rest, we compared measures of EGJ pressure morphology made with real time 3D-HRM to measures made simulating a conventional pull-through protocol and to define the pressure signatures of the diaphragmatic and LES pressure components within the 3D-HRM recording. This work is published: Nicodème F, Lin Z, Pandolfino JE, Kahrilas PJ. Esophagogastric Junction pressure morphology: comparison between a station pull-through and real-time 3D-HRM representation. *Neurogastroenterol Motil*. 25(9), e591–8 (2013).

- To assess the EGJ relaxation during deglutition, we tested the hypothesis that the 3D-HRM array using an analysis paradigm premised on finding the minimal radial pressure at each axial level (3D-eSleeve) should provide a representation of the luminal pressure gradient across the EGJ that is more relevant to predicting periods of trans-sphincteric flow using barium transit on fluoroscopy as the comparator. We also sought to adapt the IRP metric to the 3D-HRM array using the 3D-eSleeve principle (3D-IRP) and compare normative values obtained with this new paradigm to standard IRP calculations. This work is

published: Nicodème F, Pandolfino JE, Lin Z, Xiao Y, Escobar G, Kahrilas PJ. Adding a radial dimension to the assessment of esophagogastric junction relaxation: validation studies of the 3D-eSleeve. *AJP: Gastrointestinal and Liver Physiology*. 303(3), G275–80 (2012).

METHODS

1) Subjects

a) For the description of the EGJ pressure morphology at rest

Nine volunteers were recruited for this study. None of them had a history of prior gastrointestinal surgery, significant medical disease, or current use of medications for upper gastrointestinal symptoms. All subjects underwent a brief interview and examination and gave written informed consent. Dysphagia was assessed using the Impaction Dysphagia Questionnaire (IDQ, maximal score: 50; 95th percentile cutoff in controls: 2). Reflux symptoms were measured using the GerdQ (scale 0-18; positive for GERD if score ≥7) (121). The study protocol was approved by the Northwestern University Institutional Review Board.

b) For the assessment of the EGJ relaxation during the deglutition

Thirty-nine subjects were recruited during the two phases of the study. None of the subjects had a history of prior gastrointestinal surgery, significant medical disease or were currently utilizing medications for upper gastrointestinal symptoms. All subjects underwent a brief interview and examination and gave written informed consent. Dysphagia was assessed using the IDQ (maximal score: 50; 95th percentile cutoff in controls: 2). Reflux

symptoms were measured using the GerdQ (scale 0-18; positive for GERD if score ≥7) (121). The study protocol was approved by the Northwestern University Institutional Review Board.

2) Manometry assemblies

a) The standard HRM catheter

The standard HRM catheter was a 4.2 mm outer diameter solid-state manometric assembly with 36 circumferential sensors spaced 1 cm apart (Given Imaging, Duluth, GA). Each level sensor averaged the pressure signals from the 12 radially dispersed sensors into a single circumferential pressure value. The data acquisition frequency was 25 Hz. All pressure measurements were referenced to atmospheric pressure.

b) The 3D-HRM assembly

The 3D-HRM assembly was a 128-channel solid-state device incorporating a 9.0 cm 3D-HRM segment into an otherwise standard HRM array (Figure 8A). The 4.2 mm outer diameter assembly had the 3D-HRM segment positioned between 28 proximal and 4 distal standard sensing elements that were spaced 1 cm apart (119). Each standard sensor averaged the pressure signals from the 12 radially dispersed sensors into a single circumferential pressure value. The 3D segment was comprised of 12 rings of 8 radially dispersed independent pressure sensors with the rings spaced 7.5 mm apart. The

individual 3D sensing elements were 2.5 mm long and separated from the adjacent element by 5 mm. Consequently, the 9 cm 3D segment provided 96 independent pressure recordings with a radial resolution of 45° and an axial resolution of 7.5 mm (Figure 8B & 8C). The data acquisition frequency was 100 Hz.

Figure 8. Characteristics of the 3D-HRM assembly and resulting 3D-HRM views.

Panel A is a representation of the 3D-HRM catheter composed of the assembly of 32 standard HRM sensors and 12 levels of 8 radially dispersed sensors. The resulting image is a cylinder (Panel B) that can be unfolded for the 3D-HRM panoramic view (Panel C). Gray dots represent each pressure sensor in the panoramic view.

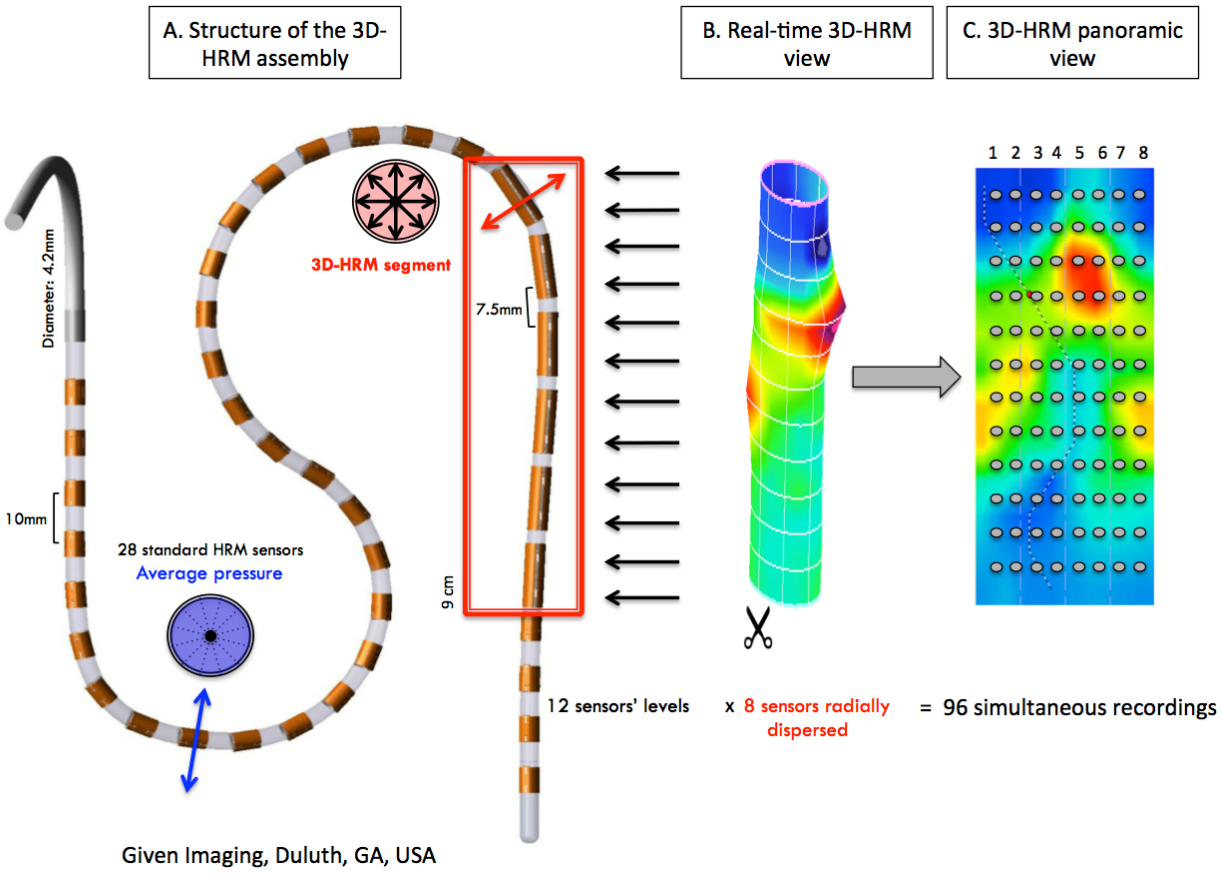

Prior to recording, each manometric assembly was calibrated at zero and 300 mmHg using the manufacturer's calibration chamber. The technical specifications provided by the manufacturer were that the accuracy of the individual elements of the 3D array were ±1 mmHg for the pressure range of 0-50 mmHg and ±1.5 mmHg in the 50-100 mmHg range.

3) Manometry protocols and data analysis

a) For the description of EGJ pressure morphology at rest

Manometry protocol

Studies were performed in the supine position after a 6-hour fast. The assembly was passed transnasally and positioned with the 3D-HRM segment straddling the EGJ. After a period of accommodation, five minutes of baseline recording was obtained during which the subjects were asked to breathe normally. A standard 10 water swallow protocol was obtained to verify that the subjects had normal motility according to the Chicago Classification (68).

The assembly was then repositioned with the 3D segment in the stomach and a station pull-through was obtained withdrawing the assembly at 5 mm increments with each station held for at least 30 seconds. The pull-through was done maintaining normal respiration, with the patient asked to minimize swallowing. The pull-through was continued until the 3D array had traversed the EGJ and the distance to the nares was recorded for each station.

Data analysis

Data were analyzed after thermal compensation using Manoview software (version 3.0, Given Imaging, Duluth, GA). Analysis subroutines were written to compare calculations of HPZ length, and the localization of respiratory inversion made with real-time 3D-HRM to the same measures made using simulations of conventional manometry from the pull-through protocol.

Four radially dispersed sensors within the 3D-HRM array (3, 6, 9, and 12 o'clock) were utilized for the simulation of conventional manometry during the station pull-through protocol. For each sensor, the upper and lower margins of the HPZ were defined by a 2-mmHg pressure increase relative to gastric pressure. The four length values were averaged to calculate the mean 'LES length', as described using conventional manometry, and a composite value was calculated as the extreme value of HPZ length. Respiratory inversion was defined as the axial position along the EGJ at which the positive pressure deflections associated with inspiration recorded in the abdomen change to negative deflections recorded in the chest. Pull-through data from the same four single sensors as for the determination of 'LES length' were used and the RIP was reported as the average of the four values.

For the real-time 3D-HRM definition of the HPZ, we determined the length characterized by a 360° circumferential pressure increase of at least 2 mmHg relative to gastric pressure as the proximal and distal limits (119). Measurements of sphincter length were made at rest and in the 5-second post-deglutitive period to capture the LES after-

contraction. The magnitude of sphincter pressure was also measured at each time as the 'maximum of the minimums' using the e-sleeve tool (122). Respiratory inversion was analyzed using the Manoview pressure inversion point tool ('PIP tool'). Using the 'PIP tool', the tracing progressively changed from a thoracic pattern to an abdominal pattern (Figure 9). Hence, respiratory inversion was also reported as the 'inversion zone' spanning the distance between these endpoints.

Figure 9. Characteristics of the RIP, using the 3D-HRM assembly.

Determination of the respiratory inversion zone using the 'PIP tool' of the Manoview software ('diamond shape' at 42.5 cm). The transition from a clearly thoracic pattern with inspiratory pressure decrement at 42 cm to a clearly abdominal pattern at 43 cm with a clear inspiratory augmentation occurred gradually, centered at 42.5 cm. In this example, the overall length of the zone was 0.9 cm, otherwise varying between 0.7 and 1.0 in the subject group as a whole.

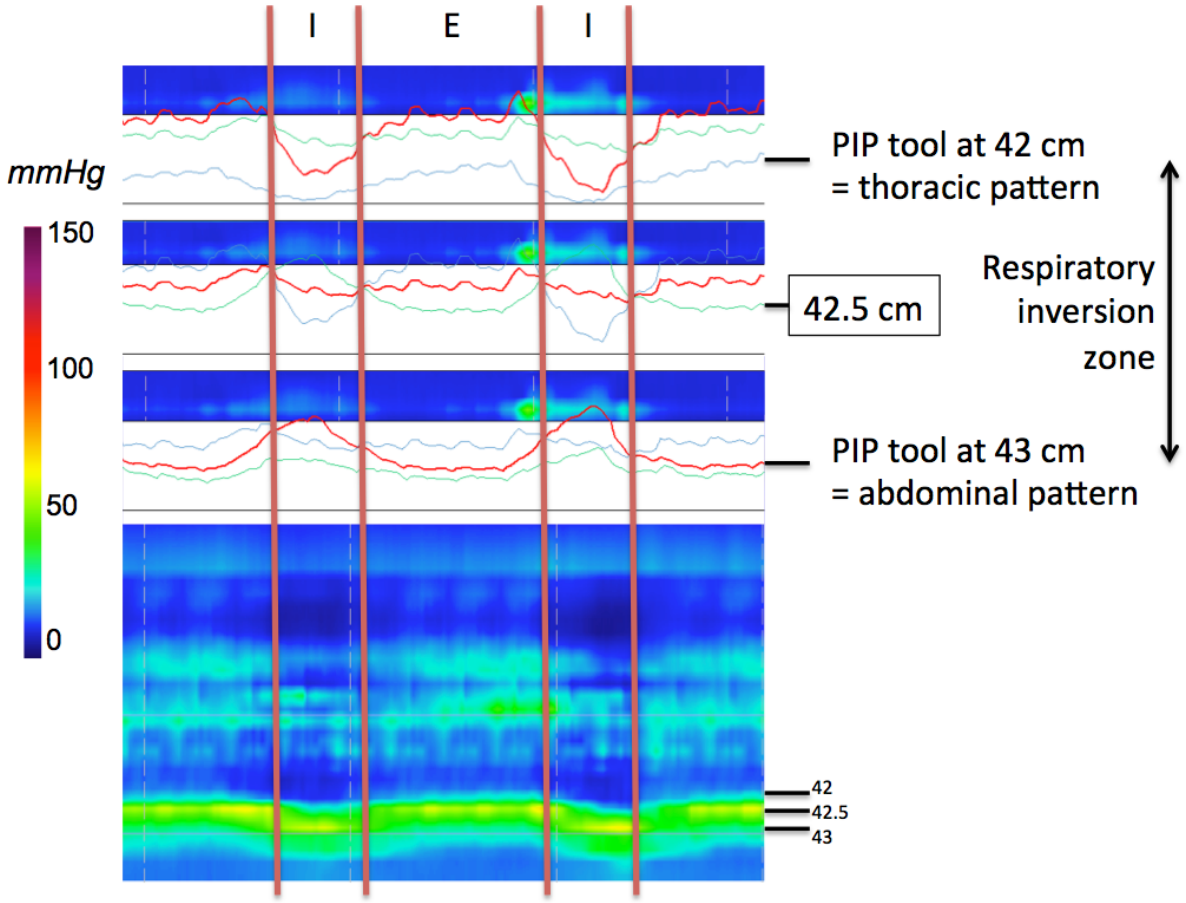

b) For the assessment of the EGJ relaxation during the deglutition

1. Phase I protocol: comparison of the IRP and 3D-IRP

Twenty-five subjects underwent manometric evaluation with both the standard HRM assembly and the 3D-HRM assembly in randomized sequence within a 30 minute time frame. Studies were performed in the supine position after a 6-hour fast and the subjects underwent a protocol that included ten 5 ml water swallows with each assembly. The assemblies were passed transnasally and positioned at the same location with at least 3 intragastric sensors in each case. During the 3D-HRM protocol, the swallow sequence was repeated twice: once with the 3D-HRM segment within the EGJ and once with the non-3D segment within the EGJ (Figure 10).

Figure 10. Positions of the HRM assemblies used for the calculation of IRP.

The standard HRM assembly is composed entirely of circumferential sensors (blue). The 3D-HRM incorporates a 9cm 3D segment (red).

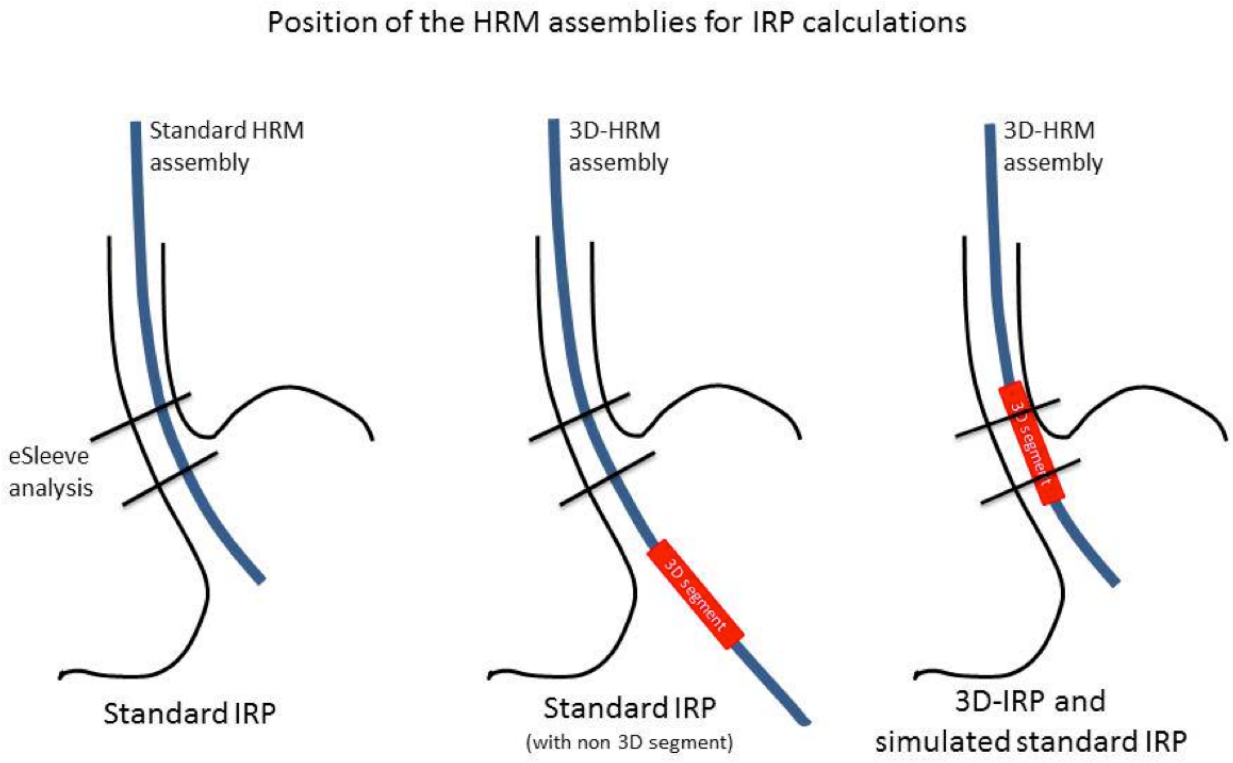

2. *Phase II protocol: assessment of accuracy for determining bolus transit*

Fourteen subjects underwent simultaneous 3D-HRM evaluation and videofluoroscopy after a 6-hour fast using a C-arm fluoroscope (Easy Diagnostics, Phillips Medical Systems, Shelton, CT). Subjects were shielded below the umbilicus with a lead apron, along with a lead collar for thyroid protection. The 3D-HRM assembly was positioned as in Phase I studies. The study protocol included recordings of two 5-ml barium swallows with the

barium injected with a syringe into the mouth and swallowed as one bolus. The interval between swallows varied from 20 to 40 seconds. During the recording, the subjects were supine on a fluoroscopy table. Real-time fluoroscopic images were recorded through a video module (ManoScanV™, Given Imaging) on the computer and synchronized with concurrent 3D-HRM recordings.

- eSleeve and IRP analysis paradigms

As applied with standard HRM, the eSleeve is an analysis tool that detects the greatest pressure within a specified segment of the recording, serving as a means for quantifying residual pressure during sphincter relaxation. The eSleeve domain is typically 4-6 cm in length and can be modified during analysis so that it encompasses the EGJ high-pressure zone. The IRP is derived from the eSleeve recording during the 10 s period after the swallow. The analysis routine finds and averages the 4 s within that post-deglutitive window with the lowest eSleeve pressure. The median for the IRP, determined from a set of 75 normal subjects was 7.9 mmHg with the upper limit of normal being 15 mmHg (15).

The 3D-HRM assembly was used to calculate IRP in three different ways: 1) exactly analogous to with the standard HRM by positioning the 3D-HRM segment within the stomach and utilizing the standard segment (Non 3D segment) of the hybrid assembly, 2) analogous to the method with the standard HRM but using the 3D-HRM segment to compute it (Figure 11A), and 3) using a novel 3D-IRP method (Figure 11B). The 3D-IRP method isolated the

minimal radial pressure at each axial sensor ring rather than using the average of the 8 sensors with the caveat being that selected sensors in adjacent sensor rings must be in proximity to each other. This concept was also incorporated into the eSleeve paradigm as the 3D-eSleeve.

Figure 11. Snapshot of pressure recordings in the 3D segment of the 3D-HRM assembly within the EGJ.

(A) Standard eSleeve generated with 12 independent pressure recordings. (B) 3D-eSleeve generated with 96 independent recordings (12 sensors levels x 8 radial sensors) utilizing the minimum radial pressure (3D-eSleeve) algorithm (Red dot is the maximum pressure of the 3D-eSleeve).

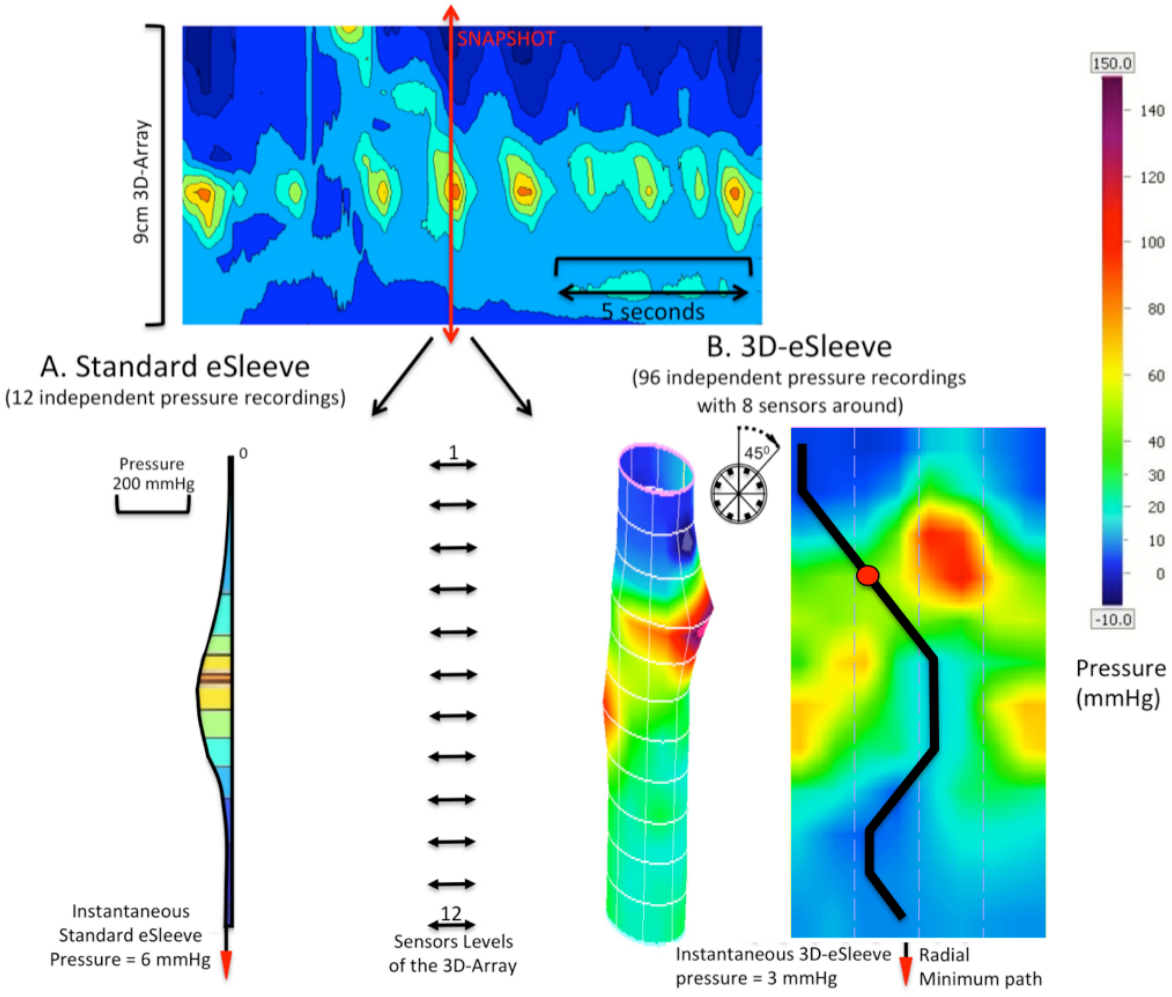

A β version of ManoView™ software (Given Imaging, Los Angeles, CA, U.S.A.) was used to calculate both IRP and 3D-IRP. MATLAB™ (MATLAB v. 2010b, The MathWorks Inc., Natick, MA, U.S.A.) programs were written to independently check these calculations and to assess the minimal number of radial sensors required to measure the 3D-IRP accurately. Simulations were done using eight sensors at 45°, four sensors at 90° [simulations with sensors #1, 3, 5, 7 and sensors #2, 4, 6, 8], 2 sensors at 180° [sensors #1 and 5], and a single sensor of the assembly. For the cases of 2 and 1 single sensor, we arbitrary selected the sensors but their position within the EGJ was unknown and consequently random, depending of the orientation of the assembly when it was passed transnasally.

- Comparing flow permissive time to bolus transit

A custom MATLAB™ program was written to calculate flow permissive time (FPT) as a derivative of: 1) the esophageal body pressure 2 cm proximal to the EGJ eSleeve domain, 2) intragastric pressure at least 2 cm distal to the EGJ eSleeve domain, 3) eSleeve pressure, and 4) 3D-eSleeve pressure (Figure 12). The FPT was defined as the time during which esophageal pressure was greater than eSleeve pressure (117). The presence or absence of bolus transit on the corresponding fluoroscopic images was coded with dichotomous values for each 0.1 s and this was compared using a 2 x 2 contingency box with the FPT. The sensitivity and specificity of the FPT utilizing either the standard eSleeve or the 3D-eSleeve to

predict bolus transit were compared. The determination of bolus transit and FPT were performed in a blinded fashion by two separate investigators.

Figure 12. Example of calculation of the flow permissive time (FPT) with the 3D-HRM assembly.

FPT was defined as the time period, consecutive or not, when the esophageal pressure was higher than the EGJ eSleeve pressure which in turn was higher than the gastric pressure. In this figure, standard FPT is present when esophageal pressure is greater than the standard eSleeve pressure, which in turn was greater than the gastric pressure; 3D-FPT is present when esophageal pressure is greater than the 3D-eSleeve pressure, which in turn was greater than the gastric pressure.

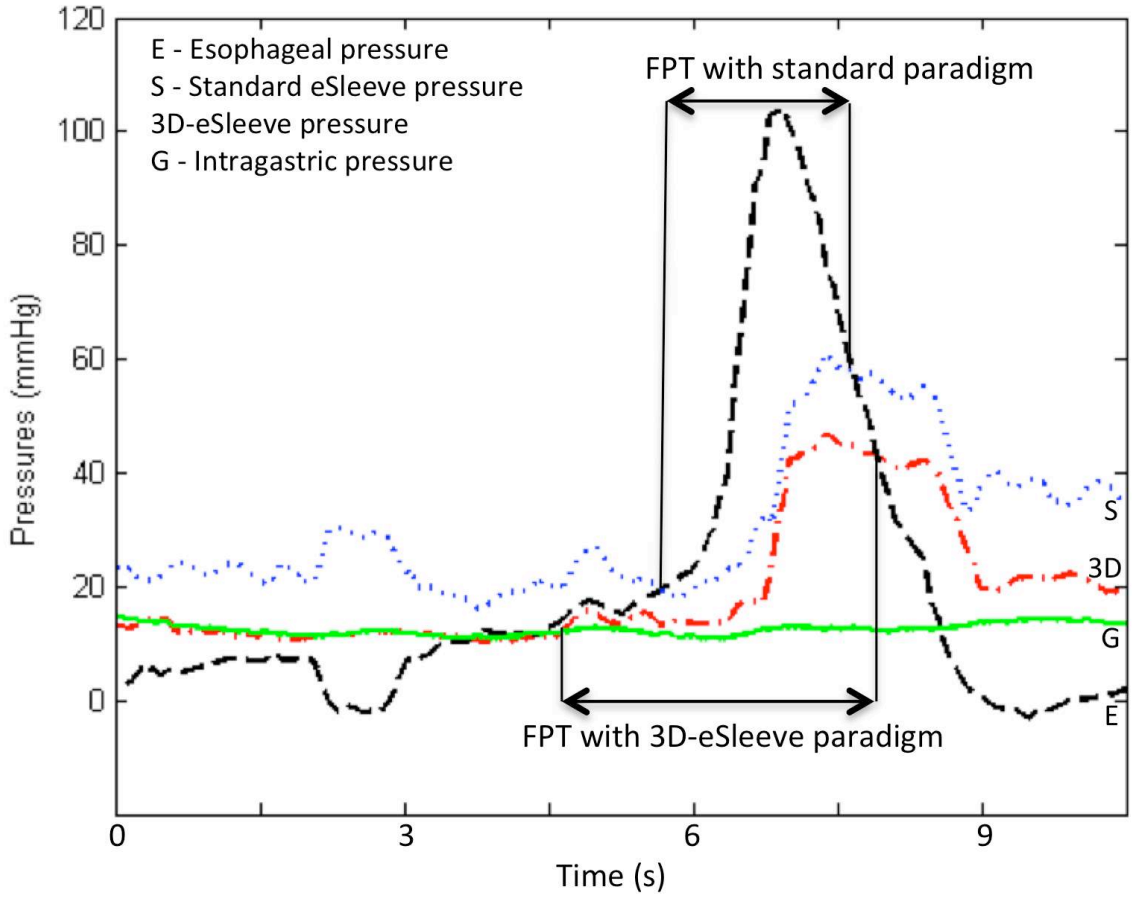

4) Statistical Analysis

Results between manometric methods at rest were compared using the Kruskal-Wallis test for independent variables, and the Wilcoxon test for the dependent variables.

For the EGJ deglutitive relaxation study, in the Phase I study, the values of the different measures of IRP were compared using the Kruskal-Wallis test and the correlation between ManoView and MATLAB™ calculations were assessed by using the Pearson correlation coefficient. Data were summarized as median [25^{th}-75^{th} percentile], unless stated otherwise. A $p<0.05$ was considered significant.

RESULTS

1) Subjects

- For the description of the EGJ pressure morphology at rest

Nine subjects (5F, ages [26, 49]) were recruited for the study. All had normal IDQ and GerdQ scores. All subjects successfully completed the intended protocol. One subject was suspected of having a hiatal hernia based on the HRM recording; this was subsequently confirmed by endoscopy. This volunteer was excluded from the determinations of HPZ length and respiratory inversion.

- For the assessment of EGJ relaxation

Twenty-five subjects (17F, ages [19; 48]) were recruited for the first phase of the study focused on comparing the measurement of IRP using the standard 360-HRM assembly with the IRP obtained with the 3D-HRM assembly utilizing the maximum of the radial minimum pressure paradigm. Fourteen new subjects (6F; ages [21; 52]) participated in the second phase of the study and underwent simultaneous 3D-HRM and videofluoroscopy to determine the efficacy of new 3D-HRM paradigms in predicting bolus transit. No subject had manometric evidence of hiatal hernia. Of the twenty-five subjects in phase I, 25 had a normal IDQ score and 2 had a borderline abnormal score of 8 and 9. Of the fourteen

subjects in phase II, 13 had a normal IDQ score and one had a borderline abnormal GerdQ score of 9. All subjects successfully completed the intended protocol.

2) 3D-HRM EGJ pressure morphology at rest

An immediate observation of 3D-HRM recordings was of their dynamic nature, varying with respiration, vascular pulsations, and swallowing. The dominant pressure peak, labeled DH_{Apex} was precisely synchronized with inspiration as evidenced by its synchrony with the occurrence of negative intrathoracic pressure (Figure 13A & 13B). In keeping with the convention established by Kwiatek, et al. (119), DH_{Apex} (referred to as the CD signal by Kwiatek) was assigned the 6 o'clock orientation in the panoramic depiction of EGJ pressure morphology created by unfolding the cylindrical pressure representation. Radially opposing DH_{Apex} (12 o'clock), split in half on the inverted V plots and located 2.7 cm [2.2-3.4] distal to DH_{Apex} was a second prominent pressure peak (DH_{Base}) that varied during respiration. Thus, the pressure signature of the diaphragmatic hiatus (DH) was found to be highly radially asymmetrical and oblique with respect to the axis of the esophagus (Figure 14). The obliqueness of the pressurization composed by the DH_{Apex} and DH_{Base} peaks is modeled in Figure 15.

Figure 13. Representative examples of 3D-HRM still images.

Figures 3A & 3B illustrate the discrete pressure peaks within the EGJ at expiration (A) and inspiration (B). Figures 3C & 3D illustrate the case of a different subject with pulsatile peaks. The shaded 'V' on the topography plots indicates the disposition of the split diaphragm signal. See text for details of peaks DH_{Apex}, DH_{Base}, V1, and V2.

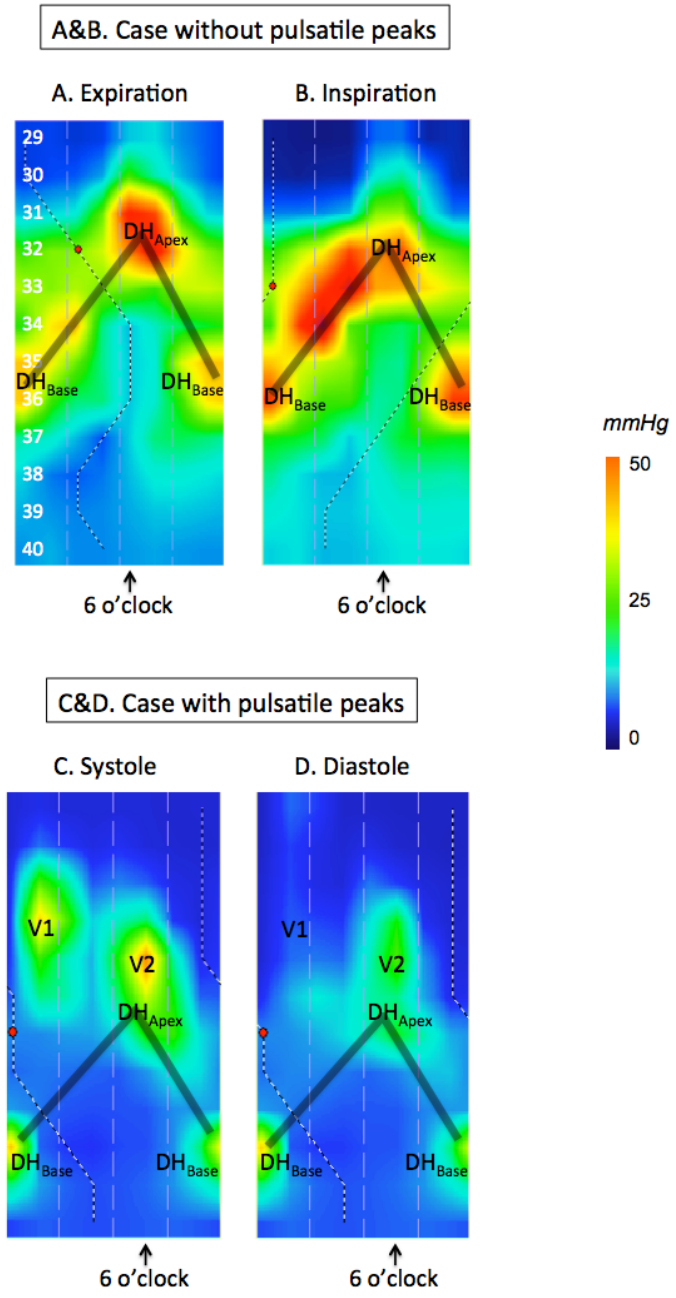

Figure 14. Sagittal view of a CT-scan of the esophagus.

This CT-scan illustrates the topographic anatomy of the esophagus. In the thorax, the distal esophagus is located between the heart in front, which is lying on the costal diaphragm, and the lower thoracic aorta in back. When the esophagus crosses the diaphragm, the CD is oblique to the axis of the esophagus.

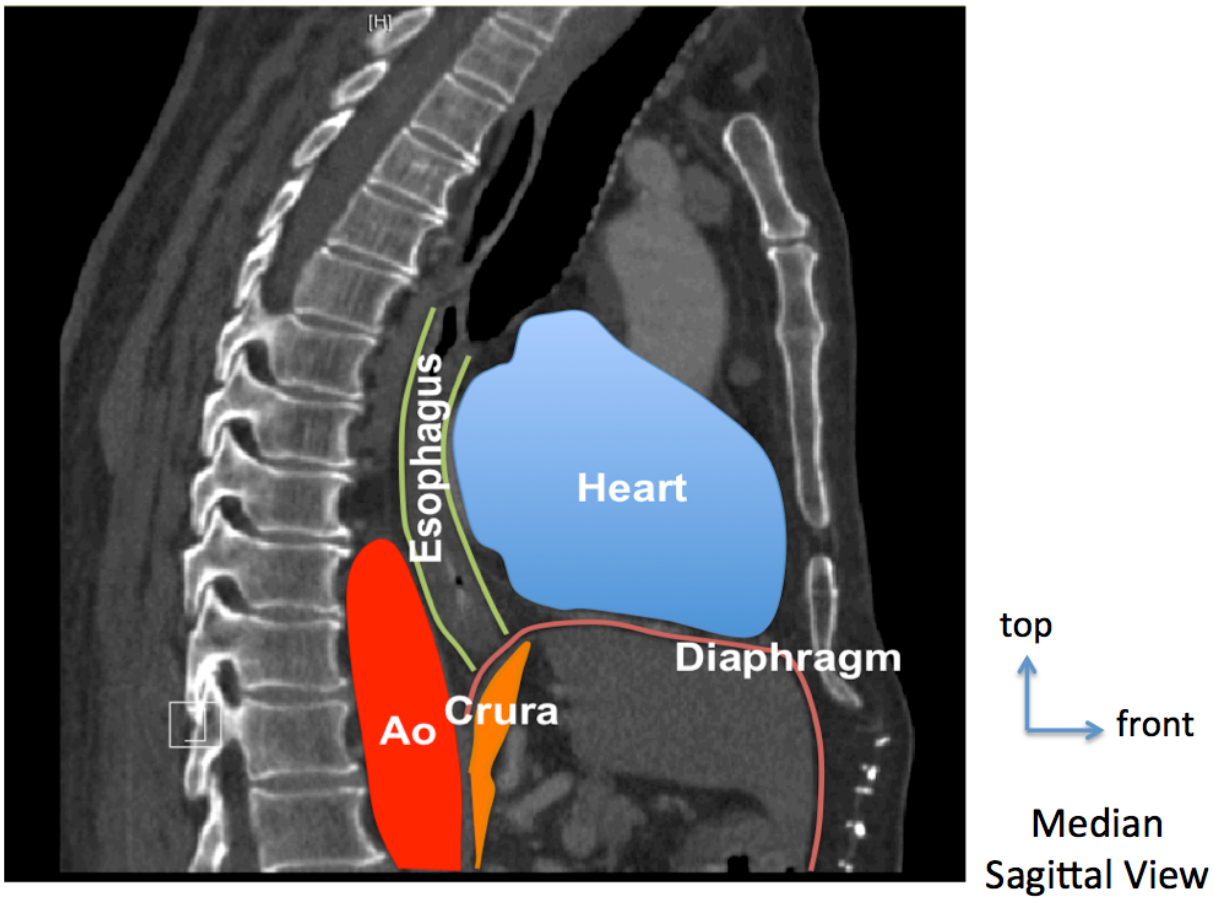

Figure 15. Schematic explanation of the inverted V plot.

The resulting real-time 3D-HRM view is a cylinder, which can be 'opened' to obtain a pressure topography panorama of the segment in the format of an inverted V plot. The orientation of the assembly relative to the EGJ was not controlled; hence, by convention the apical diaphragmatic signal is defined as 6 o'clock. The shaded 'V' on the topography plot indicates the disposition of the split diaphragm signal (red and green circles below).

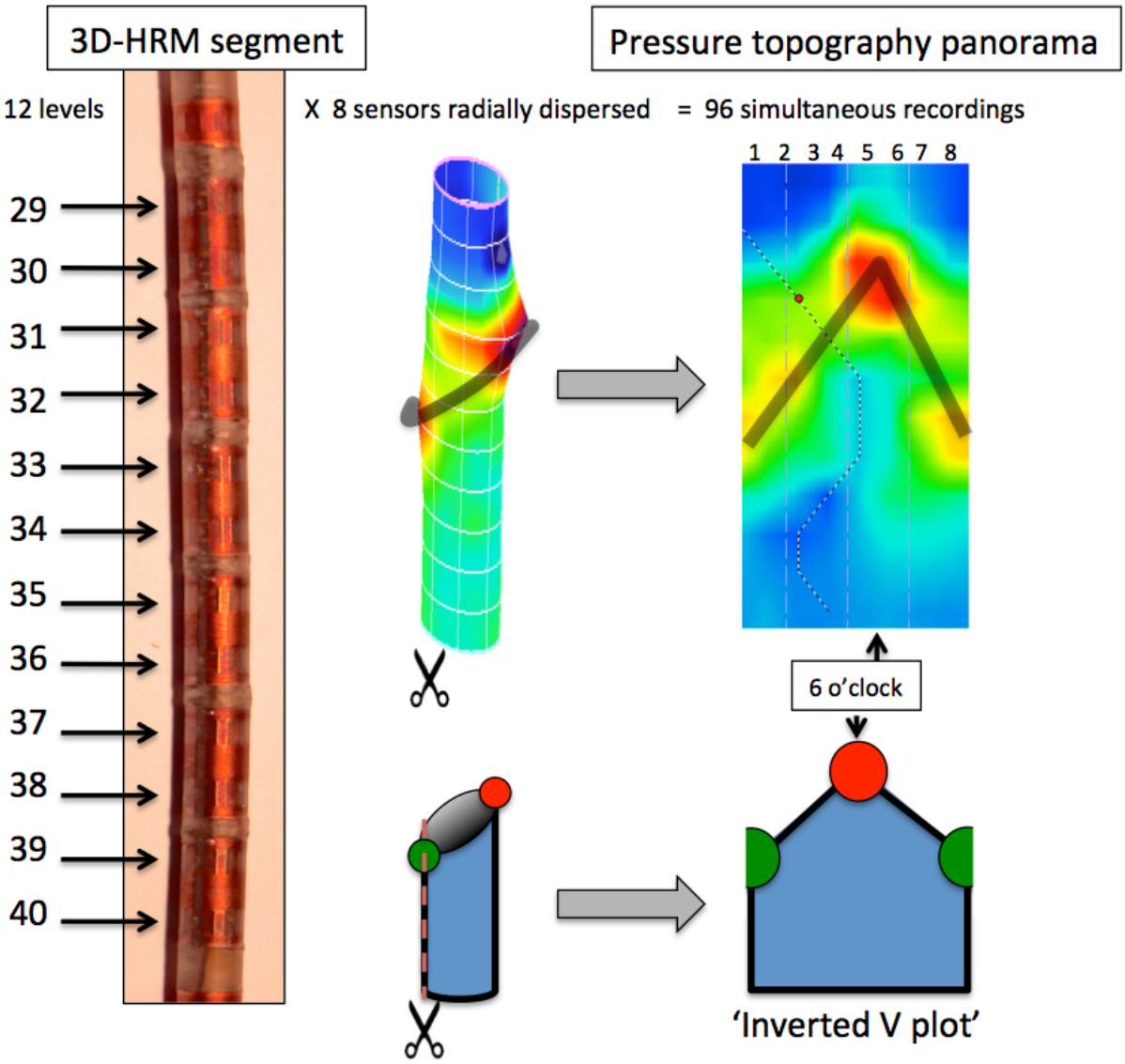

Two additional pulsatile pressure peaks were variably present (both evident in Figures 13C & 13D); both were situated in the thoracic part of the pressure topography panorama, proximal to the DH_{Apex} peak. One was situated at '6 o'clock' (labeled 'V1' in Figures 13C & 13D) and the other one was positioned at '12 o'clock' (labeled 'V2' in Figures 13C & 13D). The 'V1' peak, appearing during expiration and diminishing with inspiration, was located just above DH_{Apex}, whereas the 'V2' peak was positioned on the opposite side. These two pulsatile signals likely represent a cardiac signal and the lower thoracic aorta respectively.

Although the pressure attributable to the intrinsic LES would not be expected to vary substantially in synchrony with either respiratory or vascular pulsations, it was strongly influenced by deglutition, exhibiting both deglutitive relaxation and a profound post-deglutitive contraction (52,120). We utilized the post-deglutitive contraction to verify the pressure signature of the LES in the 3D-HRM recording (Figures 16A & 16B). In sharp distinction to the oblique orientation of the diaphragm signal, the intrinsic LES had a horizontal configuration. We also utilized the ninth volunteer (with the hiatal hernia) to confirm this interpretation of DH_{Apex} and DH_{Base} (Figure 16C). The same circumferential horizontal contraction was noted in this individual, located in the thorax above DH_{Apex}, with the inverted-V plot still present distally.

Figure 16. 3D-HRM of the EGJ at rest (Panel A), in the post-deglutitive period (Panel B), and in case of hiatal hernia (Panel C).

At rest, the inverted V plot reveals the CD (DH_{Apex} and DH_{Base}) to be the dominant pressure signals while in the post-deglutitive period, the intrinsic LES exhibits a prominent after-contraction, which, in contrast to the CD, is circumferential. The vertical red arrows represent the high-pressure zone as determined during station pull-through using sensors radially dispersed at the 3, 6, 9 and 12 o'clock radians and the blue vertical arrows represent the locus of 3D circumferential LES length. Panel C represents the case of a hiatal hernia as seen in 3D-HRM as a confirmation of our findings in normal volunteers. The shaded 'V' on the topography plots indicates the disposition of the split diaphragm signal.

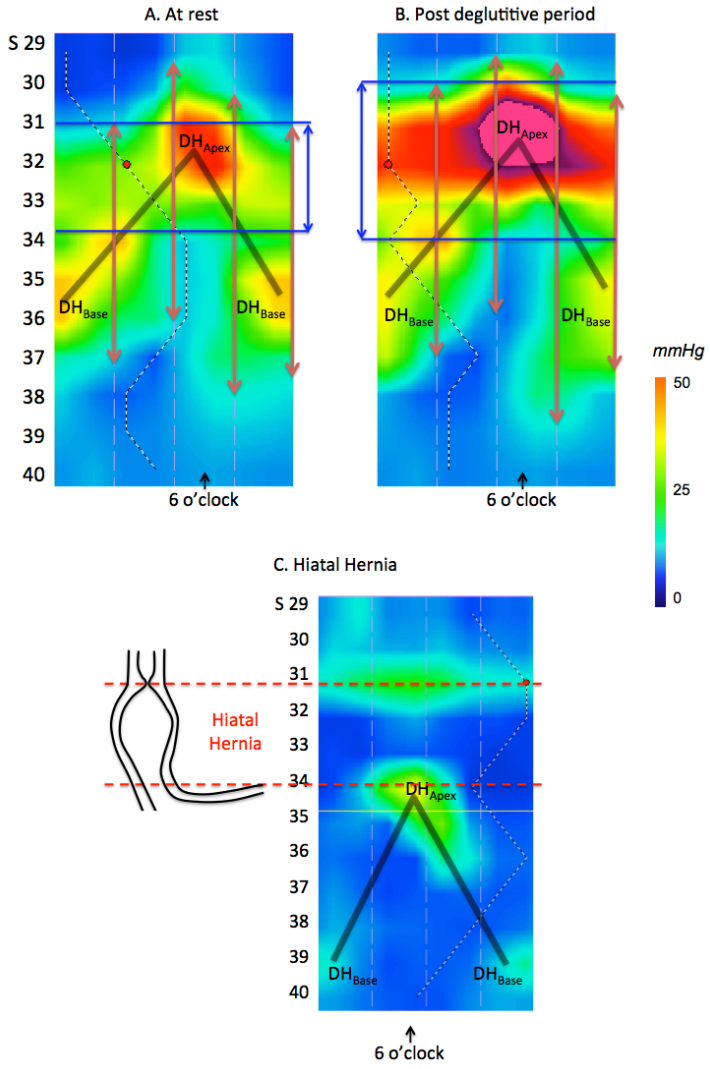

- ***High-pressure zone length***

The various measures of HPZ length are summarized in Table 2. Using simulations of conventional manometry, 'LES length' at 3, 6, 9 and 12 o'clock were different, but equally interesting the borders were different (Figures 16A & 16B), such that the composite length of the HPZ measured 8 cm [7.3-10.6 cm], more than twice the average length of each radially oriented 'LES length', calculated as 3.4 cm [3.0-3.8 cm]. On the other hand, the 3D-HRM region with circumferential horizontal pressure (LES length) was relatively short: 2.3 cm [2.2-2.6] at expiration (Table 2) with no significant difference between inspiration and expiration. The length and magnitude of LES pressure were maximized during the post-deglutitive period (Figures 16A & 16B) at which time it was significantly longer 3.7 cm [3.0-4.2] and stronger 91 mmHg [75-102] ($p<0.05$) than prior to the swallow (2.3 cm [2.2-2.6], 18.3 mmHg [15.0-19.0]).

Table 2. Localization and length of the HPZ defined by station pull-through and 3D-HRM at expiration.

	'LES length' Station Pull-through						LES length 3D-HRM	
	3 o'clock	6 o'clock	9 o'clock	12 o'clock	Average	Composite	Expiration	Inspiration
Upper border (cm)	38.3 [37-42.9]	36.3 [33.6-38.1]	40.3 [38.6-43]	40.5 [38.9-43.9]	38.8 [37.4-41.9]	36.3 [33.6-38.1]*	42.6 [41.3-45.8]	43.3 [41.5-47.1]
Lower border (cm)	41.3 [40.8-45.5]	39.8 [38.1-42.1]	44.5 [41.9-46.6]	44.5 [42.1-46.5]	42.2 [41.5-45.3]	44.5 [43.8-46.6]*	44.8 [43.6-47.7]	45.3 [44.8-49.6]
LES length (cm)	3.0 [2.5-4]	4.0 [3-4.3]	3.5 [2.5-4.2]	3.0 [2.6-5.2]	3.4 [3-3.8]	8.0 [7.3-10.6]*	2.3 [2.2-2.6]*	2.2 [2.1-2.7]*

* Different from mean pull-through value (3, 6, 9, and 12 o'clock not tested individually)

Thus, 'LES length' calculated using the simulation of the pull-through protocol was a composite of overlapping LES, diaphragmatic, and vascular pressure signals that were individually discernible in 3D-HRM by their respiratory variation, vascular pulsation, and radial orientation.

- ***Respiratory inversion***

Figure 17 illustrates representative data on the localization of the respiratory inversion zone determined by 3D-HRM and pull-through methodology. The respiratory inversion zone determined with the 'PIP tool' in 3D-HRM was located almost precisely at the DH_{Apex} pressure peak and the inversion zone averaged 0.9 cm [0.7-1.0] in length. There was no statistical difference between localization of the center of the respiratory inversion zone, determined in 3D-HRM (42.4 cm [40.5-45.5]) or by pull-through methodology (43.5 cm [40.3-45.5]).

Figure 17. Representative 3D-HRM image illustrating the 3D-HRM localization of the respiratory inversion zone using the 'PIP tool' compared to measures made using station pull-through simulations.

The 3D-HRM method tightly isolates the respiratory inversion zone within the CD signal, which is less discretely accomplished with the pull-through technique. The shaded 'V' on the topography plot indicates the disposition of the split diaphragm signal.

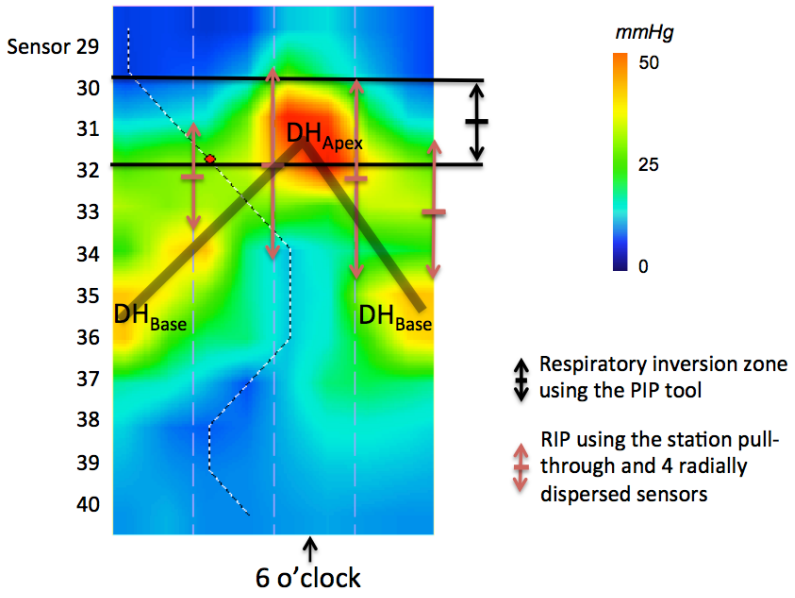

3) Assessment of EGJ relaxation during the deglutition

- ***Comparison of IRP and 3D-IRP***

The mean values and normative ranges of the IRP calculations for 25 control subjects are shown in Table 3 using the 4 different analysis protocols. There was no significant difference between IRPs calculated using the standard eSleeve, regardless of the HRM assembly. However, the 3D-IRP (calculated with the 3D-eSleeve) was significantly lower ($p<0.001$) than all other calculations of IRP. These findings suggest that an appropriate upper limit of normal for the 3D-IRP is 12 mmHg.

Table 3. Normal values for IRP and 3D-IRP (mmHg) using the standard HRM and 3D-HRM assemblies in 25 normal subjects, calculated using the β-Manoview software.

	Standard HRM	3D-HRM		
Assembly and Metric	IRP	IRP	IRP	3D-IRP
Sensing array	Standard	Standard†	3D	3D
eSleeve	Standard	Standard	Standard	3D-eSleeve
Median, mmHg	5.3*	6.5*	8*	3.1
5th−95th percentile, mmHg	0.5–17.2	1.2–19.4	2.7–24.5	0.9–12.3

†Non-3D segment of the 3D-HRM assembly is similar to the standard assembly and composed of circumferential sensors spaced 1 cm apart. *Significant difference vs. 3D-IRP ($P < 0.001$) but no significant difference between these calculations. HRM, high-resolution manometry; IRP, integrated relaxation pressure; eSleeve, electronic sleeve.

We found a good correlation ($r= 0.81$, $p<0.001$) between 3D-IRP average values calculated in MATLAB™ and those calculated in the β ManoView software for the 25 subjects of the phase I (Figure 18).

Figure 18. Correlation between 3D-IRP average values.

3D-IRP values are calculated using the β-Manoview software and using MATLAB™ (8 radial sensors) for the 25 subjects of Phase I of the study ($r=0.81$, $p<0.001$).

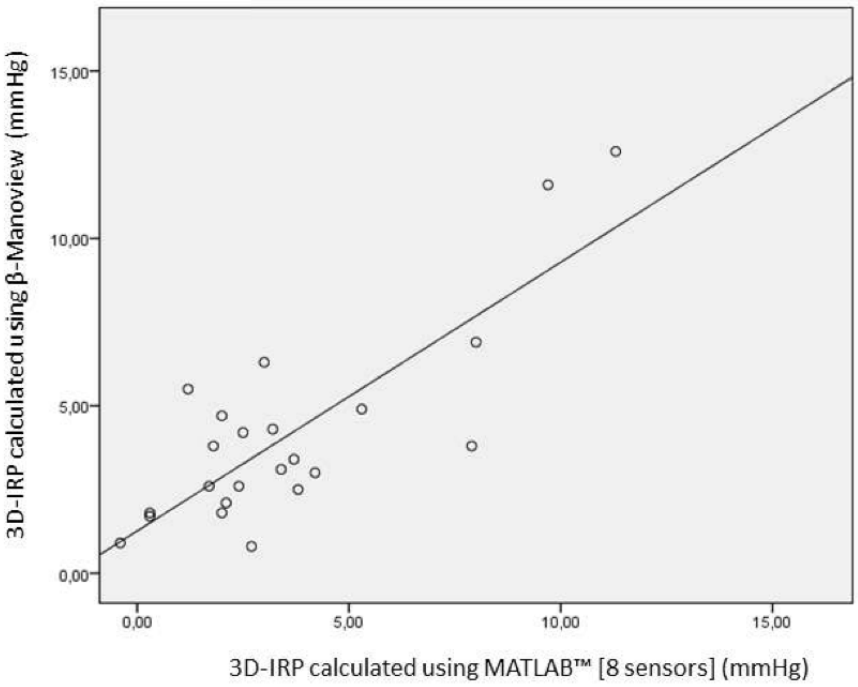

- ***Minimal radial sensor density for 3D-IRP measurement***

We used MATLAB™ simulations to compare the effect or reduced radial pressure resolution on calculated values of the 3D-IRP. Table 4 summarizes the comparison between using 8 sensors at 45°, 4 sensors at 90° [2 different calculations], 2 sensors at 180° and a single sensor. The results suggest that the calculation using 4 sensors spaced 90° slightly overestimated the value of the 3D-IRP, nevertheless with an excellent correlation with the 8-sensor analysis. Further reduction of the number of radial sensors was associated with a substantial drop in the correlation.

Table 4. MATLAB™ simulation of the 3D-IRP varying the radial resolution of the 3D assembly by selectively utilizing progressively fewer of the radial pressure sensors.

Number of sensors	8	4 (Nos. 1–3–5–7)	4 (Nos. 2–4–6–8)	2	1
Radial resolution, degrees	45	90	90	180	360
Median, mmHg	2.7	3.1	3.75	4.4	9.6
5th−95th percentile, mmHg	0.3–10.0	0.3–10.8	0.8–10.5	0.5–11.9	1.8–20.3
Correlation with the 8 sensors		$R = 0.99$ $P < 0.001$	$R = 0.98$ $P < 0.001$	$R = 0.87$ $P < 0.001$	$R = 0.44$ $P = 0.116$

- ***Using the 3D-IRP to calculate FPT***

Twenty-eight swallows were analyzed using simultaneous 3D-HRM and videofluoroscopy. The median period of bolus transit assessed with videofluoroscopy was 3.3 seconds [0.3-4.9]. The FPT was 2.1 s [0.4-4.0] with the eSleeve and 5.3 s [1.8-9.0] with the 3D-eSleeve. The presence or absence of FPT was compared to visualized bolus transit in videofluoroscopy during each tenth of a second for each swallow. The mean sensitivity and specificity of the eSleeve for predicting bolus transit were 0.55 and 0.85 respectively. In comparison, the mean sensitivity and specificity of the 3D-eSleeve were 0.78 and 0.88 respectively.

DISCUSSION RELATIVE TO THE PUBLISHED ARTICLES

These studies utilized a novel 3D-HRM manometric device comprised of a 96-sensor array to dynamically monitor the EGJ area HPZ at rest, and during the deglutition, in groups of normal subjects.

At rest, still 'images' at inspiration and expiration from the dynamic recordings were compared to simulations of a conventional pull-through method. The major findings of the study were that: 1) the dominant constituents of EGJ pressure at rest, identified by its characteristic radial and axial asymmetry, were attributable to the pressure signature of the DH, 2) sphincter length assessed by a pull-through method greatly exaggerated the length of the segment within the EGJ that had circumferential contractile pressure, and 3) the respiratory inversion zone delineated with the 'PIP tool' of the 3D-HRM software was located at the apex of the DH signal.

A major finding of interest in this study pertained to the characteristics of the pressure peaks within the EGJ area, particularly that which we attribute to the DH. The 3D-HRM pressure signature of the hiatus appeared oblique in relation to the luminal axis accounting for its extreme radial asymmetry (Figure 6). Regarding this 'obliqueness', the inverted-V pressure signal was constant among studies and this signal was clearly synchronized with inspiration as evidenced by the corresponding negative intrathoracic pressure. Hence, we propose that the inverted-V pressure signal in the 3D-HRM panoramic view is the 'pressure

signature' of the DH. Further supporting this contention was the observation that DH_{Apex} was uniformly located at the RIP. Note that, as previously suggested by Kwiatek et al (119) DH_{Apex} was very likely reflective of CD contraction, but it was not possible to be as certain regarding the genesis of DH_{Base} beyond to say that it was clearly synchronized with respiration. Given recent observations of the mobility of the LES relative to the diaphragm in prolonged recordings, periodically converting from alignment to separation (123), as well as increasing interest in the pathophysiological significance of perturbations of EGJ anatomy in GERD, where there has been increasing recognition that the DH plays a major role as an antireflux barrier since the observations by Mittal, et al. in the late 1980's (124,125). These observations beg for further studies in GERD subgroups, after determination of specific 3D-HRM parameters to quantify respective roles of EGJ components.

It was also of great interest to identify the pressure signature of the intrinsic LES within the 3D-HRM panorama of EGJ pressure (113). The key to isolating the LES component was in the post-deglutitive contraction, which doesn't involve the diaphragm. As illustrated in Figure 8, the post-deglutitive LES contraction was circumferential and oriented perpendicularly to the axis of the esophagus in both control subjects (Figure 16B) and the case of hiatal hernia (Figure 16C). The proposed horizontal orientation of LES pressure, perpendicular to the luminal axis is also consistent with its anatomical characteristic of being comprised of circular muscle with only minor helical characteristics (126).

Another observation of interest in this study was that LES length determined with 3D-

HRM was significantly shorter than 'LES length' determined by the station pull-through simulations. The lengthier pull-through measurements were attributable to the variable inclusion of pressure signals attributable to the LES, diaphragm, and vascular structures and to the misalignment of the radially oriented sensors with each other. Similar artifact was encountered in a previous study using 'standard' HRM reporting an average 'LES length' of 4.7 cm [3.3-5.3 cm] (25), presumably because of the effects of circumferentially averaging these non-circumferential, misaligned pressure constituents. Consequently, we believe that 'LES length' defined using the station pull-through incorporated all contributors to pressure within the EGJ without discerning which of the variably present ones were indeed present and without defining the spatial relationship between the LES and the diaphragm.

During deglutition, the meaning of the RIP localized in conventional manometry has been somewhat controversial since the observations of Dodds et al that movement of a pressure sensor relative to the pressure profile of the sphincter causes pressure fluctuations synchronized with respiration, but not necessarily localizing the diaphragm (127). This too was clarified using the 'PIP tool' in the current study. We observed that the locations of the RIP localized with the 'PIP tool' and DH_{Apex} exactly corresponded with each other, even though they were independent determinations. This highlights a key advantage of HRM, which is in avoiding the 'location artifact' inherent if 2D manometry technology and the ultimate genesis of the artifact described by Dodds, et al. Another consideration with

respect to the 'pseudo RIP' observed by Dodds is that the magnitude of that pressure variation cannot exceed the magnitude of LES pressure and that it would be circumferential, being the LES after all. Neither of these conditions pertained to DH_{Apex}.

A major advantage gained in the adoption of HRM with EPT over conventional manometry has been the establishment of an objective quantitative measurement of EGJ relaxation, the IRP, to distinguish between normal and abnormal EGJ relaxation (15). This study assessed whether or not a new 3D-HRM assembly could improve on this measurement with the 3D-eSleeve paradigm, an analysis premised on finding the axial maximum and radial minimum pressure at each sensor ring along the sleeve segment. The major findings of the study were that: 1) the upper limit of normal for the IRP was 12 mmHg (vs. 17 mmHg with the standard eSleeve) based on an analysis of 25 normal subjects, and 2) the residual sphincter pressure registered with the 3D-eSleeve was much more accurate in predicting intraluminal pressure gradients conducive to bolus flow (FPT) than the standard eSleeve as verified by concurrent fluoroscopy. These findings demonstrate a relevant difference between the two measurement paradigms and suggest that the 3D-eSeeeve and 3D-IRP are the superior metrics to adopt for use with 3D-HRM.

The improved accuracy of the 3D-eSleeve should prove useful in the investigation and management of esophageal disorders ranging from achalasia to gastroesophageal reflux disease (GERD) in which the assessment of EGJ relaxation is a critical variable. Resolving the detail of the EGJ high-pressure zone (HPZ) may allow one to discern whether resistance to

flow at the EGJ is due to impaired LES relaxation (128) or mechanical factors by differentiating unique features of radial symmetry and/or esophageal intrabolus pressure. The 3D analysis should also prove useful in GERD studies as the same principles that affect antegrade flow will likely impact retrograde flow of gastric juice. There is also substantial interest in defining the intra-abdominal segment of the LES and this assembly may have sufficient recording fidelity to make this measurement in real time, potentially improving upon measurements made during short interval pull-through evaluations of the LES.

One limitation of this study was that both the 3D-HRM and standard HRM assemblies studied are made by the same manufacturer (Given) making it impossible to generalize the findings more broadly. However, there is currently no way around this; there is only one solid state 3D-HRM assembly currently available. In terms of the comparator, the 3D-HRM assembly could have been compared to an HRM assembly from a different manufacturer, but the other assemblies utilized in clinical HRM do not have published normative data for the IRP, which was the focal point of the current study. A comparison of 3D-HRM to a station pull through with four radial recording sensors would be more valid, however, this technique is tedious and it is difficult to see how problems related to movement artifact can be overcome.

Although not statistically significant, the IRP calculated with the standard eSleeve paradigm using the 3D-HRM segment was greater than that with the standard HRM assembly or the proximal segment of the hybrid 3D-HRM assembly. This may be related to the

stiffness of the 3D-HRM segment, which could be reduced with lower sensor density. Our simulations suggested that 4 radial pressure orientations (90°) may be sufficient to approximate the value of 3D-IRP, and this observation may have future implications in the design and development of the next generation of the 3D-HRM assemblies, even if the present study was not designed to validate these results.

CONTINUATION OF THE DISCUSSION

Additional work was done to clarify the following points of the discussion: the pressure signature of the EGJ components and the potential role of the 3D-HRM in clinical practice, notably in cases of GERD.

1) Clarifications relative to the pressure signal of EGJ components

a) Example of Achalasia

In case of achalasia, it is widely accepted that the pressurization responsible for the dysphagia symptoms is the absence of relaxation of the intrinsic sphincter during deglutition.

Figure 19 illustrates the case of a patient with achalasia, revealing that the pressure signal due to the intrinsic sphincter is obviously circumferential at rest as well as during deglutition.

Figure 19. Case of achalasia analyzed using the 3D-HRM assembly.

Panel A shows the EGJ at rest, showing the circumferential HPZ due to the intrinsic sphincter, highlighted by the black arrow. Note that this HPZ appears stronger than in previously reported cases. Panel B illustrates the absence of deglutitive relaxation of the intrinsic sphincter.

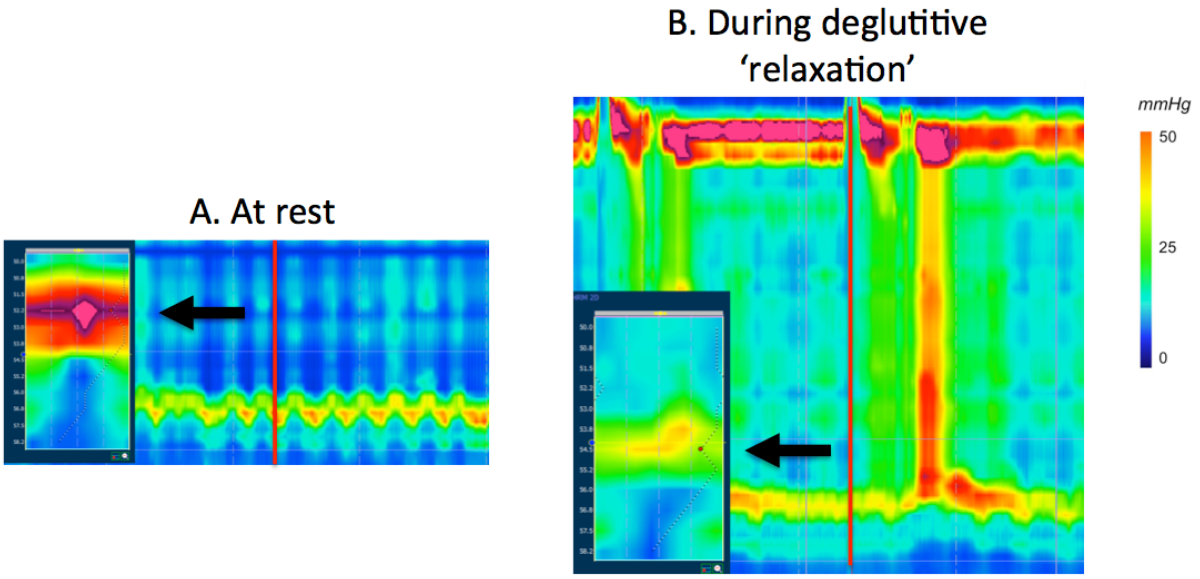

b) Wavelet transform filtering

To confirm our finding stating that the inverted-V shape was the pressure signature of the DH, we devised a way to decompose the pressure signal according to its frequency, to extract the respiratory signal from the overall signal. Indeed, the esophageal pressure signal that is recorded with manometry is a composite signal with respiratory fluctuations and vascular pulsations.

To achieve that goal, data were analyzed after thermal compensation using Manoview

software and MATLAB™ after transfer of the raw data files. A MATLAB™ program was written to apply a wavelet decomposition method similar to the one used by Lin, et al. (129) on the 96 records of the 3D-HRM segment during the resting period. The respiratory signal is a quasi-periodic signal with a frequency range from 0.15 to 0.25 Hz, the vascular signal has a frequency around 1 Hz, while the esophageal pressure signal corresponds to a frequency range less than 0.1 Hz. To identify the respiratory component contained in the pressure signal, a wavelet decomposition method was applied to the pressure signal from each radial sensor at each axial level of the 3D HRM segment. Wavelet transform filtering has recently been applied to esophageal manometric data to eliminate vascular pulsation artifacts (130). In this study, we applied a wavelet transform filtering technique to esophageal pressure data to eliminate components of the composite signal related to respiration and heartbeat.

Wavelet transform filtering is analogous to Fourier analysis. The key distinctions are that, first, whereas Fourier analysis decomposes composite signals into sine waves of varied frequency and strength, wavelet transformation uses a user-defined 'mother wavelet' as the waveform upon which signal decomposition is based. Second, whereas Fourier analysis is applied uniformly to the entire signal from start to finish, wavelet decomposition allows for 'compact support' to isolate the analysis to specified segments of the signal. Thus, the wavelet decomposition can accommodate local changes to the signal as might be anticipated in a protocol such as ours (131). The 'mother wavelet' applied is user defined and its selection depends on the waveform of the signal to be filtered.

The filtering process using wavelet decomposition is to first fit the mother wavelet to the signal to be filtered at the highest possible frequency and derive an approximation representing the original signal minus the detail coefficient representative of the portion of the original signal filtered out. In the present case, the highest possible frequency was 5 Hz. This process is then iteratively repeated, progressively halving the frequency of the mother wavelet (a process called dilation) until the mother wavelet has been dilated to such an extent that it covers the entire range of the signal. The final result is an approximation and a set of details, corresponding to the portions of the signal filtered out at each iteration (132). In practice, the number of iterations required is determined by the frequency content of the original signal.

One may hypothesize that the oblique pressure signal within the EGJ may represent the gastric sling fiber (133). However, the wavelet decomposition method reveals that the oblique signal is composed of respiratory frequencies, strongly suggesting that the signal is mainly not composed of sling fiber but composed of the DH as opposed to much lower frequencies that might be expected with the gastric sling fibers (Figure 20).

Figure 20. Filtration of the 3D data during the resting period, to differentiate pressures generated by the LES and the CD.

A dedicated MATLAB™ program decomposes the pressure signals of each of the 96 pressure recordings during the resting period, comprising inspirations and expirations (A). Each record varies with a specific frequency and records, which were not composed with significant component of respiratory frequency, were excluded (B). We hypothesize that the resultant 'map' of the 3D area (C) reveals the pressure impact of the CD. The pressure in regard of the 34th sensors' level reveals the pressure impact of the LES because the pressures are independent from the respiratory rate and circumferential in regard of the crural impact, in absence of hiatal hernia in this control population.

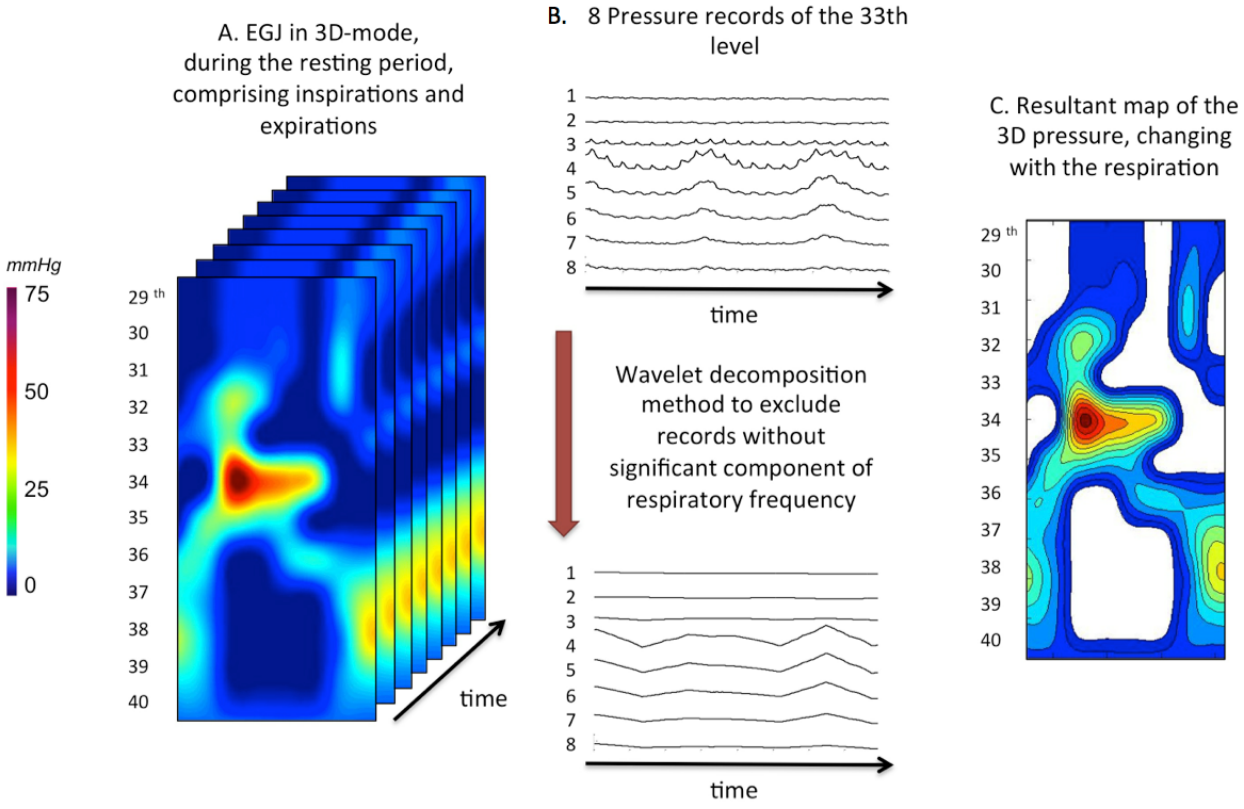

2) Potential roles for the 3D-HRM in clinical practice

As a reminder, the 3D-HRM assembly is a composite of a standard HRM catheter and a 9cm long 3D segment. Related to this design, the 3D-HRM assembly was first intended to record the EGJ pressures evident by the position of the 3D segment. Part of our previously reported research was done to assess the EGJ as a reflux barrier and it appears obvious that the first application of 3D-HRM might be for cases of GERD. However, the 3D segment can also be positioned within the UES to assess this other complex and asymmetric junction exactly the same way we did for the EGJ.

a) Roles in the evaluation of the EGJ, in GERD

-EGJ Vector volume (V-V)

Background:

A variety of manometric methodologies and metrics have been proposed to quantify the EGJ as a reflux barrier: sphincter length and RIP were described to determine the intra-abdominal LES length as a predictor of fundoplication efficacy (116). However, sphincter length, or intra-abdominal length, speaks nothing to the magnitude of closure forces at the

EGJ. Early on, it was recognized that there was substantial asymmetry of these closure forces both radially and along the length of the sphincter. Consequently, Bombeck and colleagues developed the concept of LES vector volume (V-V) in the late 1980s as a quantification of sphincter integrity (116,134). The determination of V-V required a motorized pull-through of an 8-lumen water-perfused manometry catheter with the lumens radially dispersed 45° apart and the rate of pull-though held constant so that the time axis of the plot became indicative of high-pressure zone length. The resultant data were then reconstructed into an 8-sided polygonal solid representing 3D sphincter pressure morphology and quantitative norms were established for the volume of that solid to define reflux patients with a defective valve who may benefit from surgery (116,135,136). However, since the description of the V-V, the method has not been widely used. This may relate to the obsolescence of the requisite apparatus, the impracticality of the testing procedure, and/or the requirement that the V-V measurement be done during suspended respiration.

The development of 3D-HRM assembly has the potential to greatly simplify the assessment of EGJ V-V, due to the high resolution recording both axially and radially while maintaining a stationary position. Consequently, 3D-HRM should allow for the measurement of V-V that was only possible with pull-through maneuvers in the past and this measurement can be made in real time permitting analysis of the respiratory effect. Hence, we assessed the feasibility of the calculation of EGJ V-V using the 3D-HRM assembly and to compare measures of its value using real-time 3D-HRM to analogous measures made using simulations of a conventional manometric catheter and pull-through methodology.

Methods:

We analyzed 8 volunteers at rest. We performed a station pull-through with the 3D-HRM assembly: the assembly was positioned with the 3D segment in the stomach and was obtained withdrawing the assembly at 5 mm increments with each station held for at least 30 seconds (Figure 21). The pull-through was done maintaining normal respiration, with the patient asked to minimize swallowing. The pull-through was continued until the 3D array had traversed the EGJ and the distance to the nares was recorded for each station.

For the assessment of EGJ V-V, data were analyzed after thermal compensation using Manoview software and/or Excel™ (Microsoft, Redmond Washington) after transfer of the raw data files. Analyses were constructed to compare calculations of V-V made with real-time 3D-HRM to the same measures made using simulations of conventional manometry from the pull through protocol.

Figure 21. Position of the 3D-HRM segment during the station pull-through protocol, utilized for the calculation of V-V.

A) Initial position, with the upper sensors' level positioned to record the lower part of the EGJ area. B) Intermediate position during the pull-through, used for the 3D real-time calculation of V-V. C) Final position, with lower sensors' level positioned to record the upper part of the EGJ area.

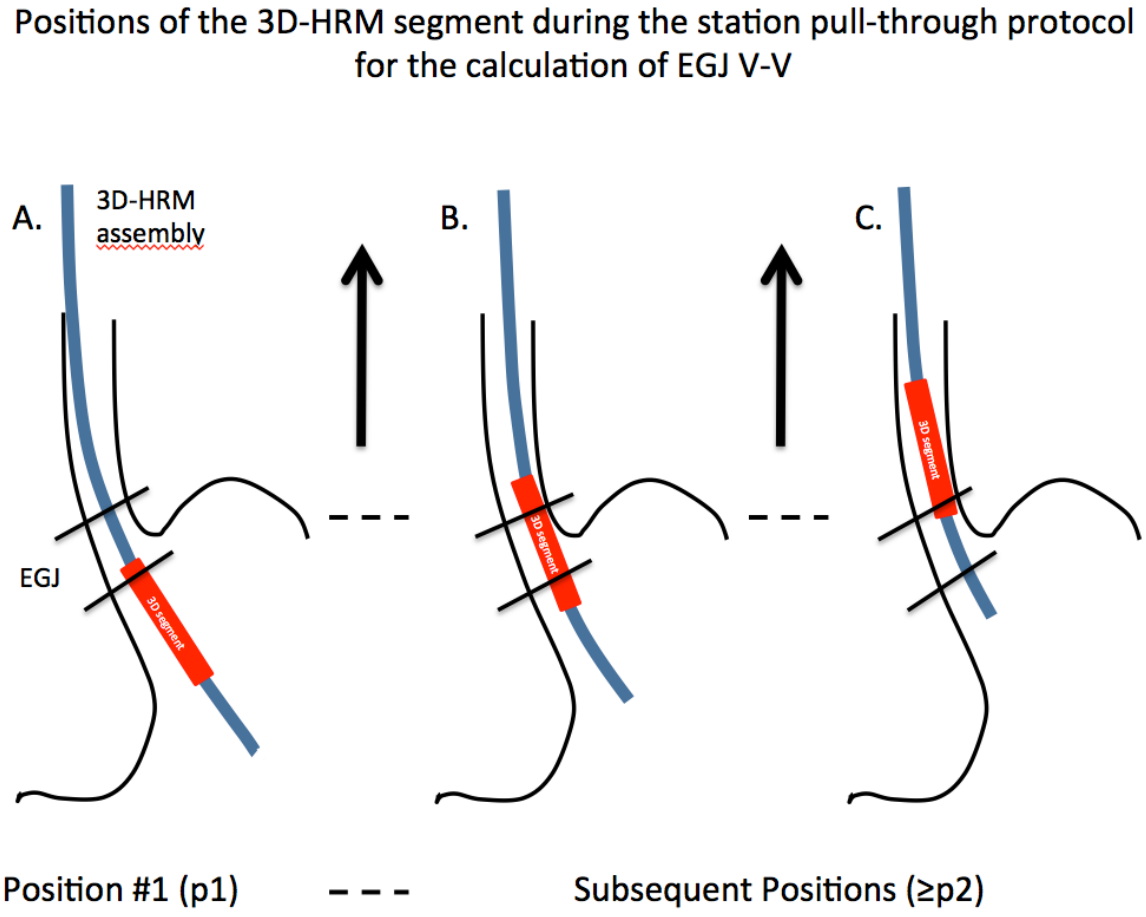

EGJ length was determined as the HPZ appearing as an inverted-V shape on 3D-HRM (137), whose upper and lower margins were defined by a 2 mmHg pressure increase relative to gastric pressure. As previously described, this method may include the vascular artifacts

into the EGJ length, so these pressure peaks were excluded for the measurement of EGJ length. This method for EGJ length calculation included both the intrinsic sphincter and the DH pressure components (Figure 22).

Figure 22. 3D-HRM still images of the EGJ.

Panel A. Representative example of 3D-HRM still image, illustrating the discrete pressure peaks within the EGJ at end-expiration. The blue vertical arrows represent the locus of EGJ length in 3D-HRM. The shaded 'V' on the topography plots indicates the disposition of the split diaphragm signal, formed by the apex of the hiatal diaphragm (DH_{Apex}) and the base of the hiatal diaphragm (DH_{Base}). Panel B. 3D representation of the EGJ, generated by the Manoview™ software is a real time representation of the EGJ V-V (dotted lines separate the EGJ by 0.75 cm sections).

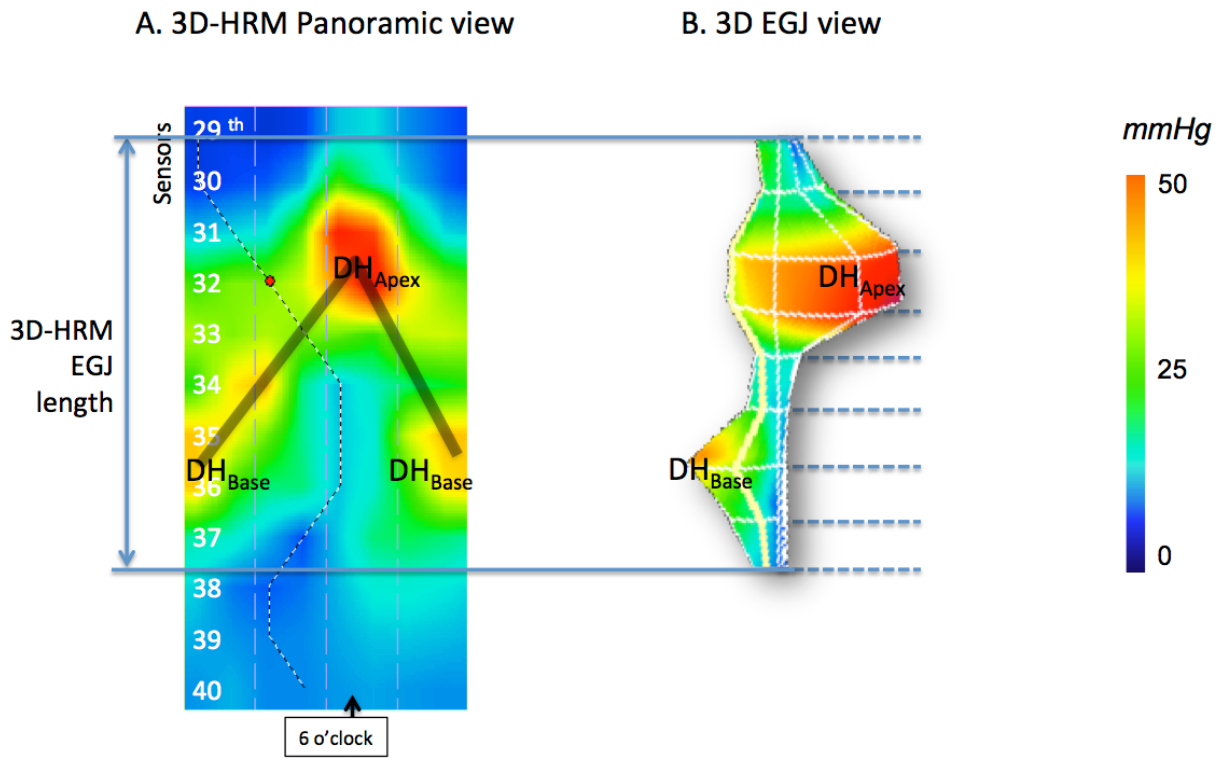

As originally described by Bombeck, V-V is a measure of EGJ integrity calculated from a motorized pull-through across the EGJ with eight radially dispersed pressure sensors (134). At each incremental position, cross sectional vector area (CSVA) was computed using the irregular polygon area formula ($CSVA = \sin(360/n)/2x(P_1xP_2 + P_2xP_3 + \ldots + P_nxP_1)$, with n=8 radial sensors). Hence, the V-V calculation requires that EGJ length be predefined and that radial pressure data be defined for every incremental position within that length. Given that each pressure-sensing element on the 3D-HRM assembly was 2.5 mm in length, we used this as the incremental length for V-V calculations. However, that approach resulted in there being two 2.5 mm gaps between each 2.5 mm sensing element. Three alternative methods were utilized to fill these gaps in the data set (Figure 23):

1) The 3D-HRM method used a single assembly position and cubic spline interpolation between pressure sensors allowing for real-time calculation of V-V;

2) Simulation method #1 of the pull-through used composite data from three assembly positions during the pull-through done in 5 mm increments; this method required no interpolation;

3) Simulation method #2 of the pull-through utilized data from a single sensor ring of the assembly at each 5 mm increment of the pull-through; this method required that the 2.5 mm gap not assessed by a pressure sensor be approximated with cubic spline interpolation.

Figure 23. Schematic representation of the methodology used for the calculation of EGJ V-V.

A. Assembly positions during the pull-through protocol with 5 mm increments. The pressure of the segment of interest (red box) is recorded by the pressure sensors during the pull-through protocol, either by a single sensor or by different sensors. B. Utilization of the recorded data using 3 different methods for the V-V calculation.

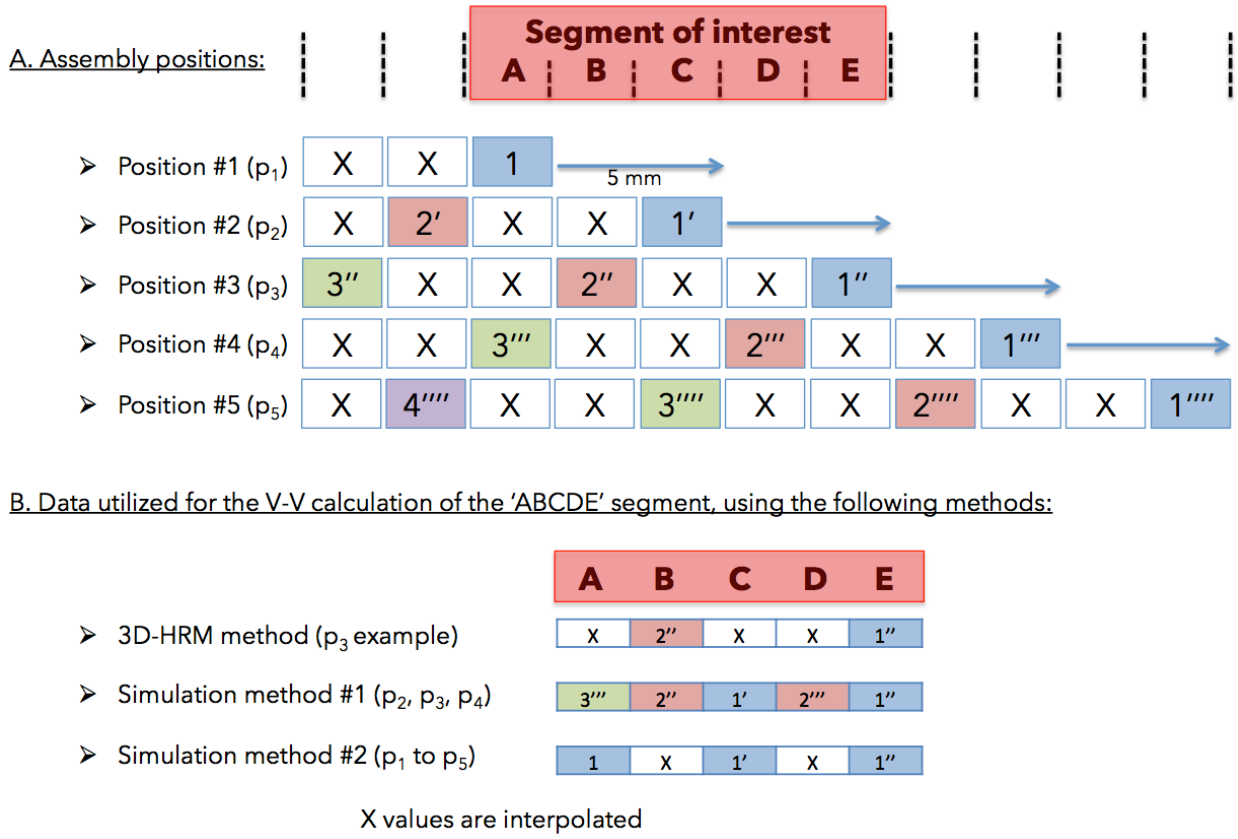

Results:

3D-HRM allowed us to differentiate the morphology of pressure signals attributable to the intrinsic sphincter (LES) and by the extrinsic components (DH and vascular pressures) (137). At rest, the DH pressure signature appeared as an inverted-V (Figure 22A), and LES pressure was almost nonexistent. Thus, measuring the pressurization generated by LES is not possible independently of the pressure attributable to the DH. Moreover, the accessory pressurization caused by the vascular signals was excluded for the determination of EGJ length. Thus, the full EGJ measured 6.0 cm long [5.8-7.0] representing the extreme limits of the inverted-V plot (Figure 22A), and was used for the calculation of EGJ V-V.

Table 5 illustrates an example of the process for the determination of EGJ V-V using the 3D-HRM real-time method at inspiration and end-expiration. The calculation of EGJ V-V in this table is the sum of the cross sectional vector areas and the interpolated pressures. Thus the EGJ V-V value incrementally increases when we include a progressively longer segment for the EGJ length. Table 5 also highlights the EGJ asymmetry, which is evident on the 3D representation of EGJ V-V (Figure 22B); this asymmetry is both radial and axial with 2 distinct axial pressure peaks.

Table 5. Example of pressures recorded at inspiration and end-expiration, with corresponding EGJ V-V ($mmHg^2$.mm) calculated using the 3D-HRM real-time method.

a. Data at inspiration

EGJ segments (cm)	*Radial pressure recording (mmHg)*								*EGJ V-V (mmHg.mm)*	
	0°	*45°*	*90°*	*135°*	*180°*	*225°*	*270°*	*315°*	*Segmental Contribution (%)*	*Cumulative contribution*
0-0.75	-1.2	-0.4	-0.9	-0.1	-1.8	-0.7	0.6	-1.8	1.1 (0.1)	1.1
0.75-1.5	2.9	2.9	2.8	6.6	40.4	35.7	51.8	5.4	3199.7 (18.0)	3200.8
1.5-2.25	50.4	24.0	21.1	18.2	16.9	14.0	14.3	16.6	4147.1 (23.3)	7347.9
2.25-3	2.0	1.1	3.8	16.3	54.7	40.3	24.2	34.2	5077.4 (28.6)	12425.3
3-3.75	2.5	2.7	5.4	8.6	12.9	8.4	2.1	0.4	1440.4 (8.1)	13865.7
3.75-4.5	-1.8	-0.6	0.6	-1.8	1.2	0.9	4.4	2.1	79.4 (0.4)	13945.1
4.5-5.25	40.1	35.7	51.8	5.4	-1.2	-0.2	-0.8	-0.1	2924.6 (16.4)	16869.8
5.25-6	1.1	0.8	4.3	2.1	2.5	2.5	5.3	8.6	911.6 (5.1)	17781.4

b. Data at end-expiration

EGJ segments (cm)	*Radial pressure recording (mmHg)*								*EGJ V-V (mmHg.mm)*	
	0°	*45°*	*90°*	*135°*	*180°*	*225°*	*270°*	*315°*	*Segmental Contribution (%)*	*Cumulative contribution*
0-0.75	3.9	7.2	4.7	4.5	4.4	5.1	5.8	5.8	74.6 (0.6)	74.6
0.75-1.5	2.5	2.5	2.5	4.7	17.8	31.8	50.0	9.2	2313.4 (17.4)	2388.1
1.5-2.25	21.3	15.3	14.1	12.8	11.6	8.4	8.9	10.7	1772.4 (13.3)	4160.5
2.25-3	5.6	6.7	19.6	39.0	27.0	17.3	26.2	32.3	3564.7 (26.8)	7725.2
3-3.75	10.3	8.8	11.9	16.2	13.6	6.0	6.1	5.8	1605.2 (12.0)	9330.4
3.75-4.5	4.5	5.3	6.1	6.4	6.6	11.1	8.8	10.8	566.6 (4.3)	9897.0
4.5-5.25	18.0	31.8	50.1	9.3	4.0	7.3	4.8	4.5	2442.5 (18.3)	12339.5
5.25-6	11.6	8.4	9.0	10.7	2.5	2.5	2.5	4.7	977.5 (7.3)	13317.0

Table 6 compares EGJ-V-V calculations between inspiration and end expiration among the 3 different methods. The Pearson correlation between the different 3 measurements for the calculation of the V-V was excellent; the worst correlation was r> 0.85;

$p<0.05$. There were no statistic differences among the methods and all methods showed significant differences between inspiration and expiration.

Table 6. Values of EGJ V-V ($mmHg^2$ x mm) at inspiration and expiration using 3 different methods for its calculation (Median [IQR]).

	3D-HRM	Pull-through method 1	Pull-through method 2	Worst Correlation	Friedman's test
EGJ V-V Inspiration	16,000 [15,350-17,000]	17,200 [16,000-19,450]	15,400 [11,300-19,300]	r>0.95; p<0.05	p=0.311
EGJ V-V Expiration	14,400 [13,000-15,000]	15,400 [14,350-18,400]	11,900 [10,600-17,000]	r>0.85; p<0.05	p=0.223

Wilcoxon test: $p<0.05$ between inspiration and expiration for the 3 methods

Discussion & Conclusion:

This additional study demonstrated that the 3D-HRM assembly permitted the calculation of EGJ V-V, using either a real-time imaging method or simulation of a pull-through protocol, resulting in statistically similar values.

The key advantages of the 3D-HRM method is that since the data are obtained with the device in a stationary position, instantaneous, dynamic measurements can be made for extended periods. Although this method required interpolation of data between recording sites positioned 7.5 mm apart on center, our findings suggest that this degree of interpolation had no significant impact on the V-V calculations. The dynamic recordings of

V-V obtained by 3D HRM graphically illustrated the dominant role of the DH in the overall EGJ pressure morphology (137). Using the characteristic axial and radial asymmetry of the diaphragm as identifying criteria, the DH contributed an estimated 85% to the total EGJ V-V. These observations are very much in line with the 'pinch-cock' model of the EGJ originally proposed by Allison in 1951 (138). Since perturbations of EGJ anatomy are increasingly recognized as important pathophysiological contributions to GERD pathophysiology (32,139,140), these observations suggest that real-time recording of V-V may contribute important insights in future pathophysiological studies of GERD subgroups.

The values of EGJ V-V calculated using the 3D-HRM are substantially greater than those previously reported in the original description of the technique (8,000 $mmHg^2$.mm [5300-12250] at end expiration (128,134,141,142). This finding is partly due to the different manometric technology used for data gathering and partly attributable to the methodology used to calculate EGJ length. With respect to manometric technology, the response characteristics of perfusion manometry are such that one would anticipate a greatly dampened signal compared to the solid-state device used in the current study (143); this would lead to an underestimation of the cross-sectional vector area at each locus within the EGJ. However, the larger consideration is probably the spatial EGJ limits used to incorporate into the V-V calculation. Although no mention of the DH contribution was made in the previous literature, we suspect that the measurement was restricted to the first pressure peak surrounding the diaphragmatic apex. Consistent with this supposition, when

restricting the measurement to a shorter length (3.75 cm), our methodology finds an EGJ V-V value that numerically correlates with the previously published values (Table 6).

EGJ pressure augmentation observed during inspiration is mainly due to diaphragmatic contraction. However, the radial asymmetry to the EGJ remains even in expiration suggesting that the diaphragmatic component of EGJ pressure can be detected throughout the respiratory cycle. Again, this is consistent with the pinchcock hypothesis put forth by Allison and also with the observation of a persistent HPZ at the hiatus in individuals who had previously undergone resection of the distal esophagus inclusive of the LES (144). Moreover, these observations highlight the cardinal contribution of the DH to EGJ pressure morphology (137). The assessment of EGJ V-V before and after hiatus hernia repair may permit to determine whether reapproximation of the crura anterior to, or posterior to, the esophagus results in a more normal physiologic outcome.

-Other area for research in GERD

As described in the review on HRM, tLESRs are responsible for most of cases of GERD in patients with or without hiatal hernia. Its recognition is complex and HRM appears more accurate to recognize them that conventional manometry (75-77). 3D-HRM with its radial

and longitudinal resolutions might be an interesting tool to differentiate tLESRs associated with reflux compared to tLESRs not associated with reflux.

Taken together with the more accurate determination of EGJ length and RIP (137), the 3D-HRM device appears to be a promising new tool in the study of GERD pathophysiology. Moreover, the results of our first studies highlight the primary role of the diaphragmatic hiatus in the pathophysiology of GERD and the crucial, but under-recognized, role of the crural repair during the anti-reflux surgery.

b) Potential role for 3D-HRM in the assessment of the UES

3D-HRM might be an interesting tool for evaluation of the UES and pharyngeal motility with the 3D segment positioned within the UES. The axial and radial resolutions of the 3D segment might improve the degree of understanding of UES and pharyngeal function, as HRM did compared to conventional manometry.

Indeed, the closely spaced sensors and rapid response time attributes of the HRM solid-state pressure sensors are particularly adapted to pharyngeal and UES physiology. UES and pharyngeal contractions have been described in control patients (145-147): normal

values for UES resting pressures were described by Takasaki *et al*. (147) and different indexes (relaxation interval, deglutitive sphincter resistance) have been proposed by Ghosh *et al*. to evaluate UES relaxation (145). However, the use of these indexes in clinical practice is currently somewhat difficult, as they require calculation using dedicated programs in MATLAB™ software.

The UES manometric signal in pathology is actually not completely understood using the conventional HRM: it has been evaluated in muscle tension dysphonia (148) and amyotrophic lateral sclerosis before and after cricopharyngeal myotomy (149). Today, the section of the cricopharyngeal muscle (150) represents almost exclusively the goal of the treatment in cases of Zenker's diverticulum and other oropharyngeal dysphagia, as oculopharyngeal muscular dystrophy (OPMD). 3D-HRM might help to define more specific causes for oropharyngeal dysphagia, and permit to propose more specific treatment.

CONCLUSIONS

3D-HRM permits real-time recording of EGJ pressure morphology facilitating analysis of the EGJ constituents responsible for its function as a reflux barrier. The axial and radial spatial resolution of the 9 cm 3D-HRM segment permit studies differentiating pressure signals within the EGJ attributable to the LES and to extrinsic structures (diaphragm and vascular artifacts). These attributes of the 3D-HRM device suggest it to be a promising new tool in the study of GERD pathophysiology. Further pathophysiological studies are anticipated in subgroups of GERD patients with reflux and with and without hiatus hernia in the hopes of evolving this into a valuable clinically technique.

During deglutition, we evaluated the feasibility of improving the measurement of IRP utilizing a novel 3D-HRM assembly and a novel 3D-eSleeve concept based on finding the axial maximum of the radial minimum pressures at each sensor ring along the sleeve segment. Our findings suggest that this approach is likely more accurate than standard HRM and other methods that utilize a radially averaged pressure within the EGJ. Although we can only speculate on how much this will improve clinical management, 3D-HRM will certainly improve the accuracy of EGJ relaxation measurements and this will certainly impact research endeavors focused on modeling EGJ function during swallowing and reflux.

ANNEXES

1) ACCURACY OF THE 3D-HRM ASSEMBLY

a. Pressure accuracy

The pressure accuracy was tested using the manufacturer's pressure chamber by applying pressure with a sphygmomanometer from 10 to 150 mmHg in increments of 10 mmHg. Each pressure was held for 5 seconds. After thermal compensation, the recorded pressures at each time and pressure increment were analyzed in Excel™.

The tested accuracy of the 3D-HRM array was such that each of the 96 sensing elements within it recorded the applied pressures in the range of 0-50 mmHg with an accuracy of ± 0.98 mmHg after thermal compensation; the maximum standard deviation (SD) was 0.4 mmHg at greater pressures.

Figure A1 illustrates the mean, maximum, and minimum pressures after thermal compensation among the 96 sensing elements at a single time point of each 10-mmHg pressure increment for the calibration test. The maximum SD was 1.2 mmHg at greater pressures. It was not possible to accurately test the recording stability over time because we were unable to hold the pressure chamber pressurization constant to the required degree of accuracy. However, as the pressurization drifted slowly downward, all sensors responded in unison.

Figure A1. Pressure accuracy of the 96 sensors of the 3D-HRM array in the testing chamber pressurized in 10 mmHg increments, after thermal compensation.

At each pressure increment, the mean of the 96 sensors as well as the maximum and minimum are indicated. The 0-40 mmHg segment of the plot is enlarged for clarity. For the range of pressures relevant to calculations of the 3D-IRP, the sensors performed within ±1 mmHg, consistent with the manufacturer's specifications.

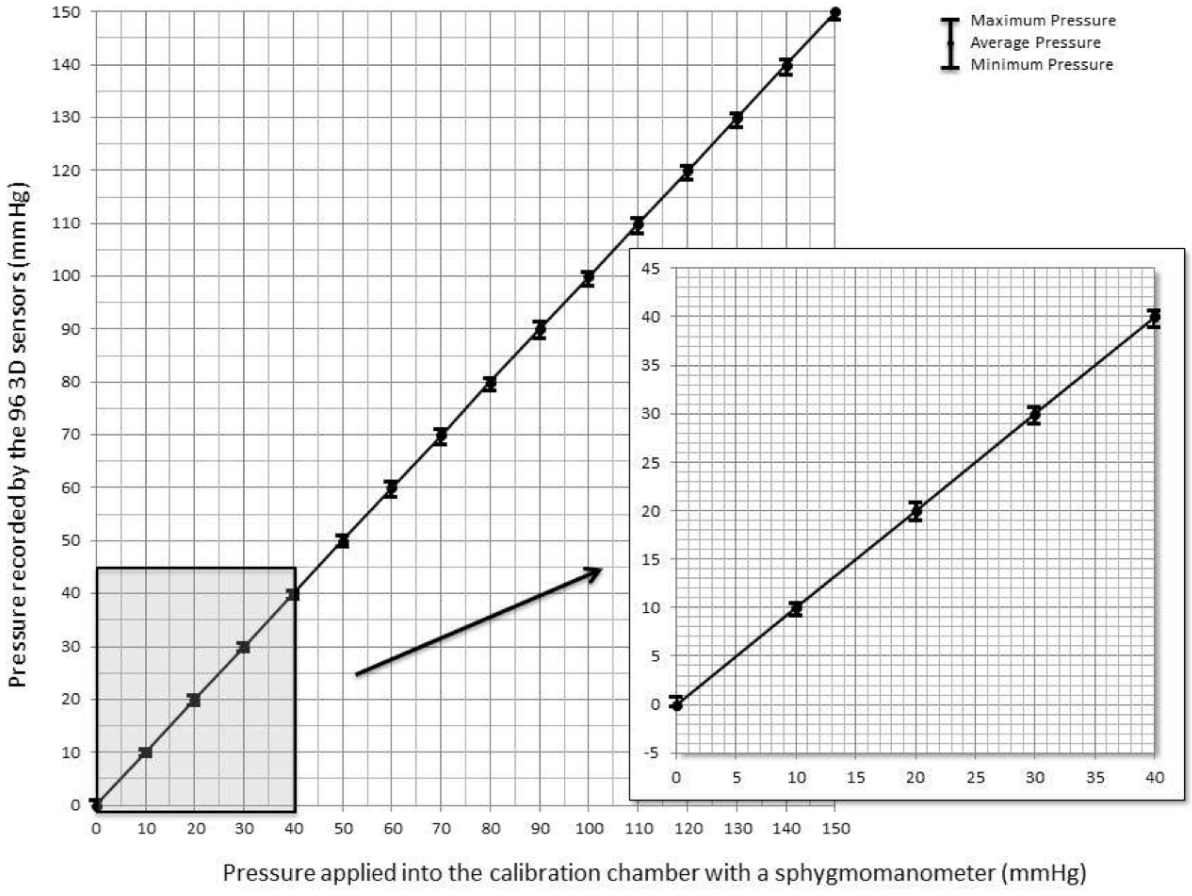

b. Length accuracy

One may discuss that the 3D-HRM assembly can overestimate the length of EGJ at the proximal and distal borders of the EGJ. The sensors are 2.5 mm long, separated by a gap of 5 mm and this technique (and all techniques) is an approximation of reality and generates some error. However, this error would be more of a problem if other available techniques were better, which is not the case. We estimate that the maximum theoretical error is ±5 mm and that this would occur if the pressure profile of the sphincter were a square wave, at one extreme exactly filling one gap between sensors or two gaps and one sensor and at the other extreme exactly covering one sensor or two entire sensors with one gap between (Figure A2). In the case of the square wave filling the gap between sensors there is potential to underestimate true sphincter length by 5 mmm and in the case of the square wave exactly covering two sensors and one gap, it would overestimate true sphincter length by 5 mm because of interpolation. In fact, that would probably be somewhat less because the hypothetical case below uses linear interpolation, whereas the HRM system uses cubic spline interpolation which would reduce the error.

Figure A2. Length accuracy of the 3D segment of the 3D-HRM assembly.

On the left, we represent the EGJ length applying a pressure on the 3D segment: the extreme values were 2.5mm (length of the pressure sensors) and 12.5mm (length of the pressure sensor plus the length of 2 gaps). In both cases, the pressure is recorded by a single pressure sensor (2.5mm) but is interpolated to 7.5mm. Thus, we estimate that the maximum theoretical error is ±5 mm.

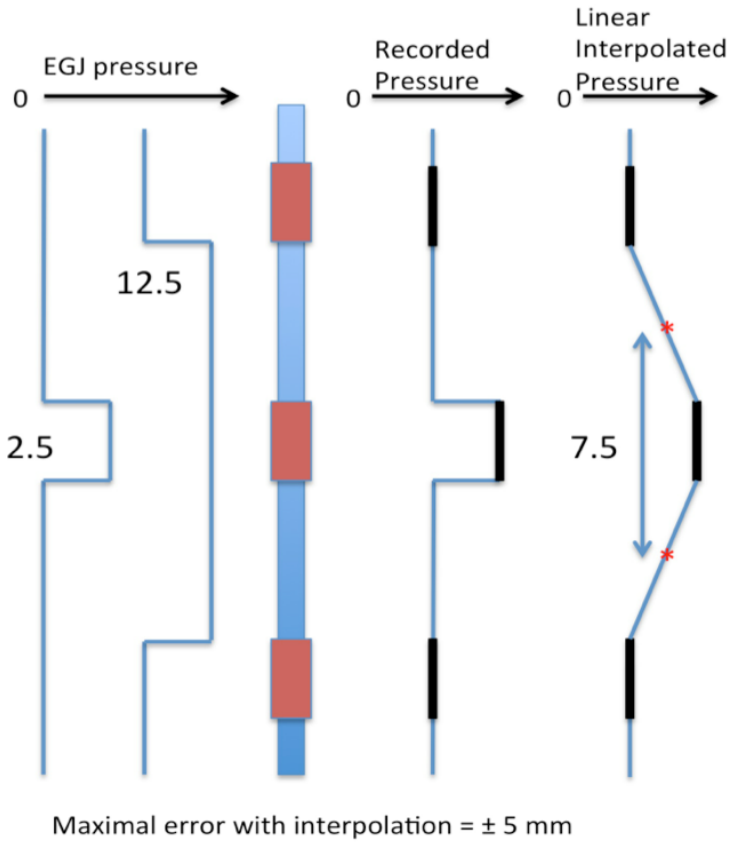

2) ABBREVIATIONS (ALPHABETIC ORDER)

AGAI	American Gastroenterology Association Institute
CART	Classification and regression tree
CD	Crural diaphragm *[Piliers du diaphragme]*
CDP	Contractile deceleration point
CFV	Contractile front velocity
CSVA	Cross sectional vector area
DCI	Distal contractile integral
DES	Diffuse esophageal spasm
DH	Diaphragmatic hiatus
DL	Distal latency
EGJ	Esophagogastric junction
EoE	Eosinophilic esophagitis
EPT	Esophageal pressure topography
FPT (3D-FPT)	Flow permissive time *[Temps permissif d'écoulement du bolus]*
GERD	Gastro-esophageal reflux disease
GerdQ	Gastro-esophageal reflux disease questionnaire
HPZ	High pressure zone
HRM (3D-HRM)	High resolution manometry *[Manométrie haute résolution]*
IBP	Intra-bolus pressure
IDQ	Impaction dysphagia questionnaire
IRP (3D-IRP)	Integrated relaxation pressure *[Pression de relaxation intégrée]*
[JOG]	*[Jonction œsophago-gastrique]*
LAGB	Laparoscopic adjustable gastric band
LES	Lower esophageal sphincter
OPMD	Oculopharyngeal muscular dystrophy
PIP	Pressure inversion point *[Point d'inversion de la pression]*
[RGO]	*[Reflux gastro-œsophagien]*
RIP	Respiratory inversion point *[Point d'inversion respiratoire]*
SD	Standard deviation
[SOI]	*[Sphincter œsophagien inférieur]*
tLESR	Transient lower esophageal sphincter relaxation
UES	Upper esophageal sphincter
V-V	Vector volume

REFERENCES

1. Kahrilas PJ, Shaheen NJ, Vaezi MF. American Gastroenterological Association Medical Position Statement on the Management of Gastroesophageal Reflux Disease. Gastroenterology. 2008 Oct;135(4):1383–5.

2. Butin JW, Olsen AM, Moersch HJ, Code CF. A study of esophageal pressures in normal persons and patients with cardiospasm. Gastroenterology. 1953 Feb;23(2):278–93.

3. Atkinson M, Ingelfinger FJ, Kramer P. The motility and pharmacology of the esophagus in cardiospasm. Gastroenterologia. 1956;86(3):174–8.

4. Sleisenger MH, Steinberg H, Almy TP. The disturbance of esophageal motility in cardiospasm: studies on autonomic stimulation and autonomic blockade of the human esophagus, including the cardia. Gastroenterology. 1953 Nov;25(3):333–48–discussion–359–63.

5. Asher MI, Coates AL, Collinge JM, Milic-Emili J. Measurement of pleural pressure in neonates. J Appl Physiol. 1982 Feb;52(2):491–4.

6. Code CF, Fyke FE, Schlegel JF. The gastroesophageal sphincter in healthy human beings. Gastroenterologia. 1956;86(3):135–50.

7. Dent J. Approaches to driving the evolving understanding of lower oesophageal sphincter mechanical function. 2007 Feb;43(1):1–14.

8. Dent J, Chir B. A new technique for continuous sphincter pressure measurement. Gastroenterology. 1976;71(2):263–7.

9. Pandolfino JE, Kahrilas PJ. American Gastroenterological Association medical position statement: Clinical use of esophageal manometry. Gastroenterology. 2005 Jan;128(1):207–8.

10. Nayar DS, Khandwala F, Achkar E, Shay SS, Richter JE, Falk GW, et al. Esophageal manometry: assessment of interpreter consistency. Clinical Gastroenterology and Hepatology. 2005 Mar;3(3):218–24.

11. Ott DJ, Richter JE, Chen YM, Wu WC, Gelfand DW, Castell DO. Esophageal radiography and manometry: correlation in 172 patients with dysphagia. AJR Am J Roentgenol. 1987 ed. 1987 Aug;149(2):307–11.

12. Clouse RE, Staiano A, Alrakawi A. Development of a topographic analysis system for manometric studies in the gastrointestinal tract. Gastrointestinal Endoscopy. 1998 Oct;48(4):395–401.

13. Clouse RE, Staiano A. Topography of the esophageal peristaltic pressure wave. Am. J. Physiol. 1991st ed. 1991 Oct;261(4 Pt 1):G677–84.

14. Pandolfino JE, Ghosh SK, Rice J, Clarke JO, Kwiatek MA, Kahrilas PJ. Classifying esophageal motility by pressure topography characteristics: a study of 400 patients and 75 controls. Am. J. Gastroenterol. 2008 Jan;103(1):27–37.

15. Ghosh SK, Pandolfino JE, Rice J, Clarke JO, Kwiatek M, Kahrilas PJ. Impaired deglutitive EGJ relaxation in clinical esophageal manometry: a quantitative analysis of 400 patients and 75 controls. Am. J. Physiol. Gastrointest. Liver Physiol. 2007 Oct;293(4):G878–85.

16. Ghosh SK, Pandolfino JE, Zhang Q, Jarosz A, Shah N, Kahrilas PJ. Quantifying esophageal peristalsis with high-resolution manometry: a study of 75 asymptomatic volunteers. Am. J. Physiol. Gastrointest. Liver Physiol. 2006 May;290(5):G988–97.

17. Pandolfino JE, Ghosh SK, Zhang Q, Jarosz A, Shah N, Kahrilas PJ. Quantifying EGJ morphology and relaxation with high-resolution manometry: a study of 75 asymptomatic volunteers. Am. J. Physiol. Gastrointest. Liver Physiol. 2006 May;290(5):G1033–40.

18. Bogte A, Bredenoord AJ, Oors J, Siersema PD, Smout AJPM. Reproducibility of esophageal high-resolution manometry. Neurogastroenterol Motil. 2011 Jul;23(7):e271–6.

19. Sweis R, Anggiansah A, Wong T, Kaufman E, Obrecht S, Fox M. Normative values and inter-observer agreement for liquid and solid bolus swallows in upright and supine positions as assessed by esophageal high-resolution manometry. Neurogastroenterol Motil. 2011 ed. 2011 Feb 22;23(6):509–e198.

20. Roman S, Damon H, Pellissier PE, Mion F. Does body position modify the results of oesophageal high resolution manometry? Neurogastroenterol Motil. 2010 Mar;22(3):271–5.

21. Xiao Y, Nicodème F, Kahrilas PJ, Roman S, Lin Z, Pandolfino JE. Optimizing the swallow protocol of clinical high-resolution esophageal manometry studies. Neurogastroenterol Motil. 2012 Oct;24(10):e489–96.

22. Basseri B, Pimentel M, Shaye OA, Low K, Soffer EE, Conklin JL. Apple sauce improves

detection of esophageal motor dysfunction during high-resolution manometry evaluation of dysphagia. Digest Dis Sci. 2011 Jun;56(6):1723–8.

23. Bernhard A, Pohl D, Fried M, Castell DO, Tutuian R. Influence of bolus consistency and position on esophageal high-resolution manometry findings. Dig. Dis. Sci. 2008;53(5):1198–205.

24. Daum C, Sweis R, Kaufman E, Fuellemann A, Anggiansah A, Fried M, et al. Failure to respond to physiologic challenge characterizes esophageal motility in erosive gastro-esophageal reflux disease. Neurogastroenterol Motil. 2011 ed. 2011 Jun;23(6):517–e200.

25. Ayazi S, Hagen JA, Zehetner J, Ross O, Wu C, Oezcelik A, et al. The Value of High-Resolution Manometry in the Assessment of the Resting Characteristics of the Lower Esophageal Sphincter. J Gastrointest Surg. 2009 ed. 2009 Sep 25;13(12):2113–20.

26. Bredenoord AJ, Weusten BLAM, Carmagnol S, Smout AJPM. Double-Peaked High-Pressure Zone at the Esophagogastric Junction in Controls and in Patients with a Hiatal Hernia: A Study Using High-Resolution Manometry. Digest Dis Sci. Kluwer Academic Publishers-Plenum Publishers; 2004;49(7/8):1128–35.

27. Bredenoord AJ, Weusten BL, Roelofs JM, Smout AJ. The gastro-oesophageal pressure inversion point revisited. Scand. J. Gastroenterol. 2003;38(8):812–8.

28. Bredenoord AJ, Weusten BLAM, Timmer R, Smout AJPM. Intermittent spatial separation of diaphragm and lower esophageal sphincter favors acidic and weakly acidic reflux. Gastroenterology. 2006 Feb;130(2):334–40.

29. Buduhan G, Orlina J, Louie B, Vallieres E, Aye R. Endoscopic and manometric position-related characteristics of the normal gastroesophageal junction. Surg Endosc. 2010 ed. 2010 Feb 21;24(9):2165–9.

30. Curcic J, Fox M, Kaufman E, Forras-Kaufman Z, Hebbard GS, Roy S, et al. Gastroesophageal junction: structure and function as assessed by using MR imaging. Radiology. 2010 ed. 2010 Oct;257(1):115–24.

31. Pandolfino JE, Serag El HB, Zhang Q, Shah N, Ghosh SK, Kahrilas PJ. Obesity: a challenge to esophagogastric junction integrity. Gastroenterology. 2006 Mar;130(3):639–49.

32. Pandolfino JE, Kim H, Ghosh SK, Clarke JO, Zhang Q, Kahrilas PJ. High-Resolution Manometry of the EGJ: An Analysis of Crural Diaphragm Function in GERD. Am J Gastroenterol. Nature Publishing Group; 2007 May;102(5):1056–63.

33. Pandolfino JE, Kwiatek MA, Ho K, Scherer JR, Kahrilas PJ. Unique features of esophagogastric junction pressure topography in hiatus hernia patients with dysphagia. Surgery. 2010 Jan;147(1):57–64.

34. Scheffer RCH, Bredenoord AJ, Hebbard GS, Smout AJPM, Samsom M. Effect of proximal gastric volume on hiatal hernia. Neurogastroenterol Motil. 2010 May;22(5):552–6–e120.

35. Endo S, Nakajima K, Nishikawa K, Takahashi T, Souma Y, Taniguchi E, et al. Laparoscopic Heller-Dor surgery for esophageal achalasia: impact of intraoperative real-time manometric feedback on postoperative outcomes. Dig Surg. 2009 ed. 2009;26(4):342–8.

36. Tibbling L, Gezelius P, Franzén T. Factors influencing lower esophageal sphincter relaxation after deglutition. WJG. 2011 ed. 2011 Jun 21;17(23):2844–7.

37. Kwiatek MA, Kahrilas PJ, Soper NJ, Bulsiewicz WJ, Mcmahon B-P, Gregersen H, et al. Esophagogastric junction distensibility after fundoplication assessed with a novel functional luminal imaging probe. J Gastrointest Surg. 2009 ed. 2010 Feb;14(2):268–76.

38. Hoshino M, Sundaram A, Srinivasan A, Mittal SK. The Relationship Between Dysphagia, Pump Function, and Lower Esophageal Sphincter Pressures on High-Resolution Manometry - Springer. J Gastrointest Surg. 2011 ed. 2012 Mar;16(3):495–502.

39. Pandolfino JE, Fox MR, Bredenoord AJ, Kahrilas PJ. High-resolution manometry in clinical practice: utilizing pressure topography to classify oesophageal motility abnormalities. Neurogastroenterol Motil. 2009 Aug;21(8):796–806.

40. Clouse RE, Staiano A. Topography of normal and high-amplitude esophageal peristalsis. Am. J. Physiol. 1993rd ed. 1993 Dec;265(6 Pt 1):G1098–107.

41. Gyawali CP, Kushnir VM. High-resolution manometric characteristics help differentiate types of distal esophageal obstruction in patients with peristalsis. Neurogastroenterol Motil. 2011 ed. 2011 Feb 9;23(6):502–e197.

42. Kushnir VM, Prakash Gyawali C. High resolution manometry patterns distinguish acid sensitivity in non-cardiac chest pain. Neurogastroenterol Motil. 2011 ed. 2011 Sep 19;23(12):1066–72.

43. Fox M, Menne D, Stutz B, Fried M, Schwizer W. The effects of tegaserod on oesophageal function and bolus transport in healthy volunteers: studies using

concurrent high-resolution manometry and videofluoroscopy. Aliment. Pharmacol. Ther. 2006;24(7):1017–27.

44. Ghosh SK, Janiak P, Fox M, Schwizer W, Hebbard GS, Brasseur JG. Physiology of the oesophageal transition zone in the presence of chronic bolus retention: studies using concurrent high resolution manometry and digital fluoroscopy. Neurogastroenterol Motil. 2008 Jul;20(7):750–9.

45. Ghosh SK, Janiak P, Schwizer W, Hebbard GS, Brasseur JG. Physiology of the esophageal pressure transition zone: separate contraction waves above and below. Am. J. Physiol. Gastrointest. Liver Physiol. 2006 Mar;290(3):G568–76.

46. Ghosh SK, Pandolfino JE, Kwiatek MA, Kahrilas PJ. Oesophageal peristaltic transition zone defects: real but few and far between. Neurogastroenterol Motil. 2008 Dec;20(12):1283–90.

47. Pohl D, Ribolsi M, Savarino E, Fruhauf H, Fried M, Castell DO, et al. Characteristics of the esophageal low-pressure zone in healthy volunteers and patients with esophageal symptoms: assessment by high-resolution manometry. Am. J. Gastroenterol. 2008;103(10):2544–9.

48. Bulsiewicz WJ, Kahrilas PJ, Kwiatek MA, Ghosh SK, Meek A, Pandolfino JE. Esophageal pressure topography criteria indicative of incomplete bolus clearance: a study using high-resolution impedance manometry. Am J Gastroenterol. 2009 Nov;104(11):2721–8.

49. Roman S, Lin Z, Kwiatek MA, Pandolfino JE, Kahrilas PJ. Weak peristalsis in esophageal pressure topography: classification and association with Dysphagia. Am J Gastroenterol. 2011 Feb;106(2):349–56.

50. Pandolfino JE, Leslie E, Luger D, Mitchell B, Kwiatek MA, Kahrilas PJ. The contractile deceleration point: an important physiologic landmark on oesophageal pressure topography. Neurogastroenterol Motil. 2010 ed. 2010 Dec 27;22(4):395–400.

51. Pandolfino JE, Lin Z, Roman S, Kahrilas PJ. The time course and persistence of "concurrent contraction" during normal peristalsis. AJP: Gastrointestinal and Liver Physiology. 2011 ed. 2011 Sep 27;301(4):G679–83.

52. Clouse RE, Staiano A, Alrakawi A, Haroian L. Application of topographical methods to clinical esophageal manometry. Am J Gastroenterol. Nature Publishing Group; 2000 Oct;95(10):2720–30.

53. Sampath NJ, Bhargava V, Mittal RK. Genesis of multipeaked waves of the esophagus:

repetitive contractions or motion artifact? AJP: Gastrointestinal and Liver Physiology. 2010 ed. 2010 Jun;298(6):G927–33.

54. Roman S, Pandolfino JE, Chen J, Boris L, Luger D, Kahrilas PJ. Phenotypes and clinical context of hypercontractility in high-resolution esophageal pressure topography (EPT). Am J Gastroenterol. 2012 Jan;107(1):37–45.

55. Hong SJ, Bhargava V, Jiang Y, Denboer D, Mittal RK. A unique esophageal motor pattern that involves longitudinal muscles is responsible for emptying in achalasia esophagus. Gastroenterology. 2010 ed. 2010 Jul;139(1):102–11.

56. Leslie E, Bhargava V, Mittal RK. A Novel Pattern of Longitudinal Muscle Contraction with Sub-threshold Pharyngeal Stimulus: A Possible Mechanism of Lower Esophageal Sphincter Relaxation. AJP: Gastrointestinal and Liver Physiology. 2011 Dec 15.

57. Roman S, Lin Z, Pandolfino JE, Kahrilas PJ. Distal Contraction Latency: A Measure of Propagation Velocity Optimized for Esophageal Pressure Topography Studies. Am J Gastroenterol. 2010 ed. 2011 Oct 26;106(3):443–51.

58. Pandolfino JE, Roman S, Carlson D, Luger D, Bidari K, Boris L, et al. Distal esophageal spasm in high-resolution esophageal pressure topography: defining clinical phenotypes. Gastroenterology. 2011 Aug;141(2):469–75.

59. Pandolfino JE, Kwiatek MA, Nealis T, Bulsiewicz W, Post J, Kahrilas PJ. Achalasia: a new clinically relevant classification by high-resolution manometry. Gastroenterology. 2008 Nov;135(5):1526–33.

60. Pratap N, Kalapala R, Darisetty S, Joshi N, Ramchandani M, Banerjee R, et al. Achalasia cardia subtyping by high-resolution manometry predicts the therapeutic outcome of pneumatic balloon dilatation. J Neurogastroenterol Motil. 2011 Jan;17(1):48–53.

61. Salvador R, Costantini M, Zaninotto G, Morbin T, Rizzetto C, Zanatta L, et al. The Preoperative Manometric Pattern Predicts the Outcome of Surgical Treatment for Esophageal Achalasia. J Gastrointest Surg. 2010 ed. 2010 Sep 10;14(11):1635–45.

62. Rohof WO, Salvador R, Annese V, Bruley des Varannes S, Chaussade S, Costantini M, et al. Outcomes of treatment for achalasia depend on manometric subtype. Gastroenterology. 2013 Apr;144(4):718–25–quize13–4.

63. Hernandez JC, Ratuapli SK, Burdick GE, DiBaise JK, Crowell MD. Interrater and intrarater agreement of the chicago classification of achalasia subtypes using high-resolution esophageal manometry. Am J Gastroenterol. 2012 Feb;107(2):207–14.

64. Jee SR, Pimentel M, Soffer E, Conklin JL. A high-resolution view of achalasia. J Clin Gastroenterol. 2008 ed. 2009 Aug;43(7):644–51.

65. Scherer JR, Kwiatek MA, Soper NJ, Pandolfino JE, Kahrilas PJ. Functional esophagogastric junction obstruction with intact peristalsis: a heterogeneous syndrome sometimes akin to achalasia. J Gastrointest Surg. 2009 ed. 2009 Dec;13(12):2219–25.

66. Galey KM, Wilshire CL, Niebisch S, Jones CE, Raymond DP, Litle VR, et al. Atypical Variants of Classic Achalasia Are Common and Currently Under-Recognized: A Study of Prevalence and Clinical Features. Journal of the American College of Surgeons. Elsevier Inc; 2011 Jul 1;213(1):155–61.

67. Hoshino M, Sundaram A, Juhasz A, Yano F, Tsuboi K, Lee TH, et al. High-resolution impedance manometry findings in patients with nutcracker esophagus. J Gastroenterol Hepatol. 2012 Mar;27(3):592–7.

68. Bredenoord AJ, Fox M, Kahrilas PJ, Pandolfino JE, Schwizer W, Smout AJPM, et al. Chicago classification criteria of esophageal motility disorders defined in high resolution esophageal pressure topography. Neurogastroenterol Motil. 2012 Mar;24 Suppl 1:57–65.

69. Nicodème F, Pandolfino JE. Esophageal Disorders Not Yet Addressed by High-resolution Manometry. J Neurogastroenterol Motil. 2013 Jan;19(1):114–5.

70. Lin Z, Kahrilas PJ, Roman S, Boris L, Carlson D, Pandolfino JE. Refining the criterion for an abnormal Integrated Relaxation Pressure in esophageal pressure topography based on the pattern of esophageal contractility using a classification and regression tree model. Neurogastroenterol Motil. 2012 Aug;24(8):e356–63.

71. Pandolfino JE. Uncovering hidden information in achalasia using esophageal pressure topography. Gastroenterology. 2013 Apr;144(4):681–4.

72. Sadowski DC, Broenink L. High-resolution esophageal manometry: a time motion study. Can. J. Gastroenterol. 2008;22(4):365–8.

73. Fox M, Hebbard G, Janiak P, Brasseur JG, Ghosh S, Thumshirn M, et al. High-resolution manometry predicts the success of oesophageal bolus transport and identifies clinically important abnormalities not detected by conventional manometry. Neurogastroenterol Motil. Wiley Online Library; 2004;16(5):533–42.

74. Babaei A, Mittal RK. Cardiovascular compression of the esophagus and spread of gastro-esophageal reflux. Neurogastroenterol Motil. 2010 ed. 2011 Jan;23(1):45–51,

e3.

75. Bredenoord AJ, Weusten BL, Timmer R, Smout AJ. Sleeve sensor versus high-resolution manometry for the detection of transient lower esophageal sphincter relaxations. AJP: Gastrointestinal and Liver Physiology. 2005 Jan 6;288(6):G1190–4.

76. Roman S, Zerbib F, Belhocine K, Varannes des SB, Mion F. High resolution manometry to detect transient lower oesophageal sphincter relaxations: diagnostic accuracy compared with perfused-sleeve manometry, and the definition of new detection criteria. Aliment Pharmacol Ther. 2011 Aug;34(3):384–93.

77. Rohof WO, Boeckxstaens GE, Hirsch DP. High-resolution esophageal pressure topography is superior to conventional sleeve manometry for the detection of transient lower esophageal sphincter relaxations associated with a reflux event. Neurogastroenterol Motil. 2011 ed. 2010 Dec 27;23(5):427–32–e173.

78. Pandolfino JE, Zhang QG, Ghosh SK, Han A, Boniquit C, Kahrilas PJ. Transient lower esophageal sphincter relaxations and reflux: mechanistic analysis using concurrent fluoroscopy and high-resolution manometry. Gastroenterology. 2006;131(6):1725–33.

79. Pandolfino JE, Ghosh SK, Zhang Q, Han A, Kahrilas PJ. Upper sphincter function during transient lower oesophageal sphincter relaxation (tLOSR); it is mainly about microburps. Neurogastroenterol. Motil. 2007 Mar;19(3):203–10.

80. Babaei A, Bhargava V, Mittal RK. Upper esophageal sphincter during transient lower esophageal sphincter relaxation: effects of reflux content and posture. AJP: Gastrointestinal and Liver Physiology. 2010 ed. 2010 May;298(5):G601–7.

81. Kuribayashi S, Massey BT, Hafeezullah M, Perera L, Hussaini SQ, Tatro L, et al. Terminating motor events for TLESR are influenced by the presence and distribution of refluxate. AJP: Gastrointestinal and Liver Physiology. 2009 ed. 2009 Jul;297(1):G71–5.

82. Bredenoord AJ, Weusten BL, Timmer R, Smout AJ. Gastro-oesophageal reflux of liquids and gas during transient lower oesophageal sphincter relaxations. Neurogastroenterol. Motil. 2006;18(10):888–93.

83. Scheffer RCH, Gooszen HG, Hebbard GS, Samsom M. The role of transsphincteric pressure and proximal gastric volume in acid reflux before and after fundoplication. Gastroenterology. 2005 Dec;129(6):1900–9.

84. Frankhuisen R, Van Herwaarden MA, Scheffer RCH, Hebbard GS, Gooszen HG,

Samsom M. Increased intragastric pressure gradients are involved in the occurrence of acid reflux in gastroesophageal reflux disease. Scand. J. Gastroenterol. 2009 ed. 2009;44(5):545–50.

85. Kwiatek MA, Post J, Pandolfino JE, Kahrilas PJ. Transient lower oesophageal sphincter relaxation in achalasia: everything but LOS relaxation. Neurogastroenterol Motil. 2009 ed. 2009 Dec;21(12):1294–e123.

86. Fouad YM, Katz PO, Hatlebakk JG, Castell DO. Ineffective esophageal motility: the most common motility abnormality in patients with GERD-associated respiratory symptoms. Am J Gastroenterol. Nature Publishing Group; 1999 Jun;94(6):1464–7.

87. Xiao Y, Kahrilas PJ, Kwasny MJ, Roman S, Lin Z, Nicodème F, et al. High-resolution manometry correlates of ineffective esophageal motility. Am J Gastroenterol. 2012 Nov;107(11):1647–54.

88. Hoshino M, Sundaram A, Mittal SK. Role of the Lower Esophageal Sphincter on Acid Exposure Revisited with High-Resolution Manometry. Journal of the American College of Surgeons. Elsevier Inc; 2011 Dec 1;213(6):743–50.

89. Hejazi RA, Reddymasu SC, Sostarich S, McCallum RW. Disturbances of Esophageal Motility in Eosinophilic Esophagitis: A Case Series. Dysphagia. 2009 ed. 2009 Aug 26;25(3):231–7.

90. Martin Martin L, Santander C, Lopez Martin MC, Espinoza-Rios J, Chavarria-Herbozo C, Gisbert JP, et al. Esophageal motor abnormalities in eosinophilic esophagitis identified by high-resolution manometry. J Gastroenterol Hepatol. 2011 ed. 2011 Sep;26(9):1447–50.

91. Roman S, Hirano I, Kwiatek MA, Gonsalves N, Chen J, Kahrilas PJ, et al. Manometric features of eosinophilic esophagitis in esophageal pressure topography. Neurogastroenterol Motil. 2011 Mar;23(3):208–14–e111.

92. Roman S, Hot A, Fabien N, Cordier JF, Miossec P, Ninet J, et al. Esophageal dysmotility associated with systemic sclerosis: a high-resolution manometry study. Dis. Esophagus. 2011 Dec 23;24:299–304.

93. Basseri B, Conklin JL, Pimentel M, Tabrizi R, Phillips EH, Simsir SA, et al. Esophageal motor dysfunction and gastroesophageal reflux are prevalent in lung transplant candidates. ATS. 2010 Nov;90(5):1630–6.

94. Kuribayashi S, Massey BT, Hafeezullah M, Perera L, Hussaini SQ, Tatro L, et al. Upper esophageal sphincter and gastroesophageal junction pressure changes act to

prevent gastroesophageal and esophagopharyngeal reflux during apneic episodes in patients with obstructive sleep apnea. Chest. 2009 ed. 2010 Apr;137(4):769–76.

95. Ahlstrand R, Savilampi J, Thorn SE, Wattwil M. Effects of cricoid pressure and remifentanil on the esophageal sphincters using high-resolution solid-state manometry. Acta anaesthesiologica Scandinavica. 2011 ed. 2011 Feb;55(2):209–15.

96. de Leon A, Ahlstrand R, Thorn SE, Wattwil M. Effects of propofol on oesophageal sphincters: a study on young and elderly volunteers using high-resolution solid-state manometry. European journal of anaesthesiology. 2010 ed. 2011 Apr;28(4):273–8.

97. de Leon A, Thorn SE, Ottosson J, Wattwil M. Body positions and esophageal sphincter pressures in obese patients during anesthesia. Acta anaesthesiologica Scandinavica. 2010 Apr;54(4):458–63.

98. de Leon A, Thorn SE, Raoof M, Ottosson J, Wattwil M. Effects of different respiratory maneuvers on esophageal sphincters in obese patients before and during anesthesia. Acta Anaesthesiologica Scandinavica. 2010 Sep 14;54(10):1204–9.

99. de Leon A, Thorn SE, Wattwil M. High-resolution solid-state manometry of the upper and lower esophageal sphincters during anesthesia induction: a comparison between obese and non-obese patients. Anesth. Analg. 2010 ed. 2010 Jul;111(1):149–53.

100. Kessing BF, Bredenoord AJ, Smout AJPM. Erroneous diagnosis of gastroesophageal reflux disease in achalasia. Clin. Gastroenterol. Hepatol. 2011 Dec;9(12):1020–4.

101. Bredenoord AJ, Draaisma WA, Weusten BL, Gooszen HG, Smout AJ. Mechanisms of acid, weakly acidic and gas reflux after anti-reflux surgery. Gut. 2008;57(2):161–6.

102. Scheffer RCH, Samsom M, Haverkamp A, Oors J, Hebbard GS, Gooszen HG. Impaired bolus transit across the esophagogastric junction in postfundoplication dysphagia. Am. J. Gastroenterol. 2005 Aug;100(8):1677–84.

103. Broeders JA, Rijnhart-de Jong HG, Draaisma WA, Bredenoord AJ, Smout AJ, Gooszen HG. Ten-year outcome of laparoscopic and conventional nissen fundoplication: randomized clinical trial. Annals of Surgery. 2009 ed. 2009 Nov;250(5):698–706.

104. Tatum RP, Soares RV, Figueredo E, Oelschlager BK, Pellegrini CA. High-resolution manometry in evaluation of factors responsible for fundoplication failure. J. Am. Coll. Surg. 2010 ed. 2010 May;210(5):611–7, 617–9.

105. Scheffer RCH, Samsom M, Hebbard GS, Gooszen HG. Effects of partial (Belsey Mark

IV) and complete (Nissen) fundoplication on proximal gastric function and esophagogastric junction dynamics. Am. J. Gastroenterol. 2006;101(3):479–87.

106. Burton PR, Brown W, Laurie C, Richards M, Afkari S, Yap K, et al. The effect of laparoscopic adjustable gastric bands on esophageal motility and the gastroesophageal junction: analysis using high-resolution video manometry. Obes Surg. 2009 Jul;19(7):905–14.

107. Burton PR, Brown WA, Laurie C, Richards M, Hebbard G, O'Brien PE. Effects of gastric band adjustments on intraluminal pressure. Obes Surg. 2009 Nov;19(11):1508–14.

108. Cruiziat C, Roman S, Robert M, Espalieu P, Laville M, Poncet G, et al. High resolution esophageal manometry evaluation in symptomatic patients after gastric banding for morbid obesity. Dig Liver Dis. 2011 Feb;43(2):116–20.

109. Burton PR, Brown WA, Laurie C, Hebbard G, O'Brien PE. Criteria for assessing esophageal motility in laparoscopic adjustable gastric band patients: the importance of the lower esophageal contractile segment. Obes Surg. 2010 Mar;20(3):316–25.

110. Burton PR, Brown WA, Laurie C, Hebbard G, O'Brien PE. Mechanisms of bolus clearance in patients with laparoscopic adjustable gastric bands. Obes Surg. 2010 Sep;20(9):1265–72.

111. Burton PR, Brown WA, Laurie C, Hebbard G, O'Brien PE. Predicting outcomes of intermediate term complications and revisional surgery following laparoscopic adjustable gastric banding: utility of the CORE classification and Melbourne motility criteria. Obes Surg. 2010 Nov;20(11):1516–23.

112. Burton PR, Brown WA, Laurie C, Korin A, Yap K, Richards M, et al. Pathophysiology of laparoscopic adjustable gastric bands: analysis and classification using high-resolution video manometry and a stress barium protocol. Obes Surg. 2010 Jan;20(1):19–29.

113. Mittal RK, Rochester DF, McCallum RW. Sphincteric action of the diaphragm during a relaxed lower esophageal sphincter in humans. Am. J. Physiol. Gastrointest. Liver Physiol. Am Physiological Soc; 1989;256(1):G139–44.

114. Mittal RK, Balaban DH. The esophagogastric junction. N Engl J Med. Mass Medical Soc; 1997;336(13):924–32.

115. Harris LD, Pope CE. The pressure inversion point: its genesis and reliability. Gastroenterology. 1966 Nov;51(5):641–8.

116. Stein HJ, DeMeester TR. Who benefits from antireflux surgery? World J Surg. 1992

Mar;16(2):313–9.

117. Ghosh SK, Kahrilas PJ, Lodhia N, Pandolfino JE. Utilizing intraluminal pressure differences to predict esophageal bolus flow dynamics. Am. J. Physiol. Gastrointest. Liver Physiol. 2007 ed. 2007 Nov;293(5):G1023–8.

118. Pandolfino JE, Ghosh SK, Lodhia N, Kahrilas PJ. Utilizing intraluminal pressure gradients to predict esophageal clearance: a validation study. Am J Gastroenterol. 2008 Aug;103(8):1898–905.

119. Kwiatek MA, Pandolfino JE, Kahrilas PJ. 3D-high resolution manometry of the esophagogastric junction. Neurogastroenterol Motil. 2011 ed. 2011/05/21; 2011 May 20;23(11):e461–9.

120. Kwiatek MA, Nicodème F, Pandolfino JE, Kahrilas PJ. Pressure morphology of the relaxed lower esophageal sphincter: the formation and collapse of the phrenic ampulla. AJP: Gastrointestinal and Liver Physiology. 2012 Feb 1;302(3):G389–96.

121. Jones R, Junghard O, Dent J, Vakil N, Halling K, Wernersson B, et al. Development of the GerdQ, a tool for the diagnosis and management of gastro-oesophageal reflux disease in primary care. Aliment Pharmacol Ther. Wiley Online Library; 2009;30(10):1030–8.

122. Nicodème F, Pandolfino JE, Lin Z, Xiao Y, Escobar G, Kahrilas PJ. Adding a radial dimension to the assessment of esophagogastric junction relaxation: validation studies of the 3D-eSleeve. AJP: Gastrointestinal and Liver Physiology. 2012 Aug;303(3):G275–80.

123. Mittal RK, Karstens A, Leslie E, Babaei A, Bhargava V. Ambulatory high-resolution manometry, lower esophageal sphincter lift and transient lower esophageal sphincter relaxation. Neurogastroenterol Motil. 2011 ed. 2012 Jan;24(1):40–2.

124. Mittal RK, Rochester DF, McCallum RW. Effect of the diaphragmatic contraction on lower oesophageal sphincter pressure in man. Gut. 1987 ed. 1987 Dec;28(12):1564–8.

125. Mittal RK, Rochester DF, McCallum RW. Electrical and mechanical activity in the human lower esophageal sphincter during diaphragmatic contraction. J. Clin. Invest. 1988 Apr;81(4):1182–9.

126. Gilbert RJ, Gaige TA, Wang R, Benner T, Dai G, Glickman JN, et al. Resolving the three-dimensional myoarchitecture of bovine esophageal wall with diffusion spectrum imaging and tractography. Cell Tissue Res. Springer; 2008;332(3):461–8.

127. Dodds WJ. Instrumentation and Methods for Intraluminal Esophageal Manometry. Arch Intern Med. American Medical Association; 1976 May 1;136(5):515–23.

128. Stein HJ, DeMeester T, Naspetti R, Jamieson J, Perry RE. Three-dimensional imaging of the lower esophageal sphincter in gastroesophageal reflux disease. Annals of Surgery. Lippincott, Williams, and Wilkins; 1991;214(4):374.

129. Lin Z, Kahrilas PJ, Xiao Y, Nicodème F, Gonsalves N, Hirano I, et al. Functional luminal imaging probe topography: an improved method for characterizing esophageal distensibility in eosinophilic esophagitis. Therap Adv Gastroenterol. 2013 Mar;6(2):97–107.

130. Najmabadi M, Devabhaktuni VK, Sawan M, Mayrand S, Fallone CA. A new approach to analysis and modeling of esophageal manometry data in humans. IEEE Trans Biomed Eng. 2009 Jul;56(7):1821–30.

131. Daubechies I. Orthonormal bases of compactly supported wavelets. Communications on pure and applied mathematics. Wiley Online Library; 1988;41(7):909–96.

132. Mallat SG. A theory for multiresolution signal decomposition: the wavelet representation. IEEE Trans. Pattern Anal. Machine Intell. IEEE; 1989 Jul;11(7):674–93.

133. Korn O, Stein HJ, Richter TH, Liebermann-Meffert D. Gastroesophageal sphincter: a model. Dis. Esophagus. 1997 Apr 1;10(2):105–9.

134. Bombeck CT, Vaz O, DeSalvo J, Donahue PE, Nyhus LM. Computerized axial manometry of the esophagus. A new method for the assessment of antireflux operations. Annals of Surgery. 1987 Oct;206(4):465–72.

135. Stein HJ, Korn O, Liebermann-Meffert D. Manometric vector volume analysis to assess lower esophageal sphincter function. Ann Chir Gynaecol. 1995;84(2):151–8.

136. Wetscher GJ, Hinder RA, Perdikis G, Wieschemeier T, Stalzer R. Three-dimensional imaging of the lower esophageal sphincter in healthy subjects and gastroesophageal reflux. Dig. Dis. Sci. Springer; 1996;41(12):2377–82.

137. Nicodème F, Lin Z, Pandolfino JE, Kahrilas PJ. Esophagogastric Junction pressure morphology: comparison between a station pull-through and real-time 3D-HRM representation. Neurogastroenterol Motil. 2013 Sep;25(9):e591–8.

138. Allison PR. Reflux esophagitis, sliding hiatal hernia, and the anatomy of repair. Surg Gynecol Obstet. 1951 Apr 1;92(4):419–31.

139. Boeckxstaens GEE. Review article: the pathophysiology of gastro-oesophageal reflux

disease. Aliment. Pharmacol. Ther. 2007 Jul 15;26(2):149–60.

140. Kahrilas PJ. GERD pathogenesis, pathophysiology, and clinical manifestations. Cleveland Clinic journal of medicine. Cleveland Clinic; 2003;70(Suppl 5):S4.

141. Andrade CG, Cecconello I, Nasi A, Zilberstein B, Filho JR, Campos Carvalho PJ, et al. Lower esophageal sphincter analysis using computerized manometry in patients with chagasic megaesophagus. Dis. Esophagus. 2006;19(1):31–5.

142. Swift GL, Smith PM, McKirdy HC, Lowndes RH. Vector volume analysis of the lower esophageal sphincter in achalasia and the effect of balloon dilation. Dis. Esophagus. 2001;14(1):54–6.

143. Dodds WJ, Stef JJ, Hogan WJ. Factors determining pressure measurement accuracy by intraluminal esophageal manometry. Gastroenterology. 1976 Jan;70(1):117–23.

144. Klein WA, Parkman HP, Dempsey DT, Fisher RS. Sphincterlike thoracoabdominal high pressure zone after esophagogastrectomy. Gastroenterology. 1993rd ed. 1993 Nov;105(5):1362–9.

145. Ghosh SK, Pandolfino JE, Zhang Q, Jarosz A, Kahrilas PJ. Deglutitive upper esophageal sphincter relaxation: a study of 75 volunteer subjects using solid-state high-resolution manometry. Am. J. Physiol. Gastrointest. Liver Physiol. 2006 Sep;291(3):G525–31.

146. Hoffman MR, Ciucci MR, Mielens JD, Jiang JJ, McCulloch TM. Pharyngeal swallow adaptations to bolus volume measured with high-resolution manometry. Laryngoscope. 2010 ed. 2010 Dec;120(12):2367–73.

147. Takasaki K, Umeki H, Enatsu K, Tanaka F, Sakihama N, Kumagami H, et al. Investigation of Pharyngeal Swallowing Function Using High-Resolution Manometry. Laryngoscope. 2008;118(10):1729–32.

148. Van Houtte E, Van Lierde K, D'haeseleer E, Van Imschoot B, Claeys S. UES pressure during phonation using high-resolution manometry and 24-h dual-probe pH-metry in patients with muscle tension dysphonia. Dysphagia. 2012 Jun;27(2):198–209.

149. Takasaki K, Umeki H, Enatsu K, Kumagami H, Takahashi H. Evaluation of swallowing pressure in a patient with amyotrophic lateral sclerosis before and after cricopharyngeal myotomy using high-resolution manometry system. Auris Nasus Larynx. 2010 ed. 2010 Oct;37(5):644–7.

150. Duranceau AC. Cricopharyngeal myotomy in the management of neurogenic and muscular dysphagia. Neuromuscul. Disord. 1997 Oct;7 Suppl 1:S85–9.